UNIVERSITAT POLITÈCNICA DE CATALUNYA
BARCELONATECH
Departament d'Enginyeria de Projectes
i de la Construcció

Environmental Engineering

DOCTORAL THESIS

Contributions to the determination of thermal behaviour of façades using quantitative internal IRT (Infrared Thermography)

Doctoral Programme:

Environmental Engineering

PhD thesis by:

Blanca Tejedor Herrán

Supervised by:

Dr. Miquel Casals Casanova

Dr. Xavier Roca Ramón

Terrassa, November 2018

“No te rindas que la vida es eso,
continuar el viaje, perseguir tus sueños,
destrabar el tiempo, correr los escombros
y destapar el cielo”
Mario Benedetti

Acknowledgements

First of all, I am really grateful for the guidance provided by my PhD supervisors, Dr. Miquel Casals and Dr. Xavier Roca. Their scientific intuition, experience and advice have been invaluable to me. Neither can I must not forget to mention my colleagues at the UPC: Dr. Marta Gangolells, Dr.Marcel Macarulla, Dr.Victor López, Dr.Maria Gonçalves, Dr. Lluc Canals, Dr.Núria Salán, Dr.Núria Forcada and Rafaela Bortolini among others.

I would like to highlight some of their expressions that helped me to grow-up as a researcher. In my first doctoral meeting, Dr. Miquel Casals told me "*A PhD thesis should be constituted by the essence of the research. In fact, it should involve a change in the society before and after its delivery. If no change is detected, the research may not be necessary to advance in our field*". Along the same lines, Dr. Marta Gangolells always mentioned, "W*riting a journal paper is a fact of embroidering, where each sentence must be drawn up with the maximum detail and care"*. Dr. Marcel Macarulla had a similar expression to add, *"One flower does not create a garden"*. All of them transmitted me that you cannot support your research with a strong statement on the basis of one single sample, because there are parameters that are not under control to generalize, but their results might be a research point to be assessed in the future. Taking all these aspects into account, the entire fruit of my publications is dedicated to them. Success does not belong to one person; it is the result of the sum of all people who are by your side. I can affirm now that I had the opportunity of working with a wonderful group of researchers (GRIC –Group of Construction, Research and Innovation) who trusted in my possibilities more than I did.

I would like to express my gratitude to all those who have facilitated the development of the measurement campaigns. In particular, at the initial stages of this research, Dr. Josep Bordonau from the Department of Electronic Engineering (ETSEIB –UPC) and Dr. Lluís Albert Bonals and Núria Vives from the Department of Heat Engines (ETSEIB –UPC). Once having developed the method, the Department of Housing and Urban Development from Terrassa for allowing access to its Council-owned buildings. Eloi Tarrés from Evowall Technology for providing a building mock-up with a low U-value and facilitating its monitoring process. My appreciation also goes to Dr. Kàtia Gaspar from the Department of Architectural Technology (UPC), a great professional and human being with whom I had the pleasure of sharing measurement campaigns in the first stages of our methods (HFM –Heat Flux Meter- and IRT –Infrared Thermography-).

I also want to acknowledge the financial support provided by the Department of Project and Construction Engineering (ESEIAAT –UPC-) at the first stage of this research. That fact alone allowed me demonstrating the applicability and the viability of the proposed method by calibration tests conducted on the laboratory. Along this line, I want to express my sincere thanks to the Industrial Engineers' Institution of Catalonia for financing part of this research through a PhD grant awarded in June 2016, and also the Terrassa City Council

for promoting this research through a PhD grant given in December 2016. Both institutions made possible the implementation of the proposed quantitative internal IRT method in several real built environments with an accurate measuring equipment.

I would also like to thank to the European Commission for giving me the grant Erasmus+ KA103 in order to develop a traineeship at *Università Politecnica delle Marche* (Ancona, Italy) from June to September 2018. I am especially grateful to the professors from the Department of Civil Engineering, Construction and Architecture for their knowledge transfer and their helpful advice, since they have allowed creating the possibility of new future research lines. Neither can I forget to mention my colleagues: Alessandra Corneli, Luigi Ridolfi and Leonardo Messi. They were the best welcoming committee to both an unknown city and a foreign country. One part of my heart will always be comprised of their smiles and our shared moments (inside and outside the UNIVPM).

I would like to dedicate my final words to my family and friends. Sometimes, your real family is created throughout your life with people who support you unconditionally without expecting anything in return. For this reason, I want to thank my parents Ana Herrán and José Tejedor, my great aunt Nica Herrán and relatives who have left us along the way (Julio Tejedor, Abilio Herrán, Rosa Papiol, Miquel Félez). In particular, my father deserves a special mention for being one of my main support columns at the engineering and human level. He steered me into the climbing and hiking world, but also into the technical field. He taught me how to combat my summits, despite bad boundary conditions, because any bad situation can be turned into a learning in any aspect of your life. He supported me when I was a child and my dream was to be a cellular biologist focused on investigation. In fact, I still have my first microscope and its original equipment and material. He always says, "*Whatever you do, it has to make you happy!*". I have to recognize that my PhD thesis has been a demanding period, but it has also been my own summit to climb. I knew which map should be followed, I had to establish a strategy for choosing the best paths of ascension to the summit, but I also had to be able to adapt to changes. Hence, my father's advice carries an invaluable weight. I also want to mention my closest friend Eva Félez, who has been like a sister to me, and her whole family. In hard times, a hug from all of them cannot be compared to anything material. Finally, I want to point out that the words of encouragement from other friends who also contributed to the finalization of this PhD thesis: Adolfo Lerin, Adrián Rivero, Oriol Huguet, Matteo Carnevali, Elena Picciafuoco and Lucia Lagrasta among others.

Abstract

Within the European framework, most of the current residential building stock does not satisfy the minimum thermal specifications. In fact, the renovation rate across the EU is estimated to be at around 1% per year. To fulfil with the goals stated by European Directives 2010/31/EU and 2012/27/EU, it is necessary to ensure a minimum discrepancy between the designed and the real building energy performance, which is also known as the energy performance gap. From a thorough literature review, it was detected that the thermal behavior of a building is often underestimated or neglected during its construction and operation stages. For this reason, an accurate non-destructive testing (NDT) should be required, improving the shortcomings given by the current modelling tools and diagnostic techniques.

The purpose of this thesis was to develop a method for determining in-situ the thermal behavior of façades under steady-state conditions using quantitative internal infrared thermography (IRT). After drawing up a numerical model to estimate the thermal transmittance (U-value) as a key parameter of the built quality, the dissertation continued with a validation process that was executed in two typical Spanish walls from different construction periods. This allowed: (i) refining the proposed method; (ii) exploring the boundaries conditions; (iii) assessing the influence of tabulated values set by international standards for wall emissivity and convective heat transfer coefficients among other aspects. The results revealed lower deviations related to the theoretical U-values (1.24 to 3.97%) for test durations of 2-3 hours. Furthermore, the results demonstrated that the use of tabulated values might entail deviations around 40% in heavy multi-leaf walls with low U-values.

Broadly, construction project documents for existing buildings, especially the oldest ones, are not available. Hence, this method may provide information about the building envelope for future refurbishment. In the case of new buildings, the method might allow the thermal behaviour of building façades to be checked according to the design parameters. Despite this, a subsequent literature review highlighted that a gap in the standardization of this method for in-situ building diagnostics is still to fill, which leads to a lack of measurement pattern. Considering this aspect, three studies were developed in order to enhance the applicability of the quantitative internal IRT within the construction industry field. Firstly, the influence of operating conditions on the determination of the measured U-value was analyzed through an experimental room with a heavy single-leaf wall tested under a wide temperature difference range ($3.8 < \Delta T < 21$ºC). Secondly, this dissertation performed tests in a public housing stock comprised of four unoccupied buildings (without electric and heating systems in operation), to assess the influence of non-transient thermophysical properties of the wall (i.e. heat capacity per unit of area) on the accuracy of the method. Thirdly, a data-processing method based on U-value time series analysis was proposed and validated through six building façades with heavy multi-leaf walls. The aim was to find a common criterion for stopping the test when it is not necessary more data to obtain a reliable result.

Having investigated the aspects mentioned above, it can be extrapolated that: (i) the optimum temperature difference range is found to be between 7 and 16ºC; (ii) the variance in the thermal transmittance could mainly be predicted by changes in the outer air temperature; (iii) the quantitative internal IRT is more accurate in heavy multi-leaf walls with high heat capacities per unit of area, reaching maximum deviations of 0.20%; (iv) the test might be executed in only 30 minutes; (v) the method could allow the assessment of aspects related to the determination of U-value of unoccupied buildings for ΔT under 10ºC, especially in Spain or European countries with a Mediterranean climate where these test conditions might represent a limitation. Hence, the decision-making could be streamlined in real built environments. In fact, this research might lead to enhanced execution of the refurbishment process in buildings that are expected to have shortcomings in 2050, in accordance with the existing literature. Consequently, it may increase the European renovation rate in the mid-term.

The dissertation concludes by outlining the main contributions of this research. The issues that were raised during the research undertaken although they could not be addressed are commented and proposed as future work.

Keywords: energy performance gap, NDT (non-destructive testing), quantitative infrared thermography, in-situ measurement, measured U-value, real built environment, building façade, operating conditions, heat capacity per unit of area, test duration

Resum

Dins del marc Europeu, la majoria dels edificis residencials actuals no satisfan els requeriments mínims tèrmics. De fet, la taxa de renovació a tota la UE s'estima entorn l'1% anual. Per complir amb els objectius establerts per les Directives Europees 2010/31/EU i 2012/27/EU, és necessari assegurar una discrepància mínima entre el rendiment energètic dissenyat i el real de l'edifici (*Energy Performance Gap*). A partir d'una revisió exhaustiva de la bibliografia, va ser detectat que el comportament tèrmic d'un edifici és sovint subestimat o negligit durant les seves etapes de construcció i operació. Per aquest motiu, una prova no destructiva (NDT) i precisa hauria de ser requerida, millorant les deficiències donades per les actuals eines de modelització i les tècniques de diagnosi.

Vist això, el propòsit d'aquesta tesi era desenvolupar un mètode per determinar in-situ el comportament tèrmic de les façanes sota condicions estacionaries utilitzant la termografia quantitativa interna (IRT). Després d'elaborar un model numèric per estimar la transmitància tèrmica (*U-value*) com a paràmetre clau de la qualitat construïda, la dissertació va continuar amb un procés de validació executat en dues parets típiques espanyoles de diferents períodes de construcció. Això va permetre: (i) refinar el mètode proposat; (ii) explorar les condicions de contorn; (iii) avaluar la influència dels valors tabulats establerts per les normatives internacionals per a l'emissivitat de la paret i els coeficients convectius de transferència de calor entre altres aspectes. Els resultats van revelar baixes desviacions respecte als valors teòrics de transmitància tèrmica (1.24 a 3.97%) per duracions de test entre 2 i 3 hores. A més a més, els resultats van demostrar que l'ús de valors tabulats podria implicar desviacions entorn al 40% en parets compostes amb baixos *U-values*.

En general, els projectes de construcció per edificis existents, especialment els antics, no estan disponibles. Per tant, aquest mètode podria proporcionar informació sobre la façana per futures rehabilitacions. En el cas d'edificis nous, el mètode podria permetre verificar el comportament tèrmic de les parets d'acord amb els paràmetres de disseny. Malgrat això, una revisió bibliogràfica posterior va posar de manifest que encara hi ha una bretxa en la estandardització d'aquest mètode per la diagnosi in-situ, la qual cosa deriva a una manca de patró de mesura. Considerant aquest aspecte, es van desenvolupar tres estudis per tal de millorar l'aplicabilitat de la termografia quantitativa interna dins el camp de la indústria de la construcció. En primer lloc, es va analitzar la influència de les condicions operatives en la determinació de la transmitància tèrmica mesurada a través d'una cambra experimental amb una façana simple sota un ampli rang de diferència de temperatura ($3.8 < \Delta T < 21$ºC). En segon lloc, aquesta dissertació va dur a terme tests en un parc d'habitatges públics constituïts per quatre pisos desocupats (sense sistemes elèctrics ni de calefacció en funcionament), amb la finalitat d'analitzar la influència de les propietats termofisiques no transitòries (ex. la capacitat de calor per unitat d'àrea) en la precisió del mètode. En tercer lloc, es va proposar i validar un mètode de processat de dades basat en l'anàlisi de sèries de temps de la *U-value* mitjançant sis parets compostes. L'objectiu era trobar un criteri comú per aturar la prova quan no són necessàries més dades per obtenir un resultat fiable.

Havent investigat els aspectes mencionats anteriorment, es pot extrapolar que: (i) el gradient de temperatura òptim es troba entre 7 i 16ºC; (ii) la variància en la transmitància tèrmica podria ser principalment atribuïda a canvis en la temperatura ambient de l'aire exterior; (iii) la IRT quantitativa interna és més acurada en parets compostes amb altes capacitats de calor per unitat d'àrea, aconseguint unes desviacions màximes del 0.20%; (iv) el test podria ser executat en només 30 minuts; (v) el mètode podria permetre l'avaluació d'aspectes relacionats amb la determinació de la *U-value* en edificis desocupats per ΔT sota 10ºC, especialment a Espanya o països europeus amb un clima mediterrani on aquestes condicions de test podrien representar una limitació. Per tant, la presa de decisions es podria simplificar en entorns construïts reals. De fet, aquesta recerca podria conduir a una millor execució del procés de rehabilitació en edificis que s'espera que tinguin deficiències l'any 2050, augmentant així la taxa de renovació europea a mig termini.

La dissertació conclou resumint les principals aportacions d'aquesta investigació. Els temes que s'han plantejat durant la recerca realitzada, i que no es van poder abordar, es comenten i es proposen com a línies de treball futures.

Paraules clau: bretxa rendiment energètic, NDT (prova no destructiva), termografia quantitativa, mesura in-situ, transmitància tèrmica mesurada, entorn construït real, façana, condicions d'operació, capacitat de calor per unitat d'àrea, duració de test

Acronyms and abbreviations

- UPC: Universitat Politècnica de Catalunya
- ETSEIB: Escola Tècnica i Superior d'Enginyeria Industrial de Barcelona
- ESEIAAT: Escola Superior d'Enginyeria Industrial, Aeronàutica i Audiovisual de Terrassa
- GRIC: Group of Construction, Research and Innovation
- UNIVPM: Università Politecnica delle Marche
- EU: European Union
- EPG: Energy Performance Gap
- NDT: Non-destructive testing
- IRT: Infrared Thermography
- BPIE: Buildings Performance Institute Europe
- EUI: Economist Intelligence Unit
- ITRE: European Parliament's Committee on Industry, Research and Energy
- IEA: International Energy Agency
- NZEB: Nearly Zero Energy Buildings
- R.D.: Spanish Royal Degree
- SAP: Standard Assessment Procedure
- HFM: Heat Flux Meter
- ISO: International Organization for Standarization
- ITC: Infrared Training Center
- CF: Contributory Factors of the Energy Performance Gap
- IFOV: Instantaneous Field of View of the IR camera
- FOV: Field of View
- EPS: Expanded Polystyrene
- ACF: Autocorrelation Function
- CP: Cumulated Periodogram
- CLT: Central Limit Theorem
- SD (or σ): Standard Deviation
- CV: Coefficient of Variation
- CI: Confidence Intervals
- IHCP: Inverse Heat Conduction Problems

Symbols

- $U_{mes\ avg}$: Average measured thermal transmittance [W/(m^2·K)]
- $U_{mes\ i}$: Instantaneous measured thermal transmittance [W/(m^2·K)]
- n: number of thermograms
- q_r: Specific heat flux by radiation [W/m^2]
- q_c: Specific heat flux by convection [W/m^2]
- ε_{WALL}: Wall emissivity [---]
- h_c: Convective heat transfer coefficient [W/(m^2·K)]
- ΔT: Temperature difference [K]
- T_{IN}: Inner air temperature [K]
- T_{OUT}: Outer air temperature [K]
- T_{WALL}: Wall surface temperature [K]
- T_{REF}: Reflected ambient temperature [K]
- σ: Stefan–Boltzmann's constant [W/(m^2·K^4)]
- λ_{air}: Thermal conductivity of the air [W/(m·K)]
- L: Height of the wall seen from inside the building [m]
- N_u: Nusselt number [---]
- G_r: Grashof number [---]
- R_a: Rayleigh number [---]
- P_r: Prandlt number [---]
- g: Gravitation [m/s^2]
- β: Volumetric temperature expansion coefficient [1/K]
- n: Air viscosity [m^2/s]
- U_t: Theoretical thermal transmittance [W/(m^2·K)]
- $\Delta U/U_t$: Deviation between the theoretical and measured thermal transmittance [W/(m^2·K) or %]
- R_t: Theoretical thermal resistance [(m^2·K)/W]
- R_{se}: Theoretical thermal resistance from outside the building [(m^2·K)/W]
- R_{si}: Theoretical thermal resistance from inside the building [(m^2·K)/W]
- Δx_i: Thickness of the layer [m]
- λ_i: Thermal conductivity of the layer [W/(m·K)]
- σU: Combined standard uncertainty [W/(m^2·K)]
- σT_{IN} and σT_{OUT}: Uncertainties associated with the environmental indoor and outdoor temperature measuring equipment [W/(m^2·K)]
- σT_{WALL}, σT_{REF} and $\sigma \varepsilon_{WALL}$: Uncertainties associated with the infrared camera when the wall surface temperature, the reflected ambient temperature and the wall emissivity are measured [W/(m^2·K)]

- k_m: theoretical heat capacity per unit of area [kJ/(m^2·K)]
- ρ_i: density of the layer [kg/m^3]
- c_{pi}: specific heat capacity of the layer [J/kg·K]
- $e_k(t)$: measurement noise [W/(m^2·K)]

Table of contents

List of figures

List of tables

Chapter 1: State of the art

This chapter provides an introduction to this thesis. The chapter is divided into four sections. The first and second ones introduce preliminary notions on energy performance gap (EPG) in buildings and the measurement techniques for determining in-situ thermal transmittance as a common indicator of the thermal quality of the building envelopes in steady-state conditions. The third section is focused on the shortcomings in the usability of the quantitative infrared thermography (IRT) as in-situ non-destructive testing (NDT). Within this context, the section shows two points of interest: (i) sources of discrepancy that could affect the accuracy of in-situ measured U-values using the quantitative IRT, based on a critical literature review; (ii) aspects related to the execution of the method in order to reduce the current duration of the data collection and post-processing. Finally, and in the fourth section, the topic addressed in this thesis is justified in the discussion of the implications.

1.1 The Energy Performance Gap and the importance of building refurbishment

Most of the current European residential stock does not satisfy the minimum thermal specifications [Itard and Meijer, 2008; Dowson et al., 2012; Gangolells and Casals, 2012; Gangolells et al., 2016]. Within the European context, over 40% of buildings were built before 1960 and 90% before 1990, and most of them will still be standing in 2050 [Itard and Meijer, 2008; Buildings Performance Institute Europe -BPIE-, 2011; Economist Intelligence Unit –EUI-, 2013; European Parliament's Committee on Industry, Research and Energy –ITRE-, 2016; Interreg Europe, 2017]. This implies that up to 110 million buildings need refurbishment [European Parliament's Committee on Industry, Research and Energy –ITRE-, 2016]. Unfortunately, the renovation rate across the EU is estimated to be very low, at around 1% per year [Itard and Meijer, 2008; Buildings Performance Institute Europe -BPIE-, 2011; Economist Intelligence Unit –EUI-, 2013; European Parliament's Committee on Industry, Research and Energy –ITRE-, 2016; International Energy Agency –IEA-, 2013; O'Grady et al., 2017a].

Nowadays, most of the energy efficiency measures are focused on maximizing the thermal performance of components [Taylor et al., 2013], since building elements may not perform as expected when they are in situ [Bordass et al., 2004; Demanuele et al., 2010; Menezes et al., 2012; Dimitrijevic et al., 2012; Guerra-Santin et al., 2013; De Wilde, 2014]. In fact, the thermal behaviour of a building is often underestimated or neglected during its construction and operation stages [Demanuele et al., 2010; Dimitrijevic et al., 2012; Menezes et al., 2012; Dowson et al., 2012; Zalejska-Jonsson, 2012; De Wilde, 2014]. In order to reduce the energy dependency and improve energy performance of buildings, two European Directives have been enforced in accordance to 2020 European Union's climate targets. Directive 2010/31/EU [European Union, 2010], also called NZEB (Nearly Zero Energy Buildings –Figure 1-), requires energy certification for

properties in order to achieve higher energy savings and guarantee adequate indoor comfort conditions for users [Albatici et al., 2010; Ficco et al., 2015]. Directive 2012/27/EU [European Union, 2012] establishes a set of binding measures to use energy more efficiently at all stages of the energy chain. As regards regulatory framework in the Spanish context, both directives were partially transposed by the R.D. 235/2013 [Spain, 2013] and R.D.56/2016 [Spain, 2016] respectively.

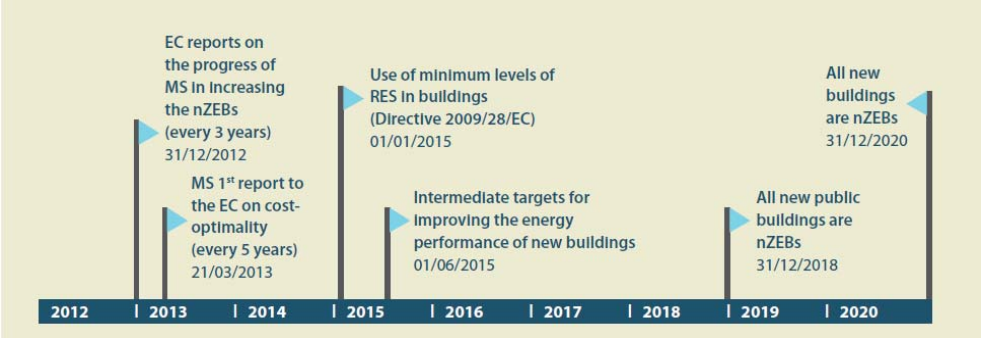

Figure 1. Share of buildings in final energy consumption in EU-28. [Source: Eurostat; BPIE]

These aforementioned directives have forced public administrations, designers, private companies and building manufacturers to ensure the minimum energy performance gap (EPG), which is the same as the minimum possible deviation between the designed and the real building energy performance [Bordass et al., 2004; Albatici et al., 2010; Demanuele et al., 2010]. Therefore, the requirements in the regulations on façades have grown and are expected to continue growing in the future [Cuerda et al., 2014]. Nevertheless, a lack of robustness has been observed in the tools used to calculate and certify building performance once the construction process has been finished [Littlewood et al., 2015]. Similarly, a high level of discrepancy has been found in the modelling of retrofit buildings [Tronchin et al., 2008; Fitton et al., 2013; Ahern et al., 2016; Marshall et al., 2017]. Simplified tools such as the Standard Assessment Procedure (SAP) in the UK or CE3X in Spain very often also underestimate thermal bridging and thermal properties of building components, since they generalize some details of the construction to reduce the management of input data [Littlewood et al., 2015; Gangolells et al., 2016]. However, feedback from building diagnosis might be used to upgrade the initial model of the building, and consequently to reduce the energy performance gap [De Wilde, 2014; Marshall et al., 2017] and improve the management of construction quality [Taylor et al., 2013].

Along this line, Ferrari et al. [2013], Nardi et al. [2014] and Soares et al. [2019] pointed out that the U-value had become a key parameter for assessing the thermal quality of the building envelope and steady-state heat transmission performance. Despite this, the measured thermal transmittance in real buildings can be rather different from that estimated by modelling and calculations [Guerra-Santin et al., 2013; Ficco et al., 2015]. For this reason, the future building diagnosis should require a precise measurement technique for determining the thermal property mentioned above.

1.2 Measurement techniques for determining U-values (thermal transmittances)

1.2.1 Background of the existing measurement techniques for determining U-values

In the last few decades, several researchers have focalized their efforts on the development and implementation of techniques for assessing building features. Some of these techniques are the following: the simulation [Emmel et al., 2007; Prada et al., 2014; Rossi et al., 2014; Liu et al., 2015], the guarded hot box method [Asdrubali et al., 2012; Vereecken et al., 2014], the automatic guarded hot plate apparatus [Kumar et al., 2013], the heat flux meter method (HFM) [Anderson, 1985; Roulet el al., 1987; Flanders, 1991; Flanders, 1992; Ahmad et al., 2014; Ficco et al., 2015; Gaspar et al., 2016; Atsonios et al., 2017] and the infrared thermography (qualitative and quantitative IRT) [Anderson, 1977; Burch et al., 1977; Burn and Schuyler, 1980; Flanders et al., 1981; McIntosh, 1981; Flanders, 1991; Straube and Burnett, 1999; Kalamees, 2007; Madding, 2008; Lucchi, 2011; Taylor et al., 2013; Meola et al., 2014; Fox et al., 2015; Barreira et al., 2016]. In fact, a combination of some of them has also been carried out to complete studies about the influence of boundary conditions on the measured U-values [Lehman et al., 2013; Tzifa et al., 2014; Albatici et al., 2015; Meng et al., 2015; Nardi et al., 2016; O'Grady et al., 2017] or to validate the results gathered by non-invasive techniques that are not fully developed (i.e. quantitative IRT) [Haralambopoulos et al., 1998; Albatici et al., 2010; Kisilewicz et al., 2010; Fokaides et al., 2011; Dall'O et al., 2013; De Freitas et al., 2014; Danielski et al., 2015].

Albatici et al. [2013] and Gaspar et al. [2016] highlighted that in-situ U-values are commonly determined by the heat flux meter (HFM) method according to ISO 9869-1:2014 [International Organization for Standardization, 2014]. The HFM consists of monitoring the heat flux rate passing through the façade and the indoor and outdoor environmental temperatures to obtain the thermal transmittance. However, this method presents some limitations. The first is that the HFM can only measure a local point of the wall and requires to be installed in different points of the wall to avoid singularities [Carbonez et al., 2014; Danielski et al., 2015; Tejedor et al., 2017]. Therefore, it does not provide accurate results for non-homogenous building elements [Danielski and Fröling, 2015]. Secondly, it requires a minimum test duration of 72 hours and a maximum of one week [ISO 9869-1:2014; International Organization for Standardization, 2014].

Within this context, infrared thermography (IRT) may be a good alternative for in-situ U-value measurements over the existing methods. IRT is a non-destructive test based on measuring the radiant thermal energy distribution (heat) emitted from an object's surface [Infrared Training Center and FLIR Systems, 2015]. Traditionally, IRT has only been used to detect thermal irregularities in building envelopes qualitatively, following EN 13187:1998 [International Organization for Standardization, 1998] and the RESNET Interim Guideline for Thermographic Inspections of Buildings [Residential Energy Services Network, 2010].

Nevertheless, quantitative IRT methods may also be adopted to determine U-values even though they are still not fully developed [Danielski and Fröling, 2015], since it is a method that provides reliable U-values of a wall area with reduced time (2-3 hours) [Albatici et al., 2010; Carbonez et al., 2014; Danielski et al., 2015; Nardi et al., 2015; Tejedor et al., 2017; Tejedor et al., 2018].

1.2.2 Quantitative Infrared Thermography (IRT)

Within the field of measuring on-site U-values with quantitative IRT, the main studies were conducted by Albatici et al. [2010], Albatici et al. [2015] and Fokaides et al. [2011]. Albatici et al. [2010] and Albatici et al. [2015] took measurements from outside the building, while Fokaides et al. [2011] carried out tests from inside the building. External thermography has several limitations. Firstly, it is more susceptible to environmental conditions than internal thermography, which provides a much more controlled environment with slower and less significant climatic fluctuations [Dall'O et al., 2009; Fokaides et al., 2011; Lucchi, 2011; Fox et al., 2016]. Secondly, many objects with unknown thermal status can reflect on the target and there is no control of the reflection index [Fokaides et al., 2011]. Finally, according to Dall'O et al. [2013], the external convective coefficient cannot be considered constant in outside tests, and must be calculated on the basis of weather conditions to achieve an acceptable result.

Jürge's equation can be used to determine the external convective heat transfer coefficient [Albatici et al., 2010; Dall'O et al., 2013; Albatici et al., 2015; Nardi et al., 2016]. This equation establishes a linear relationship between the external convective heat transfer coefficient and the wind speed. Despite being widely used in modelling, simulations and relevant calculations, Jürge's equation has several shortcomings [Palyvos et al., 2008]. The value of the convective heat transfer coefficient may be overestimated, and it may vary widely at different positions on the surface of a building [Hoyano et al., 1999; Rabadiya et al., 2012; Sham et al., 2012]. In fact, surface-to-wind angle, wind intensity and wind direction play an important role, and are strongly affected by the building's surroundings [Emmel et al., 2007; Dall'O et al., 2013; Liu et al., 2015]. Along this line, Albatici et al. [2010], Dall'O et al. [2013] and Albatici et al. [2015] highlighted that the deviation between notional and measured U-value might be higher in light walls than in heavy walls. The impact of wind speed will be greater in elements with low thermal mass, since they cool down faster. Alternatively, the external convective heat transfer coefficient can be estimated using a tabulated value stated in UNE-EN ISO 6946:2012 [International Organization for Standardization, 2012]. However, this convective heat transfer coefficient is high, a precautionary value, since it is used to determine the heat loss during the design stage of the building façade [Dall'O et al., 2013].

1.3 Shortcomings in the usability of the quantitative IRT (Infrared Thermography)

1.3.1 Accuracy of in-situ measured U-values: the main two sources of discrepancy

In general, construction project documents are not available for existing buildings, especially the oldest ones, but methods such as quantitative internal infrared thermography (IRT) can provide valuable information about in-situ thermal transmittance of the façade for future refurbishment [Tejedor et al., 2017]. To guarantee correct execution of in-situ quantitative IRT tests and accurate outcomes, some operating conditions must be fulfilled. Previous researchers stated that tests must be performed under 10-15ºC of temperature difference between outside and inside the building to ensure measurable heat exchange across the building envelope [Albatici et al., 2010; Fokaides et al., 2011; Asdrubali et al., 2012; Dall'O et al., 2013; Asdrubali et al., 2014; Biddulph et al., 2014; Kylili et al., 2014; Taylor et al., 2014; Fox et al., 2014; Barreira et al., 2017], although this parameter could be reduced to a lower level ($7 < \Delta T < 16$ºC) according to Tejedor et al. [2017].

Accuracy in the determination of the thermal behavior of façades [Gaspar et al., 2016] and the influence of operating conditions [Nardi et al., 2016] have become a widely discussed concern in recent years, regardless of the technique used for the assessment (i.e. heat flux meter –HFM-, guarded hot box, and quantitative infrared thermography, among others). For quantitative external IRT, some authors proposed a sensitivity analysis in relation to the deviation between the theoretical and measured U-values. Lehman et al. [2013] quantified the influence of climatic conditions on the surface temperature distribution in both insulated and non-insulated façades by simulations in transient regime, to derive a criterion for IRT measurements. External wall surface temperature strongly depended on wall assembly, thermal properties of materials and solar irradiation. Tzifa et al. [2014], Albatici et al. [2015] and Nardi et al. [2015] analyzed the influence of variables such as wind speed, outer and inner air temperatures and external wall surface temperature on the accuracy of U-values in steady-state conditions. Errors depended on the thermal mass and on the exposure of the wall, while wind speed was negligible for heavy walls. In addition, Albatici et al. [2015] concluded that a deviation of 50% in the determination of outer air temperature and wall surface temperature could lead to deviations from 50% (heavy walls) up to 350% (light walls) when U-values were measured by IRT. This was attributed to the use of different measuring equipment (an IR camera versus a thermo hygrometer) for low temperature values (0ºC). In this case, tests were performed in an experimental building designed for the research with five wall types.

Far fewer studies have been undertaken on quantitative internal IRT. Fokaides et al. [2011] drew up a sensitivity analysis, focused on the parameters required to determine the wall surface temperature with an IR camera. Results showed that the most sensitive parameters were the reflected ambient temperature and the assumed emissivity of the wall surface. For instance, a deviation of 1ºC in the determination of the reflected ambient temperature might lead to an error of up to 10% in the wall surface temperature.

Consequently, this might convert into a deviation of 100% in the determination of U-value [Fokaides et al., 2011]. Nardi et al. [2016] analyzed the four approaches proposed in the last few years [Madding et al., 2008; Fokaides et al., 2011; Dall'O et al., 2013; Albatici et al., 2015] in a single sample by guarded hot box. Measured U-values were plotted against the temperature difference, the reflected ambient temperature and the outdoor temperature difference. Outcomes showed better estimations of thermal transmittances for lower reflected ambient temperatures when the temperature difference increased.

As mentioned above, some authors highlighted the role of walls' thermal mass on the accuracy of measured thermal transmittances for $10 < \Delta T < 15$ºC. However, their studies were conducted on laboratories or experimental rooms using quantitative external IRT, HFM and simulation among other techniques [Albatici et al., 2010; Dall'O et al., 2013; Lehman et al., 2013; Tzifa et al., 2014; Albatici et al., 2015; Nardi et al., 2015]. U-value uncertainties provided by HFM depend on the measurement conditions that are registered, the building envelope (light or heavy wall), the data analysis (average method, black box method, LORD, among others) and the HFM' equipment [Cesaratto et al., 2013; Albatici et al., 2015; Ficco et al., 2015]. In accordance with research carried out by Rabadiya et al. [2012], the HFM can only measure a local point on the wall, and consequently it does not provide accurate results for non-homogeneous building elements. Regarding quantitative internal IRT, the influence of thermophysical properties on the accuracy of the method has not been addressed in the literature. In terms of thermal behavior of the façade, European regulation UNE-EN ISO 13786:2011 [International Organization for Standardization, 2011] introduced several thermal parameters for building envelopes (in addition to thermal transmittance), as well as their calculation procedures. Nevertheless, most are transient parameters that can be used to describe the dynamic behavior of the elements [Rossi et al., 2014]. They include thermal time shift, thermal decrement factor and periodic thermal transmittance. The only non-transient thermal parameters that might explain different accuracy values in heavy multi-leaf walls under the same operating conditions are the heat capacity per unit of area and the thermal transmittance. Normally, the effects of thermal inertia and heat capacity per unit of area (kappa value) are not considered, because data are acquired by instantaneous measurements [Nardi et al., 2016].

1.3.2 Execution of the method: data collection and post-processing

Most of the aforementioned methods present some kind of regulation or guideline concerning the main requirements and procedures to perform (i.e. guarded hot box: ASTM C177-13 [American Society for Testing and Materials, 2013], ASTM C1363-11 [American Society for Testing and Materials, 2011] and UNE-EN ISO 8990:1997 [International Organization for Standardization, 1997]; heat flux meter: ISO 9869:2014 [International Organization for Standardization, 2014]; qualitative IRT: ISO 18434-1:2008 [International Organization for Standardization, 2008], EN 13187:1998 [International Organization for Standardization, 1998] and RESNET Interim Guideline for Thermographic Inspections of Buildings

[Residential Energy Services Network, 2010]). However, a gap in the standardization of quantitative IRT for in-situ building diagnostics still needs to be filled. This aspect directly leads to a lack of measurement pattern, which can affect how the method is applied by practitioners, energy auditors or other stakeholders within the construction industry field. Implementation of quantitative IRT encompasses aspects relating to operating conditions (i.e. outdoor air temperature), thermophysical properties (i.e. kappa value or also called heat capacity per unit of area) and technical conditions (i.e. test duration and data acquisition interval) [Balaras et al., 2002; Datcu et al., 2005; Charlier, 2007; Albatici et al., 2010; Dall'O et al., 2013; Lehman et al., 2013; Taylor et al., 2013; Van De Vijver et al., 2014; O'Grady et al., 2017; Tejedor et al., 2017; Lucchi, 2018]. In previous studies of other techniques conducted in laboratories or experimental rooms, the first two aspects might be considered a source of discrepancy in the determination of the measured U-value [Lehman et al., 2013; Albatici et al., 2015; Nardi et al., 2016; Lucchi, 2018]. In the case of real built environments, the influence of the operating conditions and non-transient thermophysical properties of the wall was recently analyzed regarding to the accuracy of quantitative internal IRT for $\Delta T<10$ºC [Tejedor et al., 2018]. Such temperature gradient had been considered a limitation for the method [Vavilov, 2010; Lucchi, 2018].

Focusing on the technical conditions, some researchers underlined the difficulties of the use of quantitative IRT tests with a short sampling duration [Hoyano et al., 1999; Fokaides et al., 2011; Dall'O et al., 2013; Lucchi, 2018; Marshall et al., 2018; Nardi et al., 2018]. Kisilewicz et al. [2010] stated that data recorded by an IR camera should be collected for a sufficiently long period (an integer multiple of 24 hours) to determine the thermal resistance with reliable results, avoiding the fluctuations of both temperature and heat flows. Carbonez et al. [2014] considered that the IRT instantaneous measurements only provided a single value in time and consequently, both the applicability and accuracy of the method were limited. Nevertheless, Nardi et al. [2016] performed tests on a specimen wall of a guarded hot box using HFM and quantitative IRT in a laboratory, gathering instantaneous U-value measurements under stationary conditions and a period lower than 30 minutes.

Along this line, a thorough literature review has shown the use of different test durations and data acquisition intervals, which might also lead to a discrepancy in the assessment of in-situ U-values. The minimum test duration for the quantitative IRT method was set at 2-3 hours under stationary conditions [Albatici et al., 2010; Fokaides et al., 2011; Nardi et al., 2014; Taylor et al., 2014; Tejedor et al., 2017]. Regarding the sampling frequency, a random criterion was detected for the HFM and quantitative IRT [Bienvenido-Huertas et al., 2018]. Fokaides et al. [2011] measured the surface temperature every 20 minutes for 3 hours and the U-value resulted from the average calculation of the 10 measurements for each building element. Marinetti et al. [2012] took 30 thermograms with a sampling interval of 10 seconds. Dall'O et al. [2013] established a data acquisition interval of about 15 minutes, but only some sub-periods were suitable for the measurement. Lehmann et al. [2013] selected a sequence of single thermograms taken

at 5 minute intervals. Porras – Amores et al. [2013] recorded images every 10 seconds and temperature readings every 1 second. De Freitas et al. [2014] carried out 6 thermograms for each sunny day and at different sampling intervals (3h, 4h, 1h, 1h, 5h). Fox et al. [2015] captured images every 20 to 30 minutes. Tejedor et al. [2017] and Tejedor et al. [2018] configured all the measuring equipment with a data acquisition interval of 1 minute, recording from 120 to 180 thermograms as the maximum. Bienvenido – Huertas et al. [2018] proposed a sampling period of 15 minutes to make the subsequent data analysis easier.

1.4 Implications and justification of the thesis

The dissertation starts with a literature review to contextualize the current state of research related to the energy performance gap in buildings. This has allowed detecting the necessity of a building diagnosis testing that provides reliable results of the thermal build quality of façades with a short execution time in comparison with the existing non-invasive measurement techniques (i.e. heat flux meter –HFM-). The findings have also suggested that quantitative infrared thermography (IRT) might fulfil the requirement aforementioned, although this method is not still consolidated.

To select where it would be more suitable to conduct the tests, from inside or outside the building, the main approaches of the last ten years were analysed. According to the limitations of the external thermography, it was decided to develop a quantitative internal IRT method for determining in-situ measured U-values. UNE-EN ISO 6946:2012 [International Organization for Standardization, 2012] and ISO 9869:2014 [International Organization for Standardization, 2014] recommendations should be used as references for the test conditions and data analysis, despite of corresponding to the HFM.

The literature review also highlighted the role of operating conditions (i.e. ΔT) and thermophysical properties (i.e. heat capacity per unit of area) on the accuracy of measured thermal transmittances. Previous studies showed that tests must be executed under a temperature gradient of 10-15ºC. However, some researchers considered that such temperature difference was a limitation for the method [Vavilov et al.,2010; and Lucchi, 2018] and it could be possible to measure from 7 to 16ºC [Tejedor et al., 2017]. In fact, most of sensibility analysis to estimate the influence of both aforementioned aspects were conducted on laboratories or experimental rooms by means of simulation, guarded hot box, quantitative external IRT, among others. Taking into account the aspects exposed above, it might be interesting to explore the limits of the method from inside the building and to observe whether heat capacity per unit of area should be included as a source of discrepancy when quantitative internal IRT is implemented in real built environments, especially unoccupied buildings where ΔT is <10ºC.

Concerning the technical conditions, some researchers underlined the difficulties of the use of quantitative IRT tests with a short sampling duration (<3 hours). Indeed, it was detected a lack of measurement pattern for quantitative IRT (external and internal). For this reason, a data-processing method should be required for stopping the test when the value of the thermal transmittance is reliable.

As seen, this research might contribute: (i) to avoid mistakes in relation to operating conditions, if this building diagnostics technique is used as a tool for energy audits; (ii) to simplify the data analysis, estimating a minor sampling duration to the assumed currently. Consequently, this research might help to enhance the execution of the refurbishment process in existing buildings that are expected to have shortcomings in 2050. As regards new building façades, the method might allow to check them according to their design parameters.

Chapter 2: Objectives and research methodology

This chapter outlines the purpose, aim and objectives of this research, formulated from the discussion presented in Chapter 1, sets out the scope of the work and summarizes the methodology implemented with its limitations. Additionally, it describes the structure of the document.

2.1 Purpose, aim and objectives

The research conducted within this thesis pretends to determine quantitatively the thermal behaviour of building envelopes, helping to promote a reduction of the energy performance gap and increasing the European renovation rate in mid-term. As shown in the literature review, developing a new proposal of method based on quantitative internal IRT is a challenging task. The method should allow measuring accurately the thermal resistance or transmittance of a wall from inside the building, using a passive approach. The method should also be suitable for heavy walls, assuming one-dimensional and horizontal heat flux under steady-state conditions through the building façade. According to this, specific objectives of this dissertation were the following:

- To identify the contributory factors (CF) which may cause the Energy Performance Gap (EPG)
- To identify the existing measurement techniques for determining U-values
- To propose a quantitative internal IRT method for the in-situ measurement of the current thermal transmittance of building envelopes, achieving the minimum deviation between notional and measured U-values
- To enhance the applicability range of techniques based on quantitative IRT in the construction industry field

2.2 Overview of the research methodology and limitations of the thesis

The research methodology used in this thesis (Figure 2) includes the main steps to achieve the objectives exposed previously. More specific employed methodologies were fully described in each chapter in accordance with the aspect to be analysed.

As seen above, the lack of robustness of the current tools and the underestimation of the thermal behaviour of façades during the entire building life cycle (design, construction and operation stages) might contribute to the energy performance gap. Therefore, the extensive literature review allowed detecting the necessity of developing a quantitative internal IRT method as a building diagnosis tool as well as defining its main features.

For evaluating the feasibility of the proposed method, Thermal Engineering Laboratory of ETSEIB (UPC) was used to perform the preliminary studies and calibration tests with two samples (single-leaf and multi-leaf composite) on a thermal house with electronic regulation. For the data analyses, average method was applied. Dynamic method might also be used in accordance to standard ISO 9869-1:2014 [International Organization for Standardization, 2014]. However, this could not be applicable for data obtained from thermography, because the data acquisition interval was not the same all time in the first step of the development of the method. Thus, a more advanced software was required for next research steps. FLIR TOOLS+ [FLIR Systems, 2015] was recommended, since it allows setting a fixed sampling frequency if IR camera is connected with the computer during the monitoring process of the sample.

In order to extend and validate this approach, and considering the aspects of the previous study, several measurement campaigns were developed in two typical Spanish wall typologies from different construction periods. This second validation process allowed: (i) defining test conditions for real built environments; (ii) selecting the measuring equipment; (iii) establishing data acquisition and data post-processing in the case of buildings; (iv) defining how to determine the theoretical U-value and its deviation with respect to the measured value; (v) determining the combined standard uncertainty associated with the measuring equipment. Having applied the numerical model to calculate the measured U-value, an in-depth comparative analysis was carried out in order to quantify the influence of tabulated values shown by the regulations rather than those obtained by the proposed method.

To enhance the applicability range of techniques based on quantitative IRT in the construction industry field, it is needed to assess three groups of causal factors that might influence on the determination of in-situ measured U-values: (i) operating conditions; (ii) thermophysical properties; (iii) technical conditions. In this way, it might be established a measurement pattern. Taking into account these aspects, three steps were conducted. The details are briefly summarized below.

- The first step was focused on assessing the most influential operating conditions on the measured U-values. An experimental room with a heavy single-leaf wall was tested under a wide temperature difference range ($3.80ºC < \Delta T < 20.60ºC$). Input data of each temperature difference range was statistically analysed through a Pearson's parametric correlation with SPSS Software. To corroborate these gathered results, temperature differences (ΔT) were sorted and plotted from lowest to highest. In this way, it could be observed the evolution of the input data for the numerical model (T_{IN}, T_{OUT}, T_{WALL} and T_{REF}) and the adjustment of the measured U-value when ΔT increased. In addition, it could be established the optimum temperature difference range among other aspects.

- The second step was based on evaluating the impact of non-transient thermophysical properties. Quantitative internal IRT measurements were conducted on four real unoccupied residential buildings with heavy multi-leaf walls (without electric and heating system in operation). After determining the equation to calculate the heat capacity per unit of area (also referred to as the kappa value) in accordance with the literature, the errors of the measurements of each façade were plotted against the measured U-values and the kappa values, in order to set a relationship among the parameters.

- The third step consisted of analysing if the deviation between theoretical and measured U-values drew a trend throughout the test, obtaining more accuracy for greater test durations. Having observed the literature review, a common criterion for stopping the quantitative internal IRT test has not yet been set when the trustworthiness of the U-value is enough. Hence, this study proposed a data-processing method where the quantitative IRT measurements were assumed as a stochastic process for $N \geq 30$. To assess if the in-situ measured U-values might be a constant signal plus noise, regardless the test duration, the ACF plot and the CP were used. As regards the study of variability between instantaneous U-values of each time series for all walls, the following parameters were calculated: the mean, the SD (or σ), the CV and the 95% confidence intervals. Finally, a validation process based on MATLAB was computed.

Concerning the main limitations of this dissertation, these were established in relation to the season of the year in which the proposed method was implemented and validated, and the type of building façade that was investigated.

- All measurement campaigns were developed during the winter. The numerical model has not still been validated in Summer, since a cooler unit system is required inside the buildings. In addition, most existing units of air conditioner provide a non-stationary regime as well as a non-homogeneity of heat flux and temperature on the material to be assessed. In other words, cold air current peaks might be generated when the inner air temperature is over the set point temperature and consequently, a fluctuation of the internal parameters might be given.

- Standardized methods (i.e. HFM) were not applied to validate the results, since all tests were performed on heavy façades. Some researchers demonstrated a low discrepancy (1.3-2.6%) between the measured U-values obtained by HFM and the IRT for heavy walls, in contrast to light walls that reached discrepancies of 47.6% [Nardi et al., 2015; O'Grady et al., 2017b]. However, light walls (i.e. wood-frame insulated walls or walls with a heat capacity per unit of area lower than 150 $kJ/m^2 \cdot K$) are not erected generally in Spain.

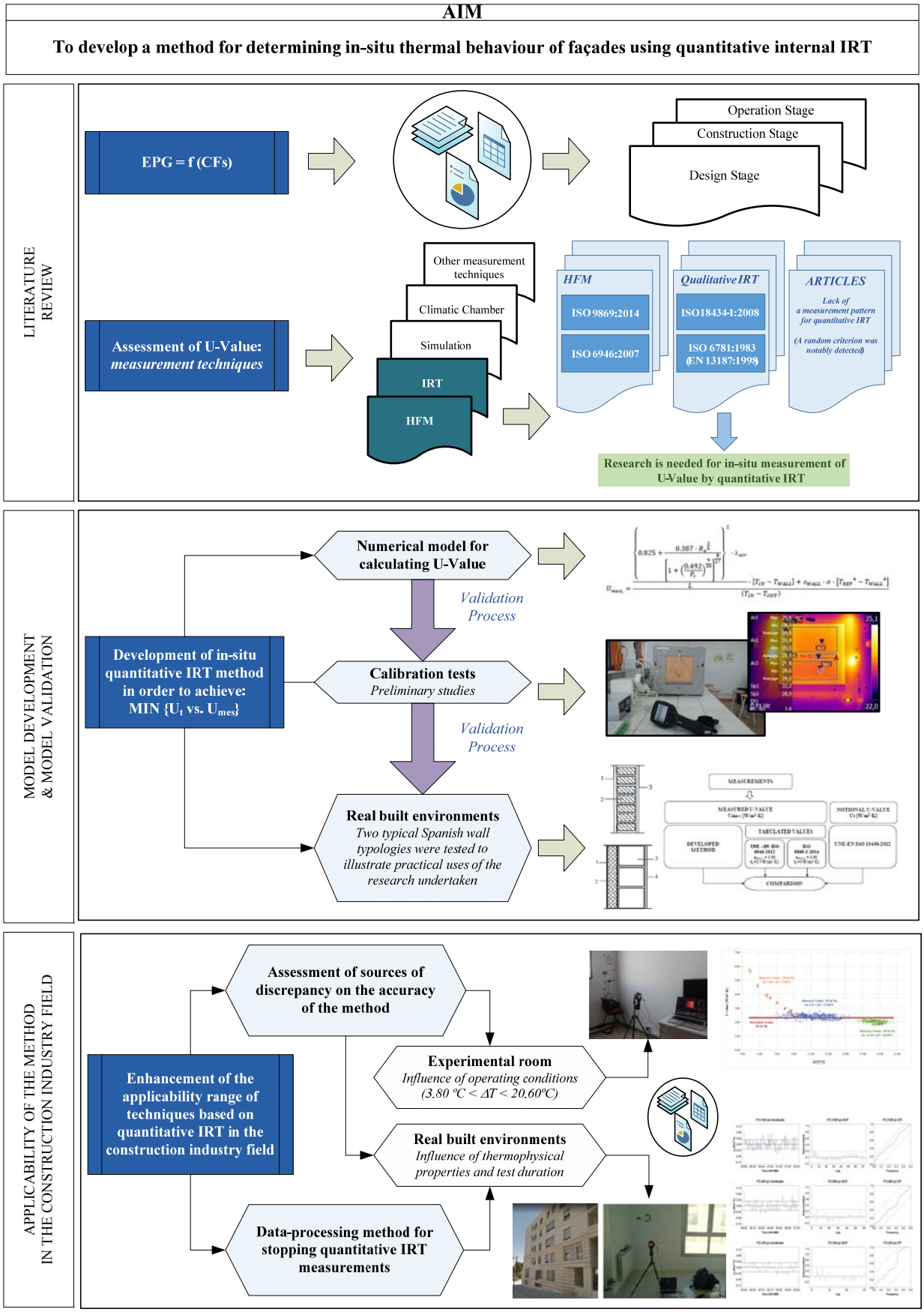

Figure 2. Overview of the methodology

2.3 Structure of the document

This PhD thesis consists of eight chapters, which are described below. Table 1 shows the structure of the document, highlighting the chapters and publications that have derived from each specific and complementary objective.

Chapter 1 presents a critical literature review about the energy performance gap related to the importance of building refurbishment, current measurement techniques for determining the thermal performance of façades and the shortcomings of the quantitative infrared thermography (sources of discrepancy on the measured U-values and execution of the method). Having outlined the main barriers to accurately in situ measure the thermophysical property aforementioned, this chapter supports the justification of the research undertaken within this thesis.

Chapter 2 presents the purpose, the main aim and specific objectives of the research project raised from the results of the previous chapter. Furthermore, it sets out the limitations and delimitations of the work before describing the research methodology and remaining structure of this dissertation.

After presenting the state of the art and the research methodology (Chapters 1 and 2), there are two chapters devoted to the development and validation of the proposed method and four chapters that are shown as a compilation of different studies that derive from the implementation of the method in an experimental room and several real built environments with heavy walls.

Chapter 3 proposes a quantitative internal IRT method for determining the thermal transmittance of building envelopes with heavy multi-leaf walls, considering the following aspects: test conditions that should be taken into account, how data acquisition and post-processing should be performed, and the determination of instantaneous and average measured U-values.

Chapter 4 shows the validation process of the proposed method through case studies, including a comparative analysis between theoretical and measured U-values. In addition, for each investigated building, such thermal parameter has also been determined using tabulated values in accordance to the current regulations, in order to check their influence on the measured U-values in comparison with those provided by the proposed method.

Having identified which equations leads to a better adjustment of the numerical model to the real built environment, it is necessary to know how to improve the shortcomings of this technique with the aim of introducing it in the market of the construction industry field. Chapter 5 is focused on assessing the influence of operating conditions on the results provided by the method. Chapter 6 evaluates the role of the thermophysical properties in the accuracy of in-situ measured U-values. Chapter 7 is based on the analysis

of the execution of the IRT technique and post-processing of the data, since a standardized test duration has not been established yet. The purpose is to define a common criterion based on U-value time series analysis for stopping the test, being possible to reduce the current sampling duration.

Chapter 8 presents the conclusions and summarizes the key findings of the dissertation, how the project has contributed to knowledge and practice regarding the stated objectives, and shows suitable areas for further research. During the research undertaken, some aspects were raised although they could not be addressed.

2.4 Related Publications

At the examination date, two works carried out into the scope of this thesis were published. The relationship among the objectives, the tasks and the related publications is represented in Table 1. With respect to the main characteristics of each paper, these are shown as follows.

Journal Paper I – Published

Tejedor, B; Casals, M; Gangolells, M; Roca, X. *Quantitative internal infrared thermography for determining in-situ thermal behaviour of façades.* Energy and Buildings 151 (2017) 187-197 < DOI: 10.1016/j.enbuild.2017.06.040>

- Area: Construction and Building Technology
- Quartile: Q1
- JCR Impact factor: 4.457 (2017)
- Number of cites: 10 (Scopus), 6 (Researchgate), 10 (Mendeley), 11 (CrossRef)

Journal Paper II – Published

Tejedor, B; Casals, M; Gangolells, M. *Assessing the influence of operating conditions and thermophysical properties on the accuracy of in-situ measured U-values using quantitative internal* infrared *thermography.* Energy and Buildings 171 (2018) 64-75 < DOI: 10.1016/j.enbuild.2018.04.011>

- Area: Construction and Building Technology
- Quartile: Q1
- JCR Impact factor: 4.457 (2017)
- Number of cites: 2 (Scopus), 1 (Researchgate), -- (Mendeley), 2 (CrossRef)

Table 1. PhD overview and related publications

RESEARCH AIM **To develop a method for determining in-situ thermal behaviour of façades using quantitative internal IRT**				
	Specific Objectives	***Tasks***	***Chapter***	***Publications***
LITERATURE REVIEW	S.O.1. To identify the contributory factors which may cause the Energy Performance Gap	T1. To classify the contributory factors of the Energy Performance Gap in function of the building life cycle	Chapter 1	Journal Paper 1
	S.O.2. To identify and examine the measurement techniques for determining U-values	T2. To focus the research on non-invasive building diagnostics techniques for in-situ U-values	Chapter 1	Journal Paper 1
MODEL DEVELOPMENT & MODEL VALIDATION	S.O.3. To propose a quantitative internal IRT method for the in-situ measurement of the current thermal transmittance of building envelopes, achieving the minimum deviation between theoretical and measured U-value	T3. To develop an accurate numerical model to measure in-situ U-values of façades using quantitative internal IRT	Chapter 3	Journal Paper 1
		T4. To validate the method in the Thermal Engineering Laboratory through calibration tests (preliminary studies)	Chapter 4	---
		T5. To validate the method in real built environments through two typical Spanish wall typologies from different periods	Chapter 4	Journal Paper 1
APPLICABILIY OF THE METHOD IN THE CONSTRUCTION INDUSTRY FIELD	S.O.4. To enhance the applicability range of techniques based on quantitative internal IRT in the construction industry field	T6. To analyse the most influential operating conditions on measured U-values, performing the proposed method on an experimental room with a heating unit to be configured	Chapter 5	Journal Paper 2
		T7. To analyse the influence of thermophysical properties on measured U-values performing the proposed method on several real built environments	Chapter 6	Journal Paper 2
		T8. To develop a data-processing method for stopping the test (< 3h)	Chapter 7	---

Chapter 3: Development of a quantitative internal IRT method

The proposed method is characterized by determining the in-situ thermal transmittance of a wall from inside the building envelope using a passive approach. This chapter describes the development of this NDT which is comprised of five steps.

In the step 1, the test conditions were specified, taking as reference the boundary conditions stated by other researchers in previous studies and the own experience at Thermal Engineering Laboratory with the calibration tests of the numerical model and the assessed existing buildings. The most relevant test conditions are related to: (i) the use of qualitative IRT for detecting anomalies in the areas to be analysed; (ii) weather limitations, since some parameters can be act as stimulus for the construction element (i.e. wind speed, rain, sun); (iii) orientation of the façade to be tested, preferably northern wall; (iv) temperature difference across the building envelope and optimum periods of the day to achieve it; (v) internal climatic conditions to ensure a stationary regime and homogenous heat flux and temperature on the material.

The second and third steps were based on establishing the minimum requirements to select the measuring equipment and their respective functions in the test, following the recommendations presented throughout the literature review and considering the aspects revealed by the tests performed in laboratory and existing buildings. In addition, a sketch of the top and front views of the position of the measuring equipment in relation to the wall were drawn up, to show the main aspects that should be taken into account during the continuous monitoring and recording of data.

The fourth and fifth steps consisted of developing the numerical model to calculate the instantaneous and average measured U-values from inside the building, assuming one-dimensional and horizontal heat flux under steady-state conditions through the building envelope.

It should be underlined that Journal Paper I [Tejedor et al., 2017] describes extensively the proposed method to determine in-situ measured thermal transmittances of façades by quantitative internal IRT. Journal Paper II [Tejedor et al., 2018] refines the numerical model for experimental rooms or unoccupied buildings when inner air temperature is found to be within the range 0-15ºC or 15-25ºC, since some tabulated values related to the properties of the airflow could be different in function of the aforementioned input parameter.

3.1 Definition of test conditions

Qualitative IRT tests are defined by EN 13187:1998 [International Organization for Standardization, 1998] and the RESNET Interim Guidelines for Thermographic Inspections of Buildings [Residential Energy Services Network, 2010]. Previous researchers have established boundary conditions for quantitative IRT tests [Grinzato et al., 1998; Hoyano et al., 1999; Martín-Ocaña et al., 2004; Aelenei et al., 2008; Albatici et al., 2010; Desogus et al., 2011; Fokaides et al., 2011; Asdrubali et al., 2012; Bagavathiappan et al., 2013; Byrne et al., 2013; Cesaratto et al., 2013; Dall'O et al., 2013; Ferrari et al., 2013; Kumar et al., 2013; Lehman et al., 2013; Ahmad et al., 2014; Asdrubali et al., 2014; Biddulph et al., 2014; Bisegna et al., 2014; De Freitas et al., 2014; Latif et al., 2014; Kylili et al., 2014; Nardi et al., 2014; Pisello et al., 2014; Rossi et al., 2014; Stazi et al., 2014; Taylor et al., 2014; Vereecken et al., 2014; Albatici et al., 2015; Ficco et al., 2015; Fox et al., 2015; Pérez-Bella et al., 2015; Maroy et al., 2017]. The most relevant are detailed below.

Tests should be performed under low values of wind speed. The recommendation is 0.2 to 1.0 m/s. This parameter can lead to greater thermal dispersion of convective factors.

Tests should be conducted on the northern façades of buildings and preferably in the early morning before sunrise and/or in the evening after sunset, to avoid solar radiation. Otherwise, the IRT survey would be conducted on transient regime. Incident solar radiation can be considered a kind of thermal stimulus that may lead to a time lag of a few hours. The wall temperature may tend to increase affecting the evaporation process in materials. In addition, incident solar radiation depends on other parameters and may not be easily predictable.

Tests must be carried out with a temperature difference (ΔT) across the building façade of at least 10-15ºC, to allow measurable heat exchange through the element. This statement was widely adopted by the majority of researchers. Nevertheless, Tejedor et al. [2017] and Tejedor et al. [2018] demonstrated that it is possible to execute quantitative internal IRT measurements from 7 to 16ºC with the proposed method. Another weather conditions such as humidity, rain and snow should be avoided 24-48 hours prior to the tests, since they can reduce the measured temperature values.

Tests should be carried out in areas of the wall without anomalies (i.e. moisture, thermal bridges and cold spots, among others). For this reason and before the on-site test, a qualitative infrared thermography inspection must be performed. It should be pointed out that the influence of the weather (wind, sun, rain, sky conditions, etc) may last for 2-6 hours, depending on the façades.

Some additional test conditions were determined from the developed research. Tests should avoid a non-stationary regime as well as a non-homogeneity of heat flux and temperature on the material. Consequently, special attention must be paid to the type of building façade, the external conditions or the

internal climatic conditions (i.e. type of heating system). Firstly, heated adjacent walls may influence the thermal behaviour of the sample that is being tested, especially in single-leaf building façades. Wall temperature in the corners tends to be higher than the rest of the wall and, consequently, U-value uncertainty may be increased. Secondly, outdoor air temperatures remain more constant during some periods of the day. The tests should be undertaken at the start of the day, to ensure an optimum temperature difference (ΔT) without peaks. Thirdly, any air current peak generated when the inner air temperature is under the set point temperature may lead to a fluctuation in internal parameters.

3.2 Selection of the measuring equipment

An IR camera, a reflector and a blackbody are needed to measure quantitatively on-site U-values by means of IRT. Thermocouples with a data logger, or a thermohygrometer, are required to monitor environmental conditions.

Several researchers have specified in their studies that the minimum requirements for an IR camera are related to: the spectral range, the spatial resolution, the temperature range, the thermal sensitivity, the frame rate and the angle of tilt. Taking into account that bodies at ambient temperature emit predominantly at 7-13 μm (spectral range), the IR camera should be selected for long wave length band [Astarita et al., 2000; Avdelidis et al., 2003; Fokaides et al., 2011; Asdrubali et al., 2012; Albatici et al., 2013; Bagavathiappan et al., 2013; Porras-Amores et al., 2013; Bisegna et al., 2014; Fox et al., 2014; De Freitas et al., 2014; Kylili et al., 2014]. The spatial resolution, also known as the Instantaneous Field of View (IFOV), is the ability of the camera to distinguish between two objects within the field of view (FOV). In other words, it is the smallest detail within the FOV that can be detected or seen at a set distance. Along this line, Bagavathiappan et al. [2013] and Fox et al. [2014] stated that FOV depends on the object to camera distance, the lens systems and the detector size. Its value represented in mrad corresponds to the size of the visible point in millimetres of a pixel at a distance of 1 metre. For building diagnosis, FOV is described in horizontal degrees by vertical degrees, 25º x 19º, and IFOV is established as 1.36 mrad. Furthermore, Bagavathiappan et al. [2013] mentioned that the temperature range is the minimum and maximum temperature values, typically -20ºC to 500ºC-; the thermal sensitivity should be selected as 0.05ºC for uncooled cameras and 0.01ºC for cooled cameras; and the number of frames acquired by the IR camera per second (frame rate) is normally set at 50Hz.

As shown in Figure 3, to avoid any reflection of the thermographer in the resulting images, the angle of tilt should be a minimum of 5º from the thermographer to the target and a maximum of 50º –from the horizontal- [Fox et al., 2014; Kylili et al., 2014].

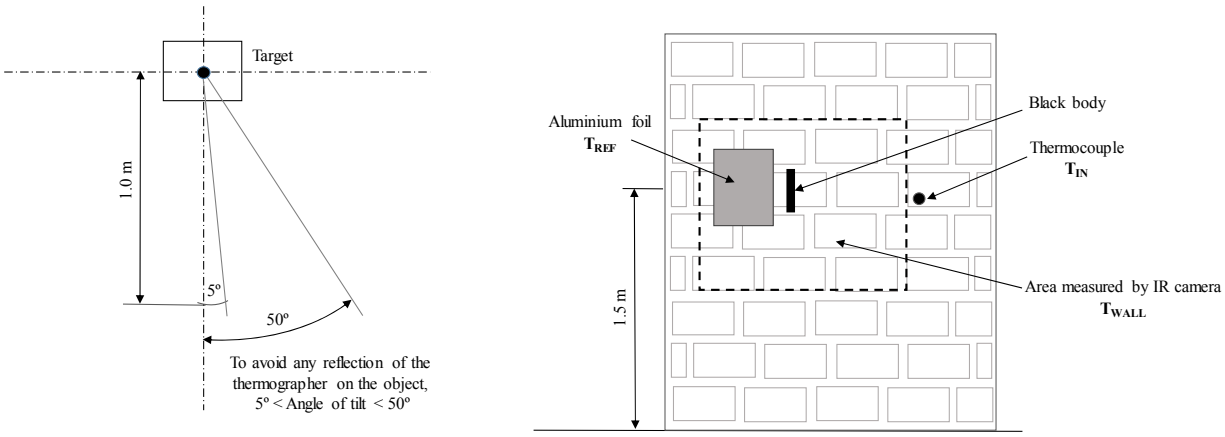

Figure 3. Top and front view of the position of the measuring equipment in relation to the wall

Before making the measurements, the IR camera should be calibrated for the wall. In other words, the reflected ambient temperature (T_{REF}) as well as the wall surface emissivity are required to compensate errors of reading with the IR camera. These parameters allow reliable surface temperature values to be obtained in the area of known emissivity during the post–processing of each thermogram [Albatici et al., 2010; Fokaides et al., 2011; Porras –Amores et al., 2013; Ohlsson et al., 2014; Albatici et al., 2015; Danielski and Fröling, 2015].

The average reading of T_{REF} represents the average temperature of the surroundings, considering the different reflection indexes. To determine this parameter, a crinkled piece of aluminium foil fixed on the surface should be used as a reflector or substitute for Lambert's radiator [Fokaides et al., 2011; Asdrubali et al., 2012; Dall'O et al., 2013; Porras –Amores et al., 2013; Nardi et al., 2014; Ohlsson et al., 2014; Danielski and Fröling, 2015; Fox et al., 2015; Nardi et al., 2016]. In order to avoid uncontrolled reflection indexes, the wall under measurement needs to be free of any object [Fokaides et al., 2011]. A blackbody is needed to measure the wall surface emissivity. In thermal radiation theory, a blackbody is considered a hypothetical object that absorbs all incident radiation and radiates a continuous spectrum, according to Planck's Law and the Stefan-Boltzmann Law. In practice, a blackbody can be a black tape, a curved plastic hosepipe (with a hole 1cm^2 wide) or a blackbody simulator fixed to the target [Astarita et al., 2000; Avdelidis et al., 2003; Fokaides et al., 2011; Bagavathiappan et al., 2013; Ohlsson et al., 2014; Danielski and Fröling, 2015]. Several blackbodies were tested in previous analysis of this PhD thesis (i.e. calibration tests of the numerical model at the Thermal Engineering Laboratory of ETSEIB –UPC-). Some of these elements were the following: a smoked metallic sheet using a candle, a tinted white tape with a black pen and a black tape. The results revealed that the smoked metallic sheet (Figure 4) did not achieved the surface temperature of the sample. Hence, the emissivity of the target could not be determined. Subsequently, a matt tinted white tape and a matt black tape were also used. The fact of being matt implies having more cavities to capture further light at microscopic level compared to bright tapes. Their emissivities were found to be around the same order. However, the black tape was the most appropriate, because the temperature of the blackbody was equal to the surface temperature of the samples.

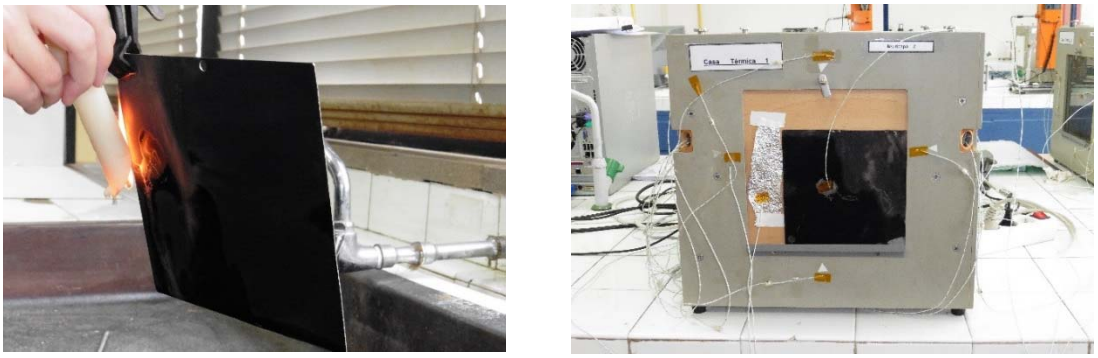

Figure 4. Images of the blackbody simulated using a smoked metallic sheet

Concerning the monitoring of environmental conditions, it should be pointed out that some uncertainties may arise in the measuring chain due to the temperature sensor and its data logger. For this reason, the type of sensor (thermocouple type K or thermistor), the position of the sensor, sensor linearity and the sensitivity, sensor drift and calibration of the element should be taken into account. Type K thermocouples with a resolution of 0.1ºC and an accuracy of ± 0.4% + 1ºC are preferred. The data logger must enable measurements within the temperature range 0 to 50ºC, and a relative humidity below 85%. In addition, the data acquisition interval should be 1 second to 3600 seconds. Nevertheless, low sampling frequency plays an important role in the autonomy of the batteries of the data logger.

In all studies conducted on this thesis, operating conditions referring to environmental parameters (T_{IN} and T_{OUT}) were measured and recorded by data loggers with type K thermocouples (TF-500, PCE –T390, PCE Iberica SL) that present a resolution of 0.1ºC and accuracy of ± 0.4% +0.5ºC. In contrast, parameters relating to the building envelope (ε_{WALL}, T_{REF} and T_{WALL}) were monitored using a reflector (crinkled piece of aluminum foil with dimensions 0.20 x 0.15 m), a blackbody (black tape with dimensions 0.01 x 0.05 m and an emissivity of 0.95) and an IR camera of long wavelength band (FLIR60bx with an IR resolution of 320 x 240 pixels and an accuracy of ±2 ºC or 2% reading at ambient temperature).

3.3 Data acquisition and post-processing

The IR camera should be positioned on a tripod perpendicular to the wall at a distance of 1.5 metres and an angle of 15º, to avoid its own reflection on the building element. This distance is enough to analyse a wide wall area characteristic of the thermal behaviour of the building façade, including the reflector foil.

Measurements should be performed and recorded over a period of 2-3 hours, with a data acquisition interval of 1 minute by the IR camera and FLIR TOOLS+ software [FLIR Systems, 2015]. Therefore, each test involves the analysis of a sequential video with 121 to 181 thermograms. All data loggers are configured to collect measurements from temperature sensors with the same data acquisition interval as the IR camera

(1 minute). Surrounding environmental conditions are also continuously monitored and recorded during the on-site test duration by data loggers and thermocouples. Post-processing of thermograms is carried out with the software mentioned above. The instantaneous readings of the wall surface temperature (T_{WALL}) and the reflected ambient temperature (T_{REF}) of each thermogram must be considered to determine the measured U-value. The average reflected ambient temperature (T_{REF}) should be measured in an area of the reflector located at 1.5 m above ground level to avoid any reflection of the ground and most of the furniture. In addition, the thermocouple of T_{IN} should be positioned at the same height. As this IRT method is performed inside the building, the height of the walls is around 2.5-3.0 m. Hence, a height of 1.5 m is acceptable to consider an average inner air temperature value, approximately equal to T_{REF}. The wall surface temperature (T_{WALL}) should be calculated by measuring the maximum, minimum and average values of the total area of the building element that is being evaluated (Figure 3).

3.4 Calculation of the measured U-value using the numerical model

In a real built environment, it can be considered that the building envelope is crossed by a one-dimensional horizontal specific heat flux (q) resulting from the processes of convection (q_c) and radiation (q_r) of the inner wall surface and its surroundings, without the influence of any kind of external thermal stimulus and under steady-state conditions. According to this, the instantaneous and average measured thermal transmittances can be expressed by Equations 1 and 2.

$$U_{mes_i} = \frac{\left\{0.825+\frac{0.387\cdot Ra^{\frac{1}{6}}}{\left[1+\left(\frac{0.492}{Pr}\right)^{\frac{9}{16}}\right]^{\frac{8}{27}}}\right\}^2\cdot\lambda_{air}}{L}\cdot[T_{IN}-T_{WALL}]+\varepsilon_{WALL}\cdot\sigma\cdot\left[{T_{REF}}^4-{T_{WALL}}^4\right]}{(T_{IN}-T_{OUT})} \quad (1)$$

$$U_{mes_{avg}} = \frac{\sum_{i=1}^{n}(q_{c_i}+q_{r_i})}{\sum_{i=1}^{n}(T_{IN_i}-T_{OUT_i})} = \frac{\sum_{i=1}^{n} U_{mes_i}}{n} \quad (2)$$

Where $U_{mes\,i}$ [W/ (m^2·K)] is the sum of the instantaneous specific heat fluxes through the building envelope by convection q_c [W/m^2] and radiation q_r [W/m^2], divided by the temperature difference (ΔT) between inside and outside the building [K]. Hence, T_{IN} denotes the inner air temperature [K] and T_{OUT} refers to the outer air temperature [K]. Other parameters in the equations are: the wall surface temperature (T_{WALL}) in [K]; the reflected ambient temperature (T_{REF}) in [K]; the emissivity of the wall (ε_{WALL}); Stefan–Boltzmann's constant (σ); the thermal conductivity of the air (λ_{air}) in [W/m·K]; the height of the wall (L) seen from inside the building in [m]; and the dimensionless parameters Rayleigh (R_a) and Prandtl (P_r) numbers for a laminar flow. Once all instantaneous measured U-values have been determined, the mean is estimated from the total number of thermograms (n) that have been assessed for the test.

As shown in the above equations, the contribution of the conduction heat transfer can be ignored for IRT measurements [Albatici et al., 2010], since the processes seen by IR camera in relation to the wall are only radiation and convection. Regarding the formulation of each term, this is extensively reported in sections 3.4.1. and 3.4.2.

3.4.1 Radiation heat transfer

To estimate the heat transfer through radiation that takes place in the infrared region, the Stefan-Boltzmann Law should be applied. During the cold season, the surroundings radiate energy to a cooler object, such as an inner wall surface, which leads to a net radiation heat loss rate (Equation 3).

$$q_r = \varepsilon_{WALL} \cdot \sigma \cdot \left[{T_{REF}}^4 - {T_{WALL}}^4\right] \quad (3)$$

Where q_r represents the specific heat flux by radiation [W/m^2]; ε_{WALL} is the emissivity coefficient of the object ($0 < \varepsilon < 1$, depending on the type of material and the temperature of the surface); σ is Stefan–Boltzmann's constant with a value of 5.67x10^{-8} [W/m^2 ·K^4]; T_{REF} denotes the reflected ambient temperature [K]; and T_{WALL} is the wall surface temperature from inside the building [K]. In contrast to Fokaides et al. [2011], the equation was not linearized.

Considering all studies carried out in this dissertation, it should be highlighted that the wall emissivity for a gypsum plaster with white paint can be estimated at 0.88.

3.4.2 Convective heat transfer

The heat energy transferred between a surface and a moving fluid at different temperatures is known as convection. Considering natural convection and laminar flow, the heat transfer per unit surface through convection (Equation 4) is known as Newton's Law of Cooling. In the same way as in heat transfer by radiation, the cooler object is the wall to be tested.

$$q_c = h_c \cdot [T_{IN} - T_{WALL}] \quad (4)$$

Where q_c belongs to specific heat flux by convection [W/m^2]; h_c is the convective heat transfer coefficient [W/m^2 ·K]; T_{IN} denotes the air temperature near the target from inside the building [K] and T_{WALL} is the wall surface temperature from inside the building [K].

According to Dall'O et al. [2013], the external convective heat transfer coefficient tabulated in UNE-EN ISO 6946:2012 [International Organization for Standardization, 2012] is a high and precautionary value, since it is used to determine the heat loss during the design stage of the building façade. Therefore, the same assumption could be made in relation to the ISO value for the internal convective heat transfer coefficient.

In base on this, several options were contemplated in function of the calculation procedure for this parameter. Such procedure was classified into dimensional and dimensionless approaches, since the second one is found to be more accurate [Sham et al., 2012]. For the first group, the dimensional equations for laminar and turbulent flow were taken from "ASHRAE 2005-Handbook: Fundamentals" [American Society of Heating, Refrigerating and Air-Conditioning Engineers, 2005]. For the second group, the main expressions were developed using thermal engineering books. Analysing the calibration tests of the preliminary studies at Thermal Engineering Laboratory of the UPC, the measurements were better fit to both a laminar flow and the equation resulting from the dimensionless approach. Hence, the internal convective heat transfer coefficient (h_c) is function of the Nusselt (*Nu*), Rayleigh (*Ra*) and Prandtl (*Pr*) numbers within this research. The Nusselt number (Equation 5) can be estimated as follows:

$$N_U = (h_c \cdot L)/\lambda_{air} \tag{5}$$

As mentioned above, h_c is the convective heat transfer coefficient [W/m^2 ·K], *Nu* is the Nusselt number [dimensionless] and *L* refers to the height of the wall [m] seen from inside the building. λ_{air} is the thermal conductivity of the fluid. Taking into account that the fluid is air, λ_{air} is equal to 0.024 W/m·K for T_{IN}= 0 - 15ºC and 0.025 W/m·K for T_{IN}= 15 - 25ºC. Even so, when the surface consists of a vertical plate such as a wall, the expression that describes the Nusselt number is the following (Equation 6):

$$N_U = \left\{ 0.825 + \frac{0.387 \cdot {R_a}^{1/6}}{\left[1+\left(\frac{0.492}{Pr}\right)^{9/16}\right]^{8/27}} \right\}^2 \tag{6}$$

Where *Ra* and *Pr* are the Rayleigh and Prandtl numbers respectively. The Prandtl number for air is considered to be 0.73 for T_{IN}= 0 - 25ºC. The Rayleigh number (Equation 8), which is the product of Grashof (Equation 7) and Prandtl numbers, should be $10^4 < Ra < 10^{10}$ for a laminar flow. It should be noted that all of these parameters are dimensionless.

$$G_r = \frac{g \cdot \beta \cdot (T_{IN} - T_{WALL}) \cdot L^3}{v^2} \tag{7}$$

$$R_a = G_r \cdot P_r = \frac{g \cdot \beta \cdot (T_{IN} - T_{WALL}) \cdot L^3}{v^2} \cdot P_r \tag{8}$$

The g refers to gravitation (9.8 m/s^2). The β is the volumetric temperature expansion coefficient [1/K], where all fluid properties should be evaluated at the film temperatures, so $\beta=1/T_m$ where $T_m= (T_{IN}+T_{WALL})/2$. The v is the air viscosity with a value of $1.4 \cdot 10^{-5}$ m^2/s for T_{IN}= 0 - 15ºC m^2/s and $1.5 \cdot 10^{-5}$ m^2/s for T_{IN}= 15 - 25ºC.

Concerning the formulation of some tabulated values (i.e. the thermal conductivity of the air, the Prandlt and Rayleigh numbers and the air viscosity), they were taken from several sources [Touloukian et al., 1970; Touloukian et al., 1970b; Keenan et al., 1983; Dixon, 2007; Shert et al., 2007], including those provided by EES Software [F-Chart Software, 2016]. Replacing by the known values, the Rayleigh number (Ra) mainly depends on the inner air temperature [K], the inner wall surface temperature [K] and the height of the wall [m]:

$$R_a = 3.18 \cdot 10^{10} \cdot \beta \cdot (T_{IN} - T_{WALL}) \cdot L^3 \tag{9}$$

From (5) and (6), the convective heat transfer coefficient becomes:

$$h_c = \frac{\left\{0.825 + \frac{0.387 \cdot R_a^{\frac{1}{6}}}{\left[1+\left(\frac{0.492}{Pr}\right)^{\frac{9}{16}}\right]^{\frac{8}{27}}}\right\}^2 \cdot \lambda_{air}}{L} \tag{10}$$

Taking into account the value of the Prandtl number, Equation 10 can be simplified:

$$h_c = (\lambda_{air}/L) \cdot \left\{0.825 + 0.325 \cdot R_a^{\frac{1}{6}}\right\}^2 \tag{11}$$

Chapter 4: Validation of the proposed quantitative internal IRT method

This chapter presents the validation process used in this thesis through two case studies. Having performed the quantitative internal IRT tests, the validation of the method consists of evaluating the accuracy of these measurements through the comparison with the theoretical U-value (U_t). A further comparative analysis is also conducted to check the influence of using tabulated values rather than the proposed method to determine the measured U-values of each building envelope. Finally, the main aspects resulting from the implementation of the method are discussed. It should be pointed out that this study was published in Journal Paper I [Tejedor et al., 2017].

4.1 Framework of the validation process

The validation process of the proposed method is divided into several parts, as shown in Figure 5.

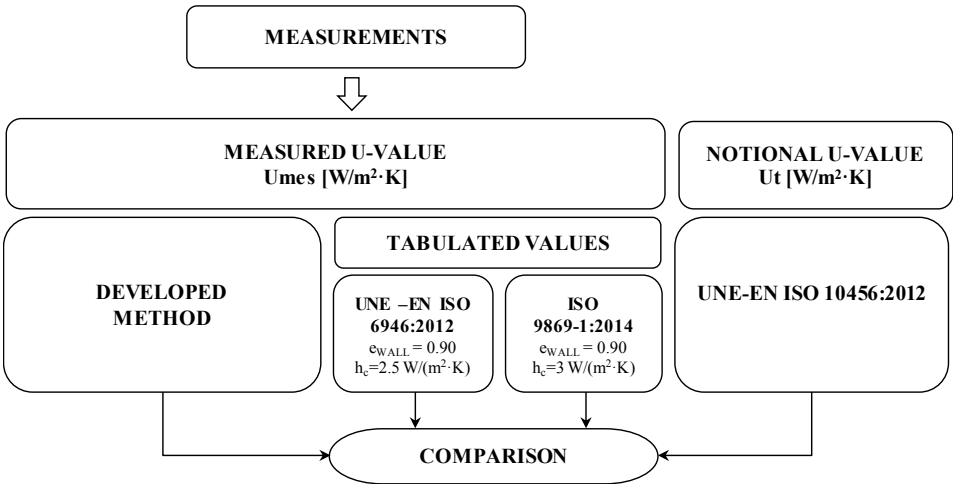

Figure 5. Flowchart of the validation process through case studies

Once all instantaneous and measured U-values have been determined by the quantitative internal IRT, the comparison with the theoretical thermal transmittance (U_t) must be undertaken. According to Ficco et al. [2015], the estimation of the notional U-value of existing buildings can be based on four approaches: (i) using data obtained by historical analysis of the building or analogies with similar buildings using specific technical databases; (ii) using nominal design data; (iii) the actual data obtained by structure identification (sampling or endoscope method); (iv) in-situ measurement using HFM.

In this study, the theoretical thermal transmittance of the building façade (U_t) was estimated for each case study through the nominal design data following the technical data available in the Spanish Technical Building Code [Spain, 2006] and European Standards such as UNE-EN ISO 10456:2012 [International Organization for Standardization, 2012] and UNE-EN ISO 6946:2012 [International Organization for Standardization, 2012]. In particular, UNE-EN ISO 10456:2012 [International Organization for Standardization, 2012] provides the thermal properties for each building material, including thermal conductivity and resistance values in function of the material density or for an interval of densities, to estimate design values [Fokaides et al., 2011; Ficco et al., 2015; Pérez –Bella et al., 2015]. The theoretical thermal transmittance (U_t) for building façades and its respective deviation with the average measured U-value ($\Delta U/U_t$) can be calculated as follows (Equations 12-13):

$$U_t = \frac{1}{R_t} = \frac{1}{R_{Si}+\sum_{i=0}^{n}\frac{\Delta x_i}{\lambda_i}+R_{Se}} = \frac{1}{0.13+\sum_{i=0}^{n}\frac{\Delta x_i}{\lambda_i}+0.04} \quad (12)$$

$$\Delta U/U_t = [(U_{mes_{avg}} - U_t)/U_t] \cdot 100 \quad (13)$$

Where R_t is the theoretical thermal resistance [(m^2·K)/W]; R_{si} and R_{se} denote the theoretical thermal resistance from inside and outside the building respectively [(m^2·K)/W]; Δx_i is the thickness of the layer in [m]; and λ_i is the thermal conductivity of the layer [W/(m^2·K)].

In accordance with ISO/IEC Guide 98-3:2008 [International Organization for Standardization, 2008] and taking into account the accuracy of the measuring equipment (sensors and infrared camera) provided by the manufacturers, the combined standard uncertainty (σU) of all measured parameters can be obtained by Equation 14:

$$(\sigma U_{mes})^2 = \left(\frac{\delta U_{mes}}{\delta T_{IN}}\right)^2 \cdot (\sigma T_{IN})^2 + \left(\frac{\delta U_{mes}}{\delta T_{OUT}}\right)^2 \cdot (\sigma T_{OUT})^2 + \left(\frac{\delta U_{mes}}{\delta T_{WALL}}\right)^2 \cdot (\sigma T_{WALL})^2 + \left(\frac{\delta U_{mes}}{\delta T_{REF}}\right)^2 \cdot (\sigma T_{REF})^2 + \left(\frac{\delta U_{mes}}{\delta \varepsilon_{WALL}}\right)^2 \cdot (\sigma \varepsilon_{WALL})^2 \quad (14)$$

Where σT_{IN} and σT_{OUT} are the uncertainties associated with the environmental indoor and outdoor temperature measuring equipment respectively. σT_{WALL}, σT_{REF} and $\sigma \varepsilon_{WALL}$ are the uncertainties associated with the infrared camera when the wall surface temperature, the reflected ambient temperature and the wall emissivity are measured respectively. Notably, some parameters of the numerical model (N_u –Nusselt number-, β-volumetric temperature expansion coefficient-, R_a –Rayleigh number- and h_c -convective heat transfer coefficient-) in relation to convective heat transfer (q_c) are a function of T_{IN} and T_{WALL}. When tabulated values are used, the procedure should be the same, but it should be considered that h_c is no longer a function of T_{IN} and T_{WALL} to be derived from Equation 1.

Having obtained the deviations and uncertainties of the proposed method for each investigated building, it should be analysed the added value that this non-invasive technique might imply to other approaches. The second part of the validation process is based on another comparative analysis, to assess the influence of using tabulated values of international standards instead of the developed method when the thermal transmittance of walls is estimated. The first standard, UNE-EN ISO 6946:2012 [International Organization for Standardization, 2012], establishes a wall surface emissivity of 0.90 and a convective heat transfer coefficient of h_c=2.5 W/m^2·K. The second standard, ISO 9869-1:2014 [International Organization for Standardization, 2014], notes the same emissivity but h_c=3 W/m^2·K. Hence, considering the instantaneous readings of T_{WALL} and T_{REF} gathered by IRT as well as the readings of the thermocouples in each test, the options to be calculated were the following:

a) U-value with the proposed method.
b) U-value maintaining the measured emissivity and using the tabulated value of h_c from UNE EN-ISO 6946:2012 [ε_{WALL} = 0.88; h_c=2.5 W/m^2·K]
c) U-value maintaining the calculated h_c and using the tabulated value of emissivity from UNE EN-ISO 6946:2012 [h_c from the method; ε_{WALL} = 0.90]
d) U-value with the tabulated values of emissivity and h_c from UNE EN-ISO 6946:2012 [ε_{WALL} = 0.90; h_c=2.5 W/m^2·K]
e) U-value maintaining the emissivity and using the tabulated value of h_c from ISO 9869-1:2014 [ε_{WALL} = 0.88; h_c=3 W/m^2·K]
f) U-value maintaining the calculated h_c and using the tabulated value of emissivity from ISO 9869-1:2014 [h_c from the method; ε_{WALL} = 0.90]
g) U-value with the tabulated values of emissivity and h_c from ISO 9869-1:2014 [ε_{WALL} = 0.90; h_c=3 W/m^2·K]

The c) and f) options produced the same result, since the tabulated value of the emissivity is equal. It should be highlighted that the value of h_c is slightly different to that obtained in a), since another value of emissivity (ε_{WALL} =0.90) involves a new analysis for each thermogram of the test and consequently, new values of T_{WALL} in the numerical model.

4.2 Validation of the method in real built environments

4.2.1 Description of the case studies

According to Gangolells et al. [2012], 59% of the current Spanish residential building stock was erected before the first thermal regulation NBE-CT-79 [Spain, 1979]. Nearly 38% of Spanish residential buildings already in use were built under NBE-CT-79 [Spain, 1979], satisfying the minimum thermal requirements. Three per cent of Spanish residential building stock was erected under Spanish Technical Building Code CTE-DB-HE1 [Spain, 2006]. Along this line, Gangolells et al. [2016] stated that 53.6% of residential buildings with energy certification had the worst energy label (E class). For these reasons, two typical Spanish wall typologies from different construction periods were chosen as case studies (Tables 2 and 3).

Table 2. Technical characteristics and thermo-physical properties of case study A (from outside to inside)

#	Case Study A	Δx_i [m]	$c_{p\,i}$ [J/Kg·K]	ρ_i [Kg/m^3]	λ_i [W/(m·K)]	R-value [(m^2·K)/W]	Sketch
1	Mortar	0.02	1000	1900	1.30	---	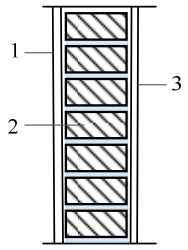
2	Perforated brick	0.14	1000	920	---	0.23	
3	Internal plaster	0.01	1000	1000-1300	0.57	---	
R_{se} = 0.04 (m^2·K)/W; R_{si} = 0.13 (m^2·K)/W; U_t = 2.31 W/(m^2·K)							

Δx_i: thickness of the layer; $c_{p\,i}$: thermal capacity of the layer; ρ_i: density of the layer; λ_i: thermal conductivity of the layer; R-value: thermal resistance of the material; R_{se}: theoretical thermal resistance from outside the building; R_{si}: theoretical thermal resistance from inside the building; U_t: theoretical thermal transmittance of the building façade.

Table 3. Technical characteristics and thermo-physical properties of case study B (from outside to inside)

	Case Study B	Δx_i [m]	$c_{p\,i}$ [J/Kg·K]	ρ_i [Kg/m^3]	λ_i [W/(m·K)]	R-value [(m^2·K)/W]	Sketch
1	Mortar	0.002	1000	1900	1.30	--	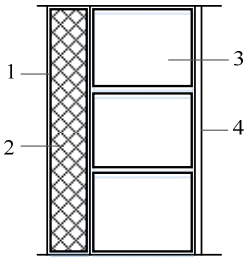
2	Insulation EPS	0.06	--	--	--	1.62	
3	Thermoclay	0.24	--	--	--	0.57	
4	Internal plaster	0.01	1000	1000-1300	0.57	--	
R_{se} = 0.04 (m^2·K)/W; R_{si} = 0.13 (m^2·K)/W; U_t = 0.42 W/(m^2·K)							

Δx_i: thickness of the layer; $c_{p\,i}$: thermal capacity of the layer; ρ_i: density of the layer; λ_i: thermal conductivity of the layer; R-value: thermal resistance of the material; R_{se}: theoretical thermal resistance from outside the building; R_{si}: theoretical thermal resistance from inside the building; U_t: theoretical thermal transmittance of the building façade.

Case study A is a single–leaf wall that is 3.26 metres high, corresponding to the typical building façade erected before NBE-CT-79 [Spain, 1979]. Case study B is a sample that is 2.54 metres high and consists of a multi-leaf wall (external insulation), built under CTE-DB-HE1 [Spain, 2006]. The main technical features and thermo-physical properties of these building façades and a sketch of them are shown in Tables 1 and 2 respectively. In accordance with the method explained above, the measurement campaign took place during January and February 2016, to ensure a temperature difference across the building façade that was within 10-15ºC.

Considering northern façades for both case studies, six tests were performed under different measuring conditions. In case study A (single-leaf wall built before NBE-CT-79, -Spain, 1979-), two tests were carried out: test A.1. was developed without heating; test A.2. was executed with the heating system switched on 48 hours previously. In case study B (multi-leaf wall erected under CTE-DB-HE1, –Spain, 2006-), the building did not have a heating system. It was observed that outside temperatures range from 0 to 5ºC between 6 am and 9 am during the winter. Moreover, inner air temperature normally remains at 12 – 14ºC in unoccupied buildings. Therefore, a temperature difference within the range of 8 to 10ºC can be ensured between the inside and outside the building.

4.2.2 Discussion of method validation results

The results of the case studies are presented in Tables 4 – 6. The comparative analysis of the measured U-values calculated using the proposed method and the theoretical U-values showed a deviation of 1.24% to 3.97%. Conversely, the deviation between the notional and the measured U-values was found to be 14 - 28% for the HFM [ISO 9869-1:2014, International Organization for Standardization, 2014] or 10 -20% for other methods of quantitative IRT developed in recent years [Albatici et al., 2010; Fokaides et al., 2011; Kylili et al., 2014; Nardi et al., 2014; Ohlsson et al., 2014; Albatici et al., 2015].

Table 4. Case study A.1. Comparison between notional and measured U-value using quantitative IRT, UNE-EN ISO 6946:2012 and ISO 9869-1:2014 (absolute deviations are presented as a percentage)

Case study A.1. **Without heating** **8.7ºC < ΔT < 9.8ºC** **181 thermograms**		**MEASURED U-VALUE** **Umes [W/m²·K]**			**NOTIONAL U-VALUE** **Ut [W/m²·K]**
		DEVELOPED METHOD	**UNE-EN ISO 6946:2012**	**ISO 9869-1:2014**	**UNE-EN ISO 10456:2012**
DEVELOPED METHOD	**ε = 0.88**	**h_c = 2.142 W/m²·K** 2.360 ± 0.280 (2.16%)	**h_c = 2.5 W/m²·K** 2.449 ± 0.278 (8.18%)	**h_c = 3 W/m²·K** 2.695 ± 0.293 (16.67%)	2.310
UNE –EN ISO 6946:2012 **ISO 9869-1:2014**	**ε = 0.90**	**h_c = 2.125 W/m²·K** 2.322 ± 0.282 (0.51%)	**h_c = 2.5 W/m²·K** 2.464 ± 0.280 (6.66%)	**h_c = 3 W/m²·K** 2.655 ± 0.295 (14.94%)	

U_{mes}: measured thermal transmittance; U_t: notional thermal transmittance; $\Delta T = T_{IN} - T_{OUT}$; ε_{WALL} = emissivity of the wall; h_c= convective heat transfer coefficient.

Table 5. Case study A.2. Comparison between notional and measured U-value using quantitative IRT, UNE-EN ISO 6946:2012 and ISO 9869-1:2014 (absolute deviations are presented as a percentage)

Case study A.2. With heating (>48h previously) 7ºC < ΔT < 15.8ºC 181 thermograms		**MEASURED U-VALUE U_{mes} [W/m²·K]**			**NOTIONAL U-VALUE U_t [W/m²·K]**
		DEVELOPED METHOD	**UNE-EN ISO 6946:2012**	**ISO 9869-1:2014**	**UNE-EN ISO 10456:2012**
DEVELOPED METHOD	**ε_{WALL} = 0.88**	**h_c = 2.370 W/m²·K** 2.339 ± 0.335 (1.24%)	**h_c = 2.5 W/m²·K** 2.395 ± 0.320 (3.71%)	**h_c = 3 W/m²·K** 2.634 ± 0.337 (14.05%)	2.310
UNE –EN ISO 6946:2012 ISO 9869-1:2014	**ε_{WALL} = 0.90**	**h_c = 2.361 W/m²·K** 2.320 ± 0.340 (0.44%)	**h_c = 2.5 W/m²·K** 2.380 ± 0.324 (3.06%)	**h_c = 3 W/m²·K** 2.617 ± 0.341 (13.28%)	

U_{mes}: measured thermal transmittance; U_t: notional thermal transmittance; $\Delta T = T_{IN}-T_{OUT}$; ε_{WALL} = emissivity of the wall; h_c= convective heat transfer coefficient.

Table 6. Case study B. Comparison between notional and measured U-value using quantitative IRT, UNE-EN ISO 6946:2012 and ISO 9869-1:2014 (absolute deviations are presented as a percentage)

Case study B Without heating 8.7ºC < ΔT < 9.8ºC 121 thermograms		**MEASURED U-VALUE U_{mes} [W/m²·K]**			**NOTIONAL U-VALUE U_t [W/m²·K]**
		DEVELOPED METHOD	**UNE-EN ISO 6946:2012**	**ISO 9869-1:2014**	**UNE-EN ISO 10456:2012**
DEVELOPED METHOD	**ε_{WALL} = 0.88**	**h_c = 1.456 W/m²·K** 0.437 ± 0.219 (3.97%)	**h_c = 2.5 W/m²·K** 0.548 ± 0.243 (30.47%)	**h_c = 3 W/m²·K** 0.602 ± 0.266 (43.32%)	0.420
UNE –EN ISO 6946:2012 ISO 9869-1:2014	**ε_{WALL} = 0.90**	**h_c = 1.451 W/m²·K** 0.436 ± 0.222 (3.80%)	**h_c = 2.5 W/m²·K** 0.547 ± 0.246 (30.15%)	**h_c = 3 W/m²·K** 0.601 ± 0.269 (42.87%)	

U_{mes}: measured thermal transmittance; U_t: notional thermal transmittance; $\Delta T = T_{IN}-T_{OUT}$; ε_{WALL} = emissivity of the wall; h_c= convective heat transfer coefficient.

Therefore, the proposed method has three advantages. Firstly, it can be used to achieve greater accuracy than other methods. Secondly, it requires less execution time. In fact, the test takes 2-3 hours in comparison to a minimum of 72 hours and maximum of one week for the HFM method. Thirdly, it allows reducing the lowest level of the temperature difference range (7 < ΔT <16ºC), in contrast to previous researches where the tests were conducted under a ΔT between 10 and 15ºC. Hence, the proposed method makes possible to measure unoccupied buildings without a heating system in operation, obtaining reliable results. However, the influence of the operating conditions on the measured U-value is an aspect that needs to be analyzed in-depth, as shown in Chapter 5 of this dissertation.

In relation to the last potential of the proposed method, it should be noted that the period of time that the internal heating system had been switched on prior to the test might not have had any influence on good heat flux transfer from inside to outside the building façade. Moreover, it might be stated that it is not required to maintain stationary conditions 48h before the measurements for existing buildings that have not been used for a long-term (i.e. case study A, Table 4) or buildings recently built without connection to the electrical grid and heating system (i.e.case study B, Table 6), because the boundary conditions have not been altered previously.

Regarding to the influence of tabulated values on the accuracy of the method, the main aspects are exposed below. For the single-leaf wall when the room was without heating (test A.1, Table 4), the proposed method had a deviation of 2.16% in comparison with 6.66% and 14.94% using tabulated values. In the same case study, when the room was heated for 48 hours prior to the test (test A.2, Table 5), the proposed method showed a deviation of 1.24% with respect to 3.06% and 13.28% using tabulated values. For the multi-leaf wall (external insulated building façade), the results were even more relevant. Considering the outcomes of Table 6 for test B, the proposed method had a deviation of 3.97% compared to 30.15% and 42.87% according to the two regulations mentioned above.

As seen, the measurements were only slightly influenced by the wall surface emissivity (ε_{WALL}). In contrast, overestimated tabulated values for the convective heat transfer coefficient can lead to high deviations in U-value. Considering Tables 4 and 5 for case study A, the discrepancy between the measured and the tabulated values of h_c was low: 2.142 W/m^2·K without heating or 2.370 W/m^2·K with heating, compared to 2.5 and 3 W/m^2·K. In accordance with Table 6, the measured h_c showed a value of 1.456 W/m^2·K in comparison with the tabulated values of 2.5 and 3 W/m^2·K. Therefore, tabulated values for the convective heat transfer coefficient (h_c) might not be suitable for heavy walls with low U-values.

This study also highlighted the importance of temperature uniformity, which is defined as the difference between the maximum and minimum inner wall surface temperature values (2-3ºC for large areas; <0.5ºC for small areas) related to input data that derives from the thermograms during the post-processing [Danielski and Fröling, 2015]. In a single leaf wall, the lower temperature uniformity and the discrepancies between the theoretical and measured U-values can be attributed to singular elements (i.e. the proportion of mortar compared to the brick for the small areas; the influence of the corner where the temperatures are higher than the rest of the wall for large areas). In contrast, a multi-leaf wall can present a higher degree of uniformity, since any part of the element has the same average wall surface temperature (Figure 6).

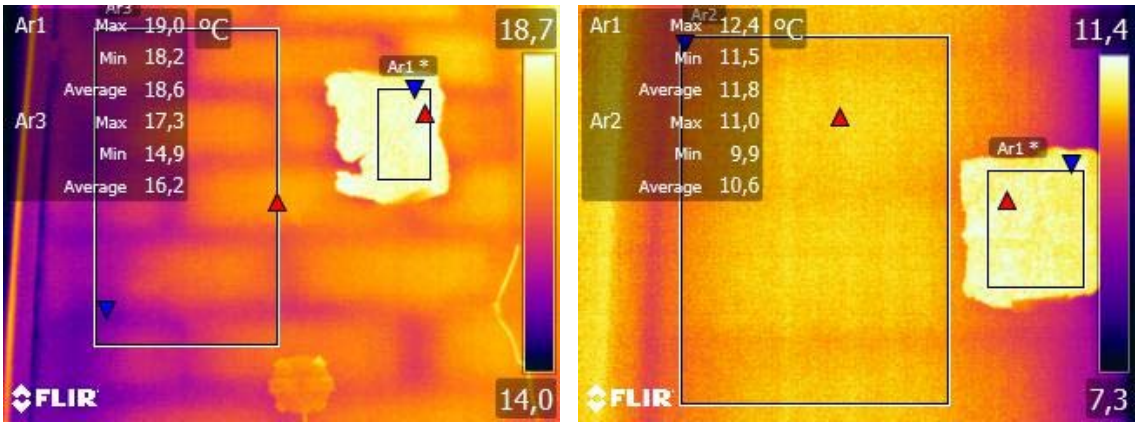

Figure 6. Wall surface temperature uniformity in case study A.2. (left) and case study B (right)

In order to quantify the influence of the aforementioned parameter on the determination of the U-value, several areas were defined in each thermogram (Figure 7). The optimum outcomes were given by an area of 104x221 (22984 pixels) for the single-leaf wall and an area of 146x212 (30952 pixels) for the multi-leaf wall. As an example of a non-homogenous wall, the results for case study A.2. were shown in Table 7. It is concluded that the quantity of pixels is not as relevant as the homogeneity of heat flux and temperature on the material in the area that is being analysed. Furthermore, it was concluded that the quantity of pixels is not as relevant as the homogeneity of heat flux and temperature on the material in the area that is being analysed (Table 7).

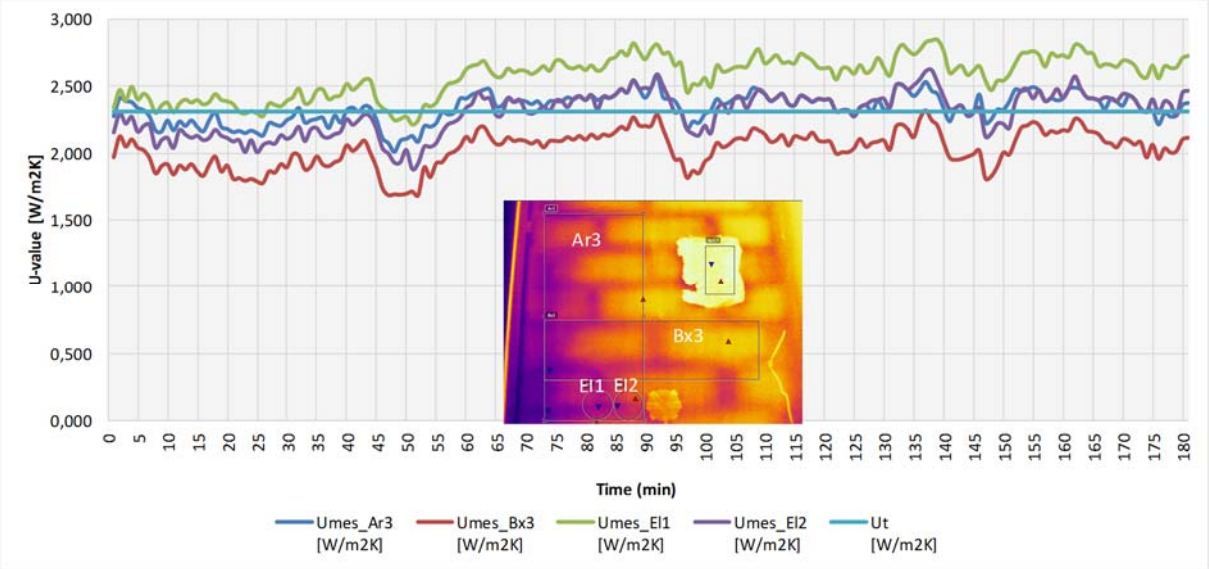

Figure 7. Case study A.2. Influence of the analysed wall area in the thermogram

Table 7. Case study A.2. Influence of the analysed wall area in the thermogram. Comparison between notional and measured U-value using quantitative IRT (absolute deviations are presented as a percentage).

AREAS	**NUMBER OF PIXELS**	**MEASURED U-VALUE U_{mes} [W/m^2·K]**	**NOTIONAL U-VALUE U_t [W/m^2·K]**
Ar3 (104 x 221)	22,984	2.339 ± 0.335 (1.24%)	2.310
Bx3 (226 x 63)	14,238	2.031 ± 0.334 (12.09%)	
EI1 (30 x 30)	900	2.575 ± 0.337 (11.49%)	
El2 (30 x 30)	900	2.299 ± 0.335 (0.49%)	

Chapter 5: Analysis of the most influential operating conditions

Having identified which equations leads to a better adjustment of the numerical model for the real built environment (Chapters 3 and 4), it is required to know how to improve this non-invasive technique with the aim of introducing it into the construction industry market. This chapter pretends to analyze the most influential operating conditions on the preciseness of in-situ measured thermal transmittance, and to determine the optimum temperature difference range for quantitative internal IRT. The assessment methodology and the main features of the measuring campaign are showed in Section 5.1. Subsequently, the results are widely discussed in Section 5.2. It should be pointed out that this study was published in Journal Paper II [Tejedor et al., 2018].

5.1 Identification of operating conditions and assessment methodology

The steps to conduct this analysis are represented in Figure 8:

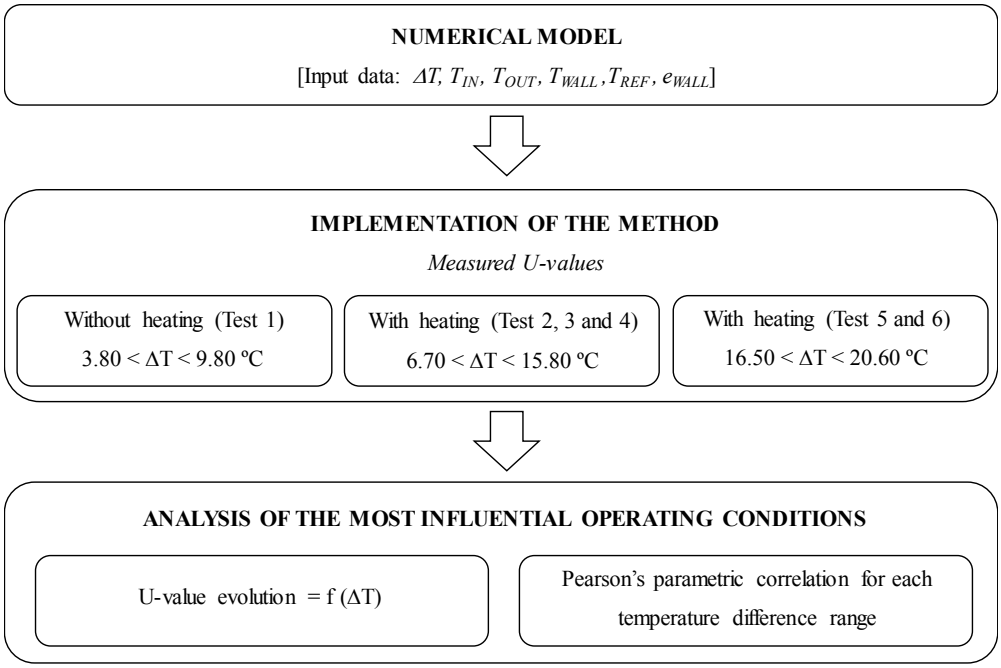

Figure 8. Flowchart of the assessment of the most influential operating conditions on U-value

In accordance with the proposed method (Chapter 3), the main operating conditions that might influence on the accuracy of measured U-values are those continuously measured by the equipment and introduced as input data in the numerical model (ΔT, T_{IN}, T_{OUT}, T_{WALL} and T_{REF}). Nevertheless, this issue must be analyzed in a controlled indoor environment under quasi steady-state conditions in order to observe the limits of the model. For this reason, a measurement campaign was performed on an experimental room located in the university with a heating unit to be configured (Figure 9) during January and February 2016.

The façade consisted of a single-leaf wall of 3.26 m height with a theoretical U-value of 2.310 W/m^2·K, since it was erected before NBE-CT-79 [Spain, 1979] without any subsequent refurbishment. As regards its internal configuration (from outside to inside), this building envelope is comprised of 20 mm of mortar, 140 mm of perforated brick wall and 10 mm of gypsum plaster.

Figure 9. Experimental room

A total of 966 thermograms were recorded to evaluate the thermal behavior of this heavy wall for an air temperature difference range from 3.80 to 20.60ºC between inside and outside the building and to determine the optimum temperature difference range for quantitative internal IRT. Measured U-values, with their respective deviations and combined standard uncertainties associated with the measuring equipment, were calculated following the method described in Section 3.5. and Section 4.1.

Finally, and to identify a significant relationship among the aforementioned variables and the measured U-value, a statistical analysis based on Pearson's correlation was computed using SPSS Statistics Software [IBM, 2017]. However, temperature difference (ΔT) is an operating condition that derives from two others (the inner and outer air temperatures near the target to be tested). Therefore, both T_{IN} and T_{OUT} should be carefully studied. It should be highlighted that the wall surface emissivity (ε_{WALL}) was not considered as a possible causal factor of deviation in this dissertation, since Tejedor et al. [2017] already demonstrated that measurements are slightly influenced by this parameter.

5.2 Influence of operating conditions on the accuracy of IRT measurements

Firstly, the analysis was carried out without heating (Test 1), under a temperature difference between inside and outside the building that ranged from 3.80 to 9.80ºC. Just one test was enough to reject this ΔT for the numerical model, since the worst outcomes were gathered for Test 1 with an average measured U-value of 3.618±0.542 W/m^2·K (Table 8 and Figure 10). The instantaneous thermal transmittances were found to be

overestimated, specifically 140-150% higher than the theoretical value when the temperature difference was around 3ºC-4ºC. This percentage was reduced to ~100% when ΔT ranged from 4 to 5ºC and 60% under 6ºC. Subsequently, three tests were conducted for a temperature difference between 7 and 16ºC (Tests 2, 3 and 4 in Table 8 and Figure 10). The measurements of 543 thermograms were found to better fit the theoretical U-value, with the average measured U-value equal to 2.396±0.304 W/m^2·K (deviation of 3.73%). Finally, two tests were performed for 16 <ΔT< 21ºC (Tests 5 and 6 in Table 8 and Figure 10), showing similar results. In this case, the average measured thermal transmittance was found to be 2.017±0.194 W/m^2·K, so was underestimated by 12.66% in relation to the theoretical U-value. Therefore, a third test for this temperature difference range was deemed not to be necessary.

Table 8. Measured U-values using quantitative internal IRT (absolute deviations are presented as percentages)

Measured U-value U_{mes} **[W/(m²·K)]**					
Test 1	**Test 2**	**Test 3**	**Test 4**	**Test 5**	**Test 6**
3.80<ΔT< 9.80ºC	**7.90<ΔT< 14.90ºC**	**6.70<ΔT< 15.30ºC**	**7<ΔT< 15.80ºC**	**16.60<ΔT< 20.40ºC**	**16.50<ΔT< 20.60ºC**
121 thermograms	**181 thermograms**	**181 thermograms**	**181 thermograms**	**121 thermograms**	**181 thermograms**
3.618±0.542		2.396 ±0.304		2.017±0.194	
(56.63%)		(3.73%)		(-12.66%)	

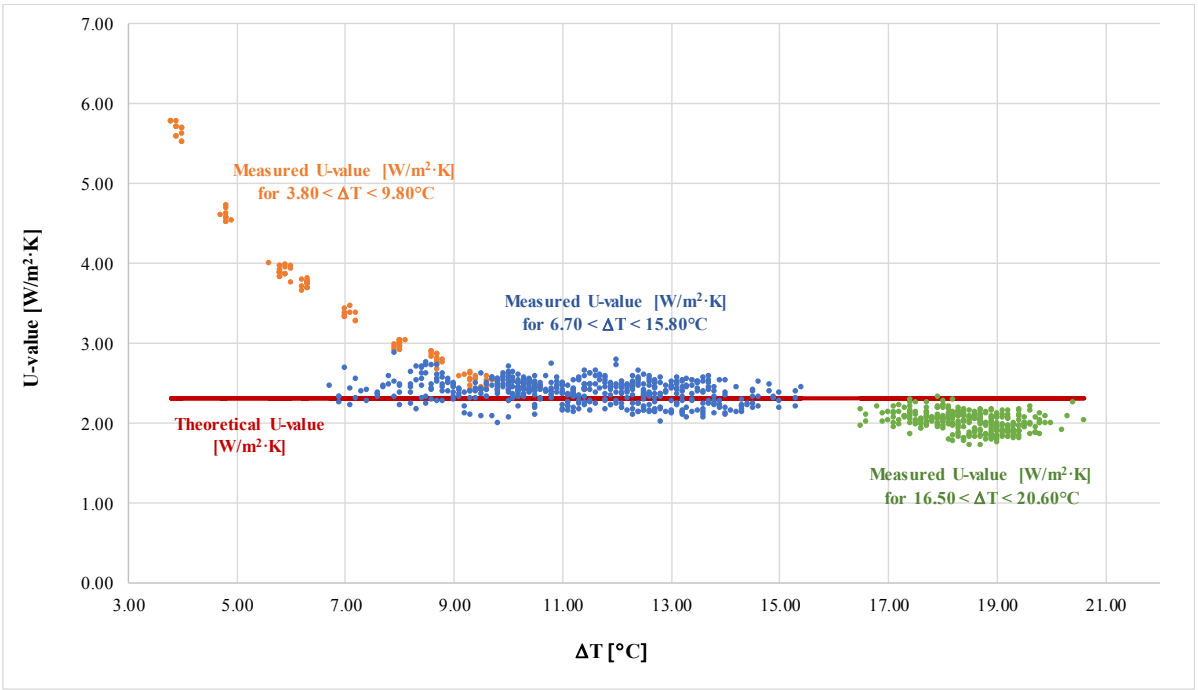

Figure 10. Measured thermal transmittance for 3.80 < ΔT < 20.60ºC

As mentioned above, a further statistical analysis of input data was also drawn up for each temperature difference range using a t-test analysis, specifically a Pearson's parametric correlation (r-value). A normal distribution at 95% confidence level was assumed in SPSS software [IBM, 2017]. The results are summarized in Tables 9 to 10, where the r^2 value indicates how a variable can be predicted by changes in another one [Love et al., 2002; Forcada et al., 2012]. Notably, the tables provide the r-value. To obtain the percentage of variance in thermal transmittance due to each operating condition, the square value of Pearson's correlation coefficients (r-value) should be calculated and multiplied by 100.

Figures 11 to 13 corroborate the results gathered from the statistical analysis. These figures illustrate the relationship among the operating conditions and the measured U-values (blue points) with respect to the theoretical U-values (red lines), as temperature differences (ΔT) are sorted and plotted from lowest to highest. In this way, and for the three ΔT ranges evaluated above (3.80 <ΔT <9.80ºC; 7 <ΔT <16ºC; 16 <ΔT<21ºC), it can be observed the evolution of the input data for the numerical model (T_{IN}, T_{OUT}, T_{WALL} and T_{REF}) and the adjustment of the measured U-value to the expected value when ΔT increases.

According to the results (Table 9), for a temperature difference range from 3.80 to 9.80ºC (Test 1), the thermal transmittance absolutely depends on ΔT (r=-0.963) as a direct consequence of outer air temperature near the target (r=+0.973). Data showed that 94.67% of the variance in thermal transmittance could be attributed to changes in T_{OUT}, being the percentage of correlation between T_{OUT} and ΔT of 99.40%. As corroborated by Figure 11, T_{OUT} and the measured U-value describe the same decreasing trend when ΔT values increase, whereas other operating conditions (inner air temperature, wall surface temperature and reflected ambient temperature) remain practically constant. The registered values of T_{IN} were around 15ºC; T_{WALL} and T_{REF} were remained in 11ºC and 14ºC respectively. It should be noted that T_{WALL} was found to be the parameter with the least influence on the measured U-value (2.46%), considering results of Table 9.

Table 9. Correlation matrix for measured U-values and operating conditions for 3.80 < ΔT < 9.80°C

	Umes	**ΔT**	**T_{IN}**	**T_{OUT}**	**T_{WALL}**	**T_{REF}**
Umes	1					
ΔT	-0.963**	1				
T_{IN}	-0.426**	0.584**	1			
T_{OUT}	0.973**	-0.997**	-0.522**	1		
T_{WALL}	0.157	-0.075	0.468**	0.122	1	
T_{REF}	-0.214*	0.310**	0.674**	-0.264**	0.899**	1

*** Correlation is significant at the 0.01 level (2-tailed); n=121*

** Correlation is significant at the 0.05 level (2-tailed; n=121*

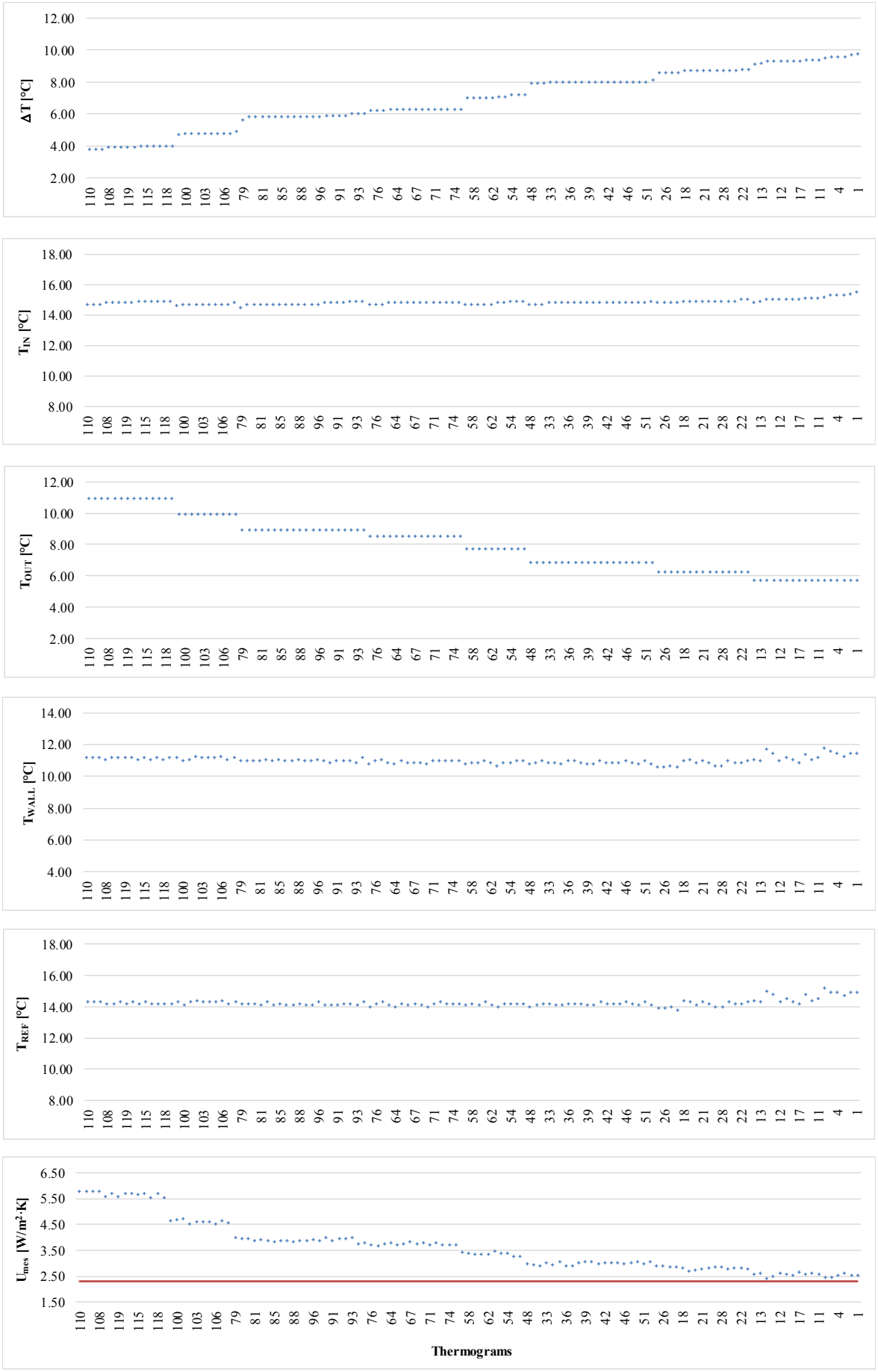

Figure 11. Influence of operating conditions on the measured U-value for $3.80 < \Delta T < 9.80$ºC

For a temperature difference range between 7 and 16ºC (Table 10 and Figure 12), correlation data revealed that the thermal transmittance was only significantly related to the outer air temperature near to the target (r=+0.469). In this case, the r^2 was low, indicating that only 22% approximately of the variance in the measured U-value could be predicted by changes of T_{OUT}. In addition, a negative Pearson's correlation value between ΔT and T_{OUT} (r=-0.848) indicated that 71.91% of the variance in ΔT could be caused by decreases in T_{OUT}.

Table 10. Correlation matrix for measured U-values and operating conditions for 7 < ΔT < 16°C

	Umes	**ΔT**	**T_{IN}**	**T_{OUT}**	**T_{WALL}**	**T_{REF}**
Umes	1					
ΔT	-0.296**	1				
T_{IN}	0.270**	0.376**	1			
T_{OUT}	0.469**	-0.848**	0.171**	1		
T_{WALL}	0.108*	-0.534**	0.460**	0.830**	1	
T_{REF}	0.077	-0.370**	0.563**	0.714**	0.975**	1

*** Correlation is significant at the 0.01 level (2-tailed); n=543*

** Correlation is significant at the 0.05 level (2-tailed; n=543*

This analysis did not show any significant relationships between the thermal transmittance and the other operating conditions. As seen in Figure 12, the inner air temperature (T_{IN}), the wall surface temperature (T_{WALL}), and the reflected ambient temperature (T_{REF}) remained practically constant. The majority of datapoints of T_{IN} were from 20 to 22ºC throughout the temperature difference range. In the case of T_{WALL} and T_{REF}, the measurements were roughly concentrated between 14-16º for T_{WALL} and 16-18ºC for T_{REF}. Besides this, the influences of these three parameters on the measured U-value were very low. Their corresponding r^2 values expressed as a percentage were found to be 7.29%, 1.17% and 0.59% respectively (Table 10).

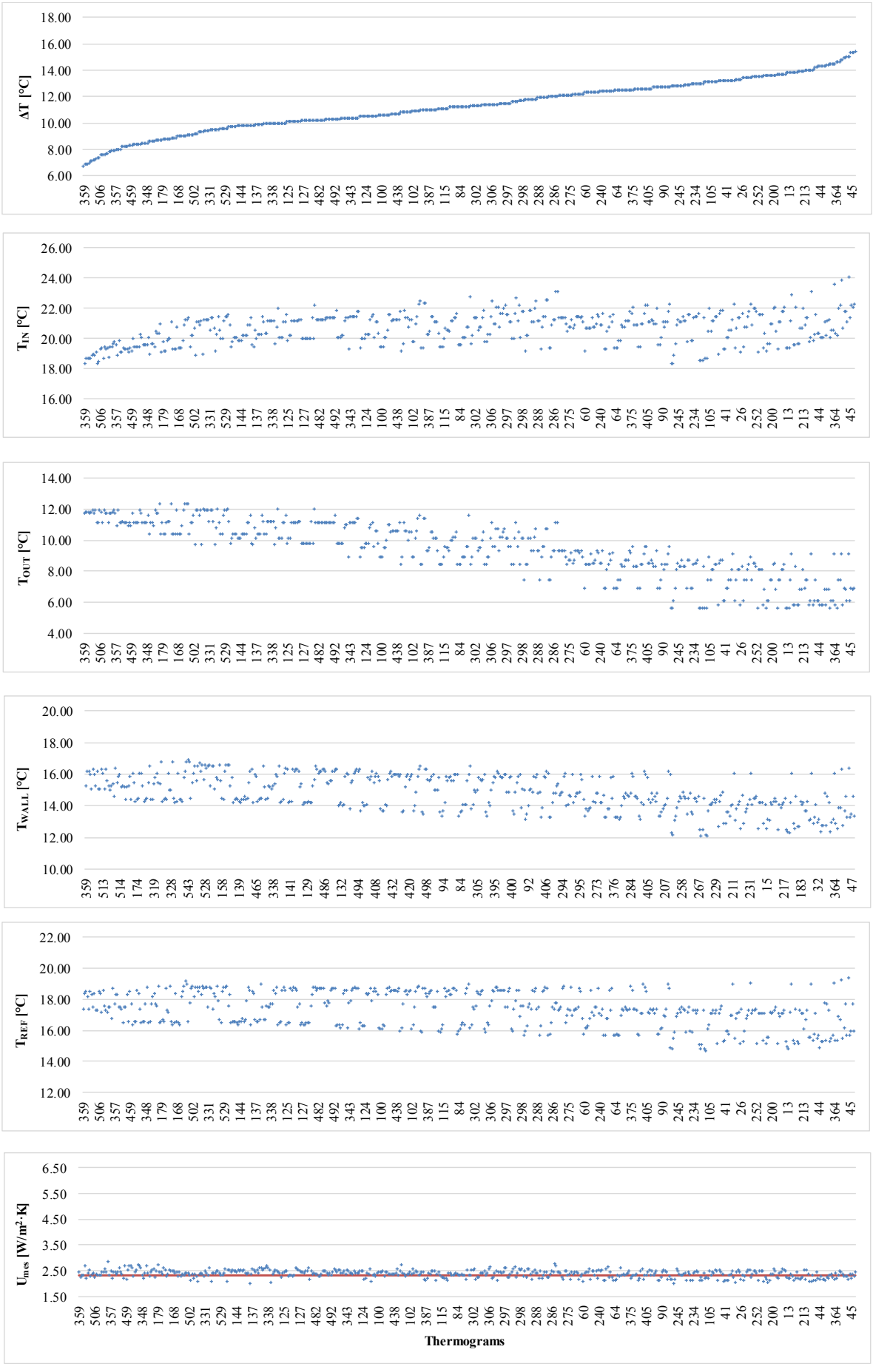

Figure 12. Influence of operating conditions on the measured U-value for 7 < ΔT < 16ºC

Along the lines of Nardi et al. [2016], the findings also showed an underestimation of measured U-value when the temperature difference and reflected ambient temperature increased ($16 < \Delta T < 21$ºC and $18 < T_{REF} < 20.1$ºC, respectively). All Pearson's coefficients for the measured U-value were found to be negative. In this case (Table 8 and Figure 13), the data showed that 35.64% of the variance of the measured U-values could be predicted by changes in T_{WALL}. In addition, higher correlation coefficients revealed that the majority of T_{WALL} measurements could have been produced by changes in T_{REF} (97.02%) and T_{IN} (80.46%). At higher inner air temperatures, the surroundings (including furniture and white walls) reflect more on the target and consequently might have affected the readings of the wall surface temperature. Wall surface temperatures gathered from 12 to 16ºC seemed to be more stable ($14.5 < T_{REF} < 17.9$ºC), giving deviations regarding the theoretical U-value of under ±5%. However, a decreasing trend of the measured U-value was observed for $T_{WALL} > 16$ºC, reaching deviations of measured U-values of around -15%.

Table 11. Correlation matrix for measured U-values and operating conditions for 16 < ΔT < 21°C

	Umes	**ΔT**	**T_{IN}**	**T_{OUT}**	**T_{WALL}**	**T_{REF}**
Umes	1					
ΔT	-0.352**	1				
T_{IN}	-0.353**	0.876**	1			
T_{OUT}	-0.211**	0.356**	0.763**	1		
T_{WALL}	-0.597**	0.657**	0.897**	0.857**	1	
T_{REF}	-0.468**	0.608**	0.888**	0.905**	0.985**	1

** *Correlation is significant at the 0.01 level (2-tailed); n=302*

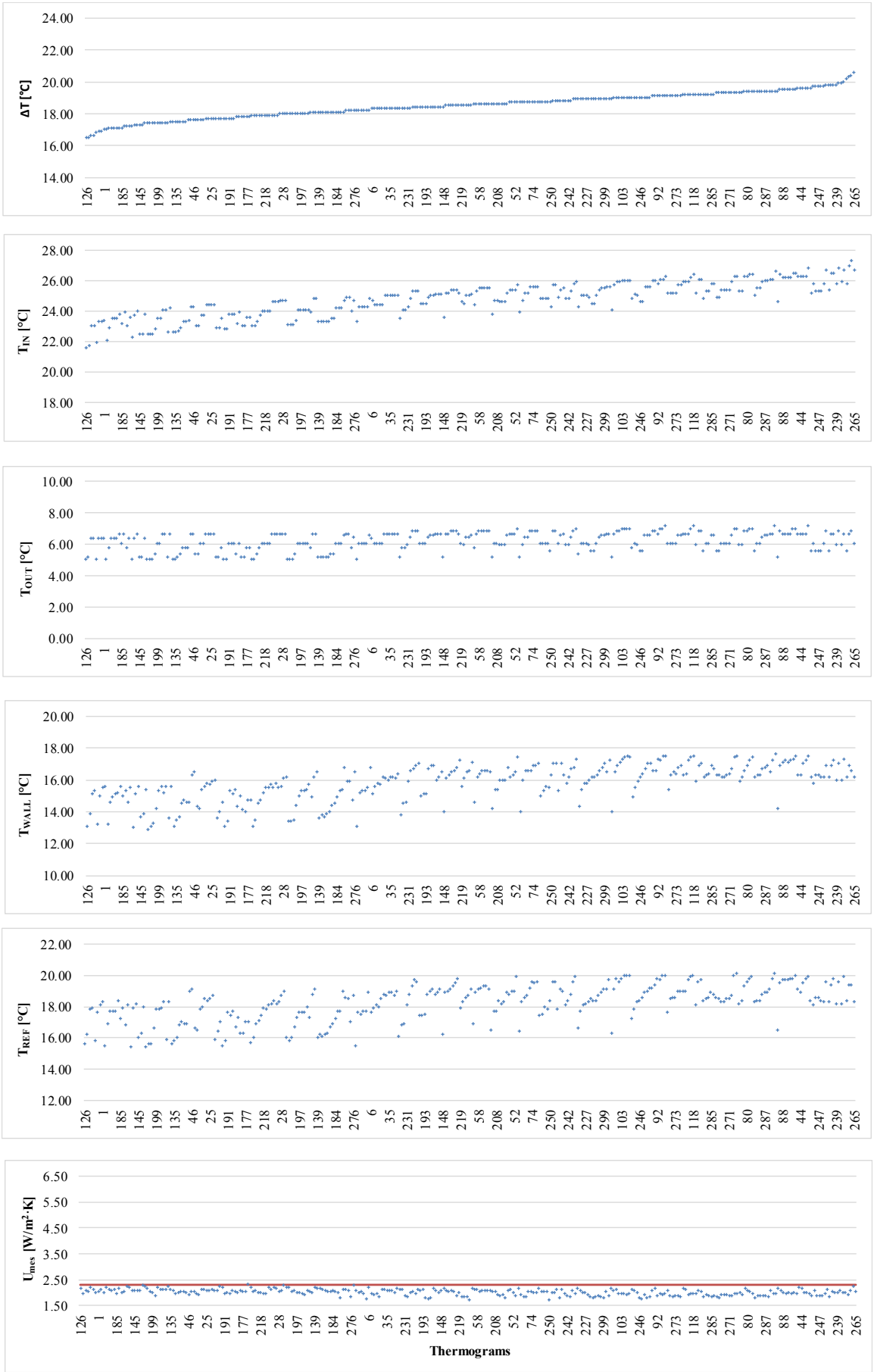

Figure 13. Influence of operating conditions on the measured U-value for $16 < \Delta T < 21$ºC

It should be noted that the relationship between T_{WALL} and T_{REF} was observed in the three ΔT ranges, where the measurements of T_{WALL} were highly correlated with T_{REF}. In fact, the reflected ambient temperature is a measurement parameter that is required to compensate errors of wall surface temperature readings with the IR camera. In addition, the percentages of r^2 value for T_{REF} in relation to the variance in thermal transmittance ascended along the wide temperature difference (80.82% for $3.80 < \Delta T < 9.80$ºC; 95.06% for $7 < \Delta T < 16$ºC; 97.02% for $16 < \Delta T < 21$ºC).

Finally, although testing procedures in quasi steady-state conditions might have influenced the variability of some measurements (swinging trend of instantaneous measurements for values of the same order), it can be considered that all obtained outcomes were reliable. A single-leaf wall is quite sensitive to outer air temperature, due to a lack of insulation layer. In addition, a temperature difference range from 7 to 16ºC might be considered the optimum.

Chapter 6: Analysis of the influence of thermophysical properties on the proposed method

Chapter 5 allowed knowing which was the optimum temperature difference range and which operating conditions could affect the determination of the thermal transmittance during the implementation of the method in an experimental room. Assuming the premise of the Section 5.2., which stated that only 22% of the variance in the measured U-value could be attributed to changes of T_{OUT} when the temperature difference range is set between 7 and 16ºC, Chapter 6 aims to evaluate the impact of thermophysical properties in several real unoccupied buildings ($\Delta T < 10$ºC) under quasi steady-state conditions. The literature review (Chapter 1) underlined walls' thermal mass as a source of inaccuracy on the determination of the measured thermal transmittance for $10 < \Delta T < 15$ºC. It should be highlighted that this study was published in Journal Paper II [Tejedor et al., 2018].

6.1 Identification of thermophysical properties and assessment methodology

In contrast to the operating conditions (Chapter 5), the thermophysical properties include aspects of the building envelope which cannot be controlled by the thermographer. However, they might also influence the accuracy of the quantitative internal IRT. Assuming that the method proposed in Chapter 3 was executed in quasi steady-state conditions, measured U-value and theoretical heat capacity per unit of area of each façade were the only non-transient thermophysical properties to be considered in this research. Measured U-value should be calculated using the specifications reported in Chapters 3 and 4. Heat capacity per unit of area (also referred to as the kappa value or k_m) defines the quantity of heat to be stored by an element for later release and characterizes the thermal mass [Ficco et al., 2015]. Hence, a wall with a high potential to accumulate heat has a high thermal mass. According to UNE-EN ISO 13786:2011 [International Organization for Standardization, 2011], the theoretical heat capacity per unit of area (k_m) can be determined by Equation 15 (considering that the summation is over all layers in the element):

$$k_m = (\sum \Delta x_i \cdot \rho_i \cdot c_{pi})/1000 \quad (15)$$

Where k_m [kJ/m^2·K] is the theoretical heat capacity per unit of area; Δx_i is the thickness of the layer [m]; ρ_i is the density of the layer [kg/m^3]; and c_{pi} is the specific heat capacity of the layer [J/kg·K].

This simplified method was found to be suitable for this study, since the building envelope can be taken as a plane component and the approximation is not used to define the thermal inertia of the wall. However, it might provide overestimations in comparison to the results obtained from dynamic thermal characteristics.

Taking into account the aspects mentioned above, four unoccupied residential buildings with heavy multi-leaf walls were tested from January to February 2017, ensuring the same internal boundary conditions among samples and similar external weather conditions. It should be noted that these unoccupied buildings form part of public housing stock and have no electric or heating system in operation. Indeed, some of them (Façades 2, 3 and 4) have not been in-use since they were built. In the case of Façade 1, the housing had not been occupied for years, since it needed to be refurbished in accordance with current regulations. Therefore, stable environmental conditions were accomplished in accordance to Section 4.2. and Section 5.2. During the performance of the method, the doors and windows remained closed.

Façades 1 (Figure 14) and 2 were erected under NBE-CT-79 [Spain, 1979], while Façades 3 (Figure 15) and 4 were built under the Spanish Technical Building Code CTE-DB-HE1 [Spain, 2006]. Table 12 shows the configuration and the main technical features of the four analyzed façades. Notably, endoscopy analyses could not be performed. The thicknesses of each layer were taken from the construction project documents. Concerning other technical features of façades, some construction project documents provided the thermal resistances of each layer. Other documents contained the conductivities and thermal resistances of each layer of the wall, and even the manufacturers' datasheets. Values of density and specific heat capacity were taken from UNE-EN ISO 10456:2012 [International Organization for Standardization, 2012] and the existing literature [Albatici et al., 2010; Kumar et al., 2013; Rossi et al., 2014]. Theoretical U-values were estimated following the recommendations of Section 4.1.

Figure 14. Measuring campaign in Façade 1

Figure 15. Measuring campaign in Façade 3

Table 12. Configuration and technical features of the façades (from outside to inside)

	N# layer	Material layer	Δx_i [m]	λ_i [W/(m·K)]	ρ_i [kg/m^3]	$c_{p\,i}$ [J/(kg·K)]	$R_{t\,i}$ [(m^2·K)/W]	L [m]	U_t [W/(m^2·K)]
Façade 1	1	Perforated brick wall	0.140	---	1140	1000	0.180	2.50	0.657
	2	Insulation EPS	0.030	0.033	30	1400	0.909		
	3	Non-ventilated air cavity	0.020	---	1	1004	0.160		
	4	Hollow brick wall	0.050	---	1000	1000	0.070		
	5	Gypsum plaster	0.010	0.300	1150	1000	0.033		
Façade 2	1	Insulation EPS	0.080	0.038	20	1400	2.125	2.70	0.362
	2	Perforated brick wall	0.140	---	1140	1000	0.180		
	3	Non-ventilated air cavity	0.050	---	1	1004	0.180		
	4	Hollow brick wall	0.040	---	1000	1000	0.090		
	5	Gypsum plaster	0.010	0.570	1150	1000	0.018		
Façade 3	1	Limestone wall	0.030	2.300	2395	920	0.013	2.51	0.480
	2	Reinforced concrete wall	0.250	2.300	2400	1000	0.109		
	3	Rock wool insulation	0.064	0.037	40	840	1.730		
	4	Plasterboard	0.016	0.250	825	1000	0.064		
Façade 4	1	Mortar	0.002	1.300	1900	1000	0.002	2.54	0.420
	2	Insulation EPS	0.060	---	20	1400	1.620		
	3	Thermoclay	0.240	---	910	719	0.570		
	4	Gypsum plaster	0.010	0.570	1150	100	0.018		

Δx_i: thickness of the layer; λ_i: thermal conductivity of the layer; ρ_i: density of the layer; $c_{p\,i}$: specific heat capacity of the layer; $R_{t\,i}$: theoretical thermal resistance of the layer; L: height of the wall; U_t: theoretical thermal transmittance of the building façade.

6.2 Influence of U-value and kappa value on method accuracy

For the first time, a study on quantitative internal IRT was undertaken in real unoccupied residential buildings with heavy multi-leaf walls under ΔT <10ºC. The results are presented in Table 13 and Figures 16-17. As shown in Table 13, and because of testing in several real built environments, *ΔT* values were slightly lower (6ºC < ΔT < 10ºC) than optimal (7ºC < ΔT < 16ºC) specified in Section 5.2. During the tests, the inner air temperature of the unoccupied buildings remained at 12-14ºC and outside temperatures ranged from 0 and 5ºC between 6 am and 9 am. By way of example, the operating conditions and the instantaneous measured U-values were plotted over time in Façade 4 (Figure 16).

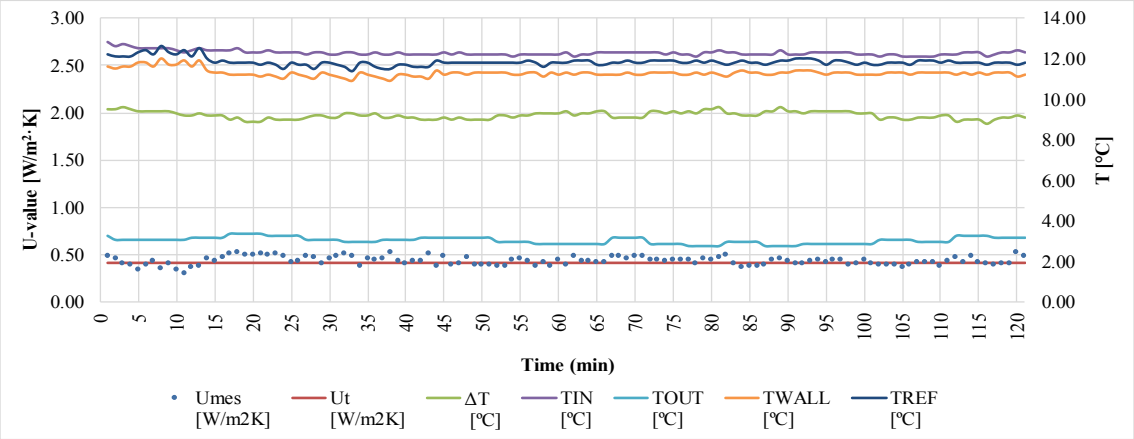

Figure 16. Operating conditions and instantaneous measured U-values over time in Façade 4

The results lead to the conclusion that heavy multi-leaf walls are less sensitive and provide more reliable results than heavy single-leaf walls for low temperature difference values (*ΔT*< 7ºC) under quasi steady-state conditions. In general, U-values measured using the proposed method showed deviations under 4% in most samples (Table 13), except for Façade 2. As shown in Figure 17, where the deviations $\Delta U/U_t$ (%) are plotted against the measured U-value, the percentage of deviation decreased as building envelopes presented greater thermal transmittance. Hence, multi-leaf walls with lower U-values might be more difficult to assess (i.e. Façade 2 had a deviation of 9.34%; Table 13).

Table 13. Theoretical thermophysical characteristics and measured U-values using quantitative internal IRT (deviations between theoretical and measured U-values are expressed as a percentage)

	Façade 1 **6.8<ΔT< 8.7°C** **121 thermograms**	**Façade 2** **7.6<ΔT< 9.1°C** **121 thermograms**	**Façade 3** **5.8<ΔT< 8.2°C** **121 thermograms**	**Façade 4** **8.70<ΔT< 9.80°C** **121 thermograms**
Notional Kappa value **κ_m [kJ/(m²·K)]**	222.38	213.39	685.88	174.01
Notional U-value **U_t [W/(m²·K)]**	0.657	0.362	0.480	0.420
Measured U-value **U_{mes} [W/(m²·K)]**	0.665±0.214 (1.19%)	0.396±0.270 (9.34%)	0.481±0.330 (0.20%)	0.437±0.219 (3.97%)

This analysis also demonstrated that façades with high theoretical heat capacities per unit of area might give low deviations (Figure 17), as detailed below. Façades 3 and 4, whose measured thermal transmittances were 0.481±0.330 W/m²·K and 0.437±0.219 W/m²·K, presented deviations of 0.20% and 3.97% respectively (Table 13, Figure 17). Despite being under the same test conditions, these multi-leaf walls with similar U-values had different accuracy levels in relation to theoretical U-values. In the case of Façade 3, the theoretical heat capacity per unit of area was found to be over 3 times higher than the estimated value for Façade 4 (Figure 17).

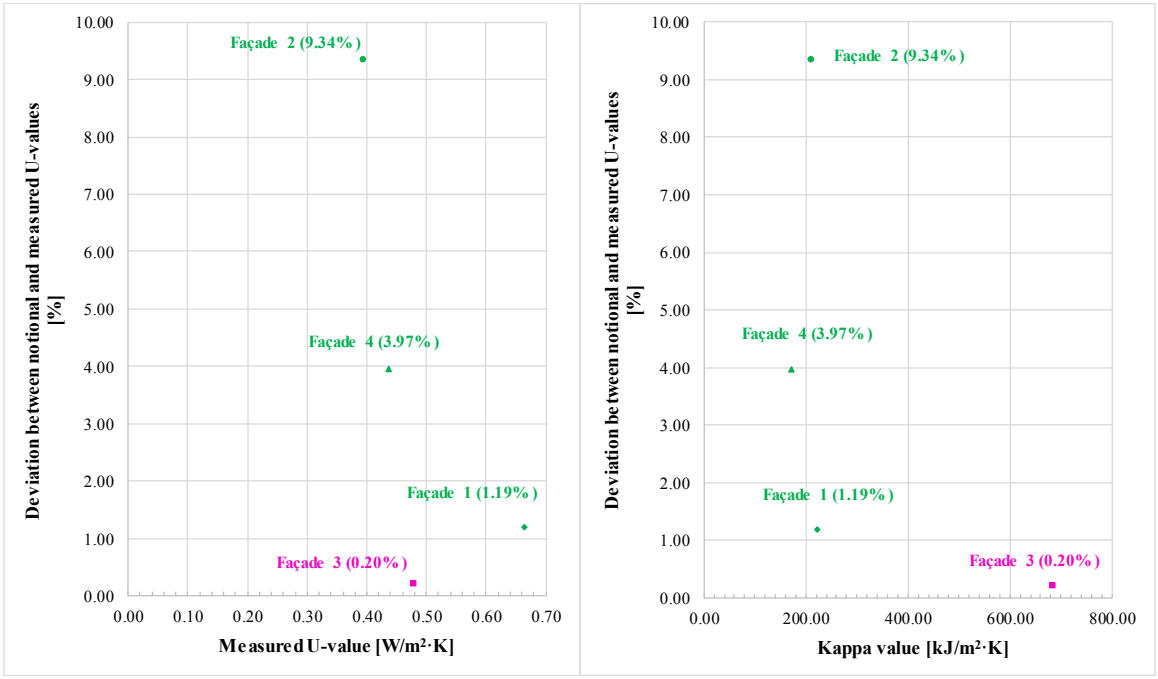

Figure 17. Deviation between the theoretical and measured U-value plotted against the thermal transmittance determined by quantitative internal IRT as well as the kappa value

Chapter 7: Analysis of the influence of test duration

As mentioned in the literature review, some researchers highlighted the limitations of using quantitative IRT tests with a short test duration. Having evaluated the thermal behaviour of different heavy multi-leaf walls (Chapter 6), and taking into account the previous recommendations (Chapters 3 to 5), this last study pretends to assess the third shortcoming in the usability of the quantitative internal IRT (Chapters 1 to 2) through two hypothesis. In the traditional approach, it is assumed that a greater test duration leads to more accuracy. Thus, the first hypothesis should check if the deviation between theoretical and measured U-value follows a trend over time. The second hypothesis, as long as first one is not affirmative, consists of assuming IRT measurements as a constant signal plus a random error. The aim is to develop a data-processing method based on U-value time series analysis, finding a common and objective criterion in order to stop the in-situ NDT when it is not necessary more data to obtain a reliable result. To validate this proposal, the System Identification Tool of MATLAB is applied, modelling the IRT measurements and observing when the signal is constant.

7.1 The role of test duration on the accuracy of IRT measurements

Previous researches underlined the difficulties of using a short-lasting tests [Hoyano et al., 1999; Kisilewicz et al. 2010; Fokaides et al., 2011; Dall'O et al., 2013; Carbonez et al., 2014; Lucchi et al., 2018; Marshall et al., 2018; Nardi et al., 2018]. For this reason, the first hypothesis of this study (H1) was focused on analysing if the deviation between the theoretical and measured U-value ($\Delta U/U_t$) decreased as sampling duration was longer, according to the traditional approach.

The measurement campaigns were conducted on six typical Spanish heavy multi-leaf walls from January to March 2017, to ensure a correct implementation of the method in accordance with Chapters 3 to 6. The details of each investigated building envelope are exposed below, with information drawn from the construction documents (Figure 18 and Table 14).

Façades F1 to F4 belonged to apartments of the same unoccupied buildings shown in Chapter 6. F1 was 2.50 m high and 0.25 m thick. It consisted of a perforated brick wall, EPS insulation, a non-ventilated air cavity, a hollow brick wall and gypsum plaster as an inner material layer. F2 was characterized by being the highest wall (2.70 m) and 0.32 m thick. It was comprised of external EPS insulation, a perforated brick wall, a non-ventilated air cavity, a hollow brick wall, and gypsum plaster. As seen, F1 and F2 were mainly differentiated by the position of the first two material layers. F3 was made from a limestone wall, reinforced concrete wall, rock wool insulation and plasterboard. This wall was 2.51 m high and 0.36 m thick. F4 was made of mortar, EPS insulation, a thermoclay layer and gypsum plaster on the internal face. Its dimensions

were 2.54 m high and 0.31 m thick. F5 belonged to an occupied residential building with walls 2.45 m high and 0.38 m thick. It was comprised of a stone wall, EPS insulation, a perforated brick wall and gypsum plaster. Finally, F6 was a new prefabricated panel whose dimensions were 2.64 m high and 0.30 m thick. Regarding the internal assembly, this building envelope consisted of a mortar layer, lightweight concrete, PIR insulation, a non-ventilated air cavity, another layer of lightweight concrete, and gypsum plaster.

Concerning their period of construction, façades F1, F2 and F5 were erected under the first thermal regulation that came into force (NBE-CT-79 [Spain, 1979]), satisfying the minimum thermal requirements. The rest of the building envelopes were built under the current Spanish Technical Building Code (CTE-DB-HE1 [Spain, 2006]). Notably, endoscopy tests could not be carried out. The main technical features of each wall layer were taken from the construction project documents and the manufacturers' datasheets (Table 14). Section 4.1. and Section 6.1. were undertaken to determine the theoretical U-value and the heat capacity per unit of area respectively.

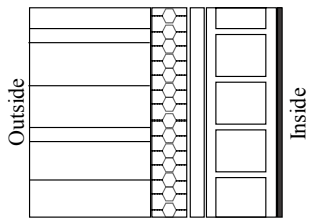

F1

Period of construction: 1981-1985

$U_t = 0.657\ W/(m^2 \cdot K)$; $k_m = 222.38\ kJ/(m^2 \cdot K)$

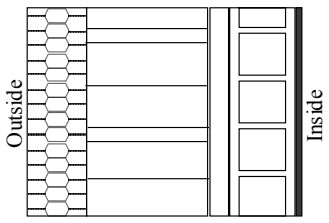

F2

Period of construction: 2005-2013

$U_t = 0.362\ W/(m^2 \cdot K)$; $k_m = 213.39\ kJ/(m^2 \cdot K)$

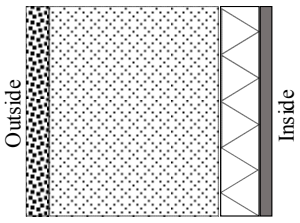

F3

Period of construction: 2006-2013

$U_t = 0.480\ W/(m^2 \cdot K)$; $k_m = 685.88\ kJ/(m^2 \cdot K)$

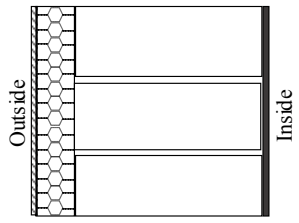

F4

Period of construction: 2007-2015

$U_t = 0.420\ W/(m^2 \cdot K)$; $k_m = 174.01\ kJ/(m^2 \cdot K)$

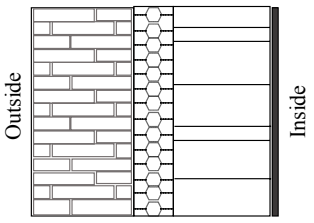

F5

Period of construction: 1990-1994

$U_t = 0.586\ W/(m^2 \cdot K)$; $k_m = 603.54\ kJ/(m^2 \cdot K)$

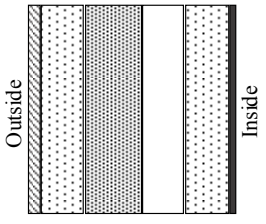

F6

Period of construction: 2015-2016

$U_t = 0.252\ W/(m^2 \cdot K)$; $k_m = 243.80\ kJ/(m^2 \cdot K)$

Figure 18. Schematic sections of the building envelopes and their year of construction

Table 14. Configuration and technical features of the façades (from outside to inside)

	N#	Material layer	Δx_i [m]	λ_i [W/(m·K)]	ρ_i [kg/m^3]	$c_{p\,i}$ [J/(kg·K)]	$R_{t\,i}$ [(m^2·K)/W]	U_t [W/(m^2·K)]	k_m [kJ/(m^2·K)]
F1	1	Perforated brick wall	0.140	---	1140	1000	0.180	0.657	222.38
	2	Insulation EPS	0.030	0.033	30	1400	0.909		
	3	Non-ventilated air cavity	0.020	---	1	1004	0.160		
	4	Hollow brick wall	0.050	---	1000	1000	0.070		
	5	Gypsum plaster	0.010	0.300	1150	1000	0.033		
F2	1	Insulation EPS	0.080	0.038	20	1400	2.125	0.362	213.39
	2	Perforated brick wall	0.140	---	1140	1000	0.180		
	3	Non-ventilated air cavity	0.050	---	1	1004	0.180		
	4	Hollow brick wall	0.040	---	1000	1000	0.090		
	5	Gypsum plaster	0.010	0.570	1150	1000	0.018		
F3	1	Limestone wall	0.030	2.300	2395	920	0.013	0.480	685.88
	2	Reinforced concrete wall	0.250	2.300	2400	1000	0.109		
	3	Rock wool insulation	0.064	0.037	40	840	1.730		
	4	Plasterboard	0.016	0.250	825	1000	0.064		
F4	1	Mortar	0.002	1.300	1900	1000	0.002	0.420	174.01
	2	Insulation EPS	0.060	---	20	1400	1.620		
	3	Thermoclay	0.240	---	910	719	0.570		
	4	Gypsum plaster	0.010	0.570	1150	100	0.018		
F5	1	Stone wall	0.180	2.200	2300	1000	---	0.586	603.54
	2	Insulation EPS	0.040	0.040	24	1340	---		
	3	Perforated brick wall	0.150	0.350	1140	1000	0.180		
	4	Gypsum plaster	0.015	0.570	1150	1000	0.018		
F6	1	Mortar	0.015	0.550	---	---	---	0.252	243.80
	2	Lightweight concrete	0.060	0.125	---	---	---		
	3	PIR insulation	0.080	0.028	---	---	---		
	4	Non-ventilated air cavity	0.060	---	---	---	0.180		
	5	Lightweight concrete	0.070	0.125	---	---	---		
	6	Gypsum plaster	0.015	0.430	---	---	---		

Δx_i: thickness of the layer; λ_i: thermal conductivity of the layer; ρ_i: density of the layer; $c_{p\,i}$: specific heat capacity of the layer; $R_{t\,i}$: notional thermal resistance of the layer; L: height of the wall; U_t: notional thermal transmittance of the building façade; k_m: the heat capacity per unit of area of the building façade

To check the hypothesis H1, the measured U-values of each wall were determined for 2 hours of sampling duration, following Section 3.5. Their respective deviations ($\Delta U/U_t$) were calculated according to Section 4.1. and plotted against time (120, 60, 30 and 15 minutes). A fluctuation of the optimum test duration might imply that it cannot be set a common criterion to facilitate the decision-making during the in-situ building diagnosis.

As can be observed in Figure 19, the optimum deviations between the theoretical and measured U-values drew fluctuations over time. In other words, they did not trend to decrease with more minutes of test duration. The lowest gap was obtained by F3 and F4 with only 30 minutes of test, since $\Delta T/U_t$ were found to be 0% and 1.19% respectively. F1 and F5 presented a deviation of 0.46% and 3.41% under 60 minutes of test. The best results for F2 and F6 were gathered at 120 minutes, achieving an error of 9.39% and 1.98% respectively. Therefore, the traditional approach cannot be used for standardizing this NDT and consequently, the development of a data-processing method is required for stopping the quantitative internal IRT measurements.

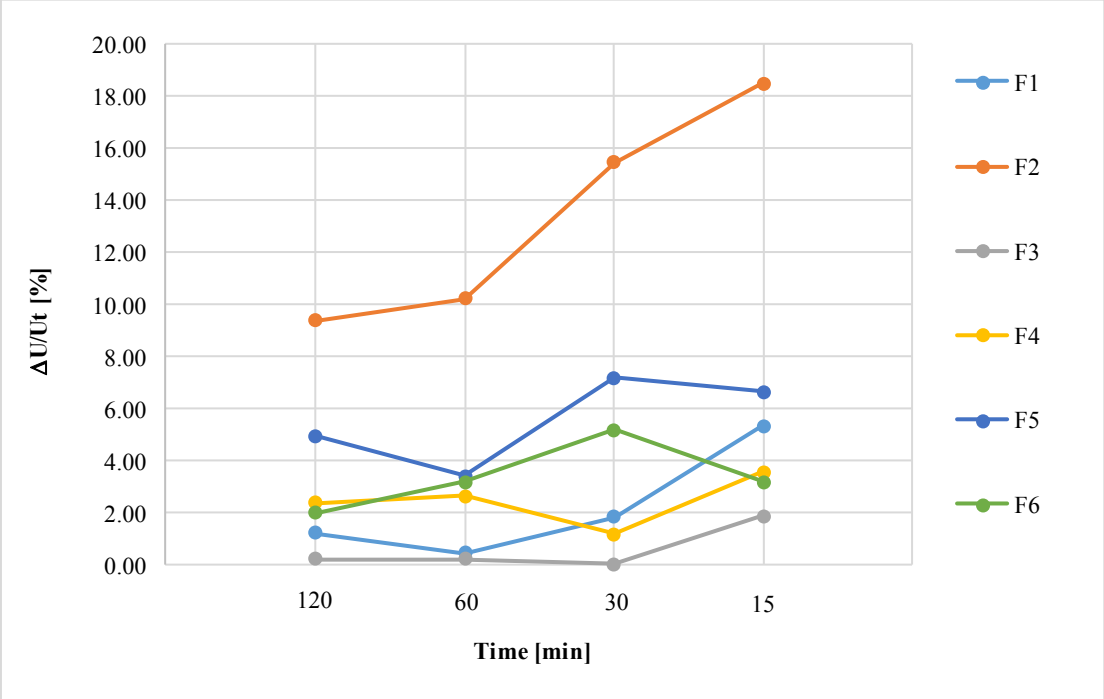

Figure 19. Deviation of the measured U-values over time

7.2 Development of a data-processing method for stopping quantitative IRT tests

7.2.1 U-value time series analysis

The proposed data-processing method is represented in Figure 20.

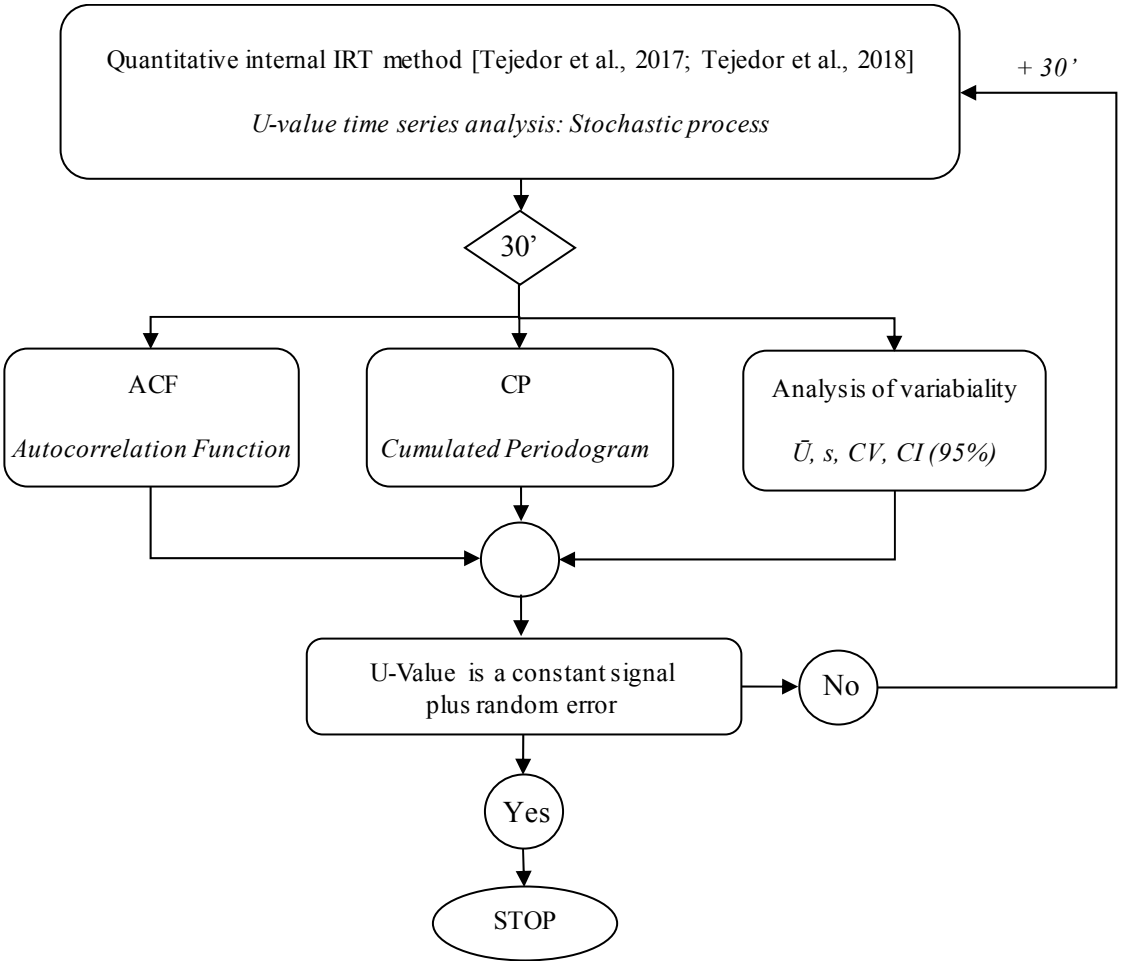

Figure 20. Flowchart of the proposed data-processing method

Theoretically, the instantaneous measured U-values ($U_{mes\ i}$) should define a constant mean over time that would be known as $U_{mes\ avg}$ or $\bar{U}$ [W/ ($m^2 \cdot K$)] and would be obtained at the end of an IRT survey from a specific number of thermograms (n), as shown in Equation 2 of Section 3.5.

Nevertheless, it can be assumed that the quantitative internal IRT measurements describe a stochastic process of underlying data in practice, since a time series is a set of consecutive samples collected over a time interval and they are ubiquitous in any field that involves data monitoring [Yaffee et al., 2000; Mahan et al., 2015]. Moreover, time series can lead to an understanding of evolving processes or provide information about trends [Mahan et al., 2015].

Figure 21 is shown to support the aforementioned assumption. The instantaneous measured U-values draw a constant signal as a function of time with a certain noise [e_k *(t)*] that is characterized by random values with a constant mean and variance, normally and independently distributed, and uncorrelated (Equation 16). In accordance with Mahan et al. [2015], this last aspect is known as "white noise".

$$U(t) = \bar{U} + e_k(t) \tag{16}$$

Hence, the hypothesis of a stochastic process comprised of a constant signal plus white noise might be evaluated for a U-value time series with different test durations.

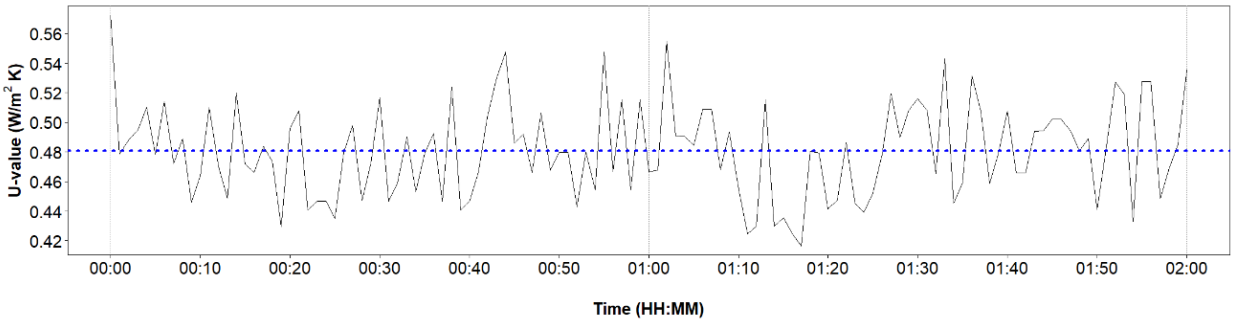

Figure 21. Example of a quantitative internal IRT test taken as a stochastic process

In accordance with the statement exposed above, the measurement noise [e_k *(t)*] might also be determined over time, assuming this parameter as the residuals if [*U(t)*] is modelled as a constant signal (Equation 17). To confirm that the measurement noise is fitted to white noise, the autocorrelation function (ACF) and the cumulated periodogram (CP) were used. Both had been used on previous studies for other fields that involved monitored data [Andersen et al., 2000; Bacher et al., 2011; Macarulla et al., 2017; Macarulla et al., 2018].

$$e_k(t) = \bar{U} - U(t) \tag{17}$$

The ACF measures the correlation between observations at different times [Meko, 2010]. When a process is non-stationary, it does not tail away to zero quickly or cut-off after finite number of steps [Mahan et al., 2015]. Hence, the ACF of the signal should not contain statistically significant terms more than the number expected by chance. This number depends on the number of lags or delays [Mahan et al., 2015], which is one time unit for the first-order autocorrelation [Meko, 2010].

The CP is the vector of partial sums of the periodogram, normalized by the sum of all of elements. Since the Fourier transform of the residuals is obtained by a linear transformation with an orthogonal matrix, the real and imaginary parts of the transform model would still be distributed independently and normally [Rust et al., 2008]. The test is focused on constructing two lines parallel to the one above and passing through the

points ±5% point of the Kolomogorov-Smirnov statistics. These aforementioned lines define a 95% confidence level band for white noise [Fuller et al., 1996; Rust et al., 2008].

In both statistical tests, the analysis was performed for 120, 60 and 30 points that correspond to the minutes of test duration. The limitation related to the minimum data points was supported as follows. Roughly speaking, a sample size of at least 40-100 repeat observations was recommended. Otherwise, due to sampling error, the estimated functions might not contain enough information for a meaningful identification [Box and Jenkins, 1976; Anderson et al., 1977; Huitema et al., 1991; De Carlo et al., 1993; Lúnden et al., 2000]. However, statisticians and researchers adopted a general criterion based on the central limit theorem (CLT) in which the sample size should be $N \geq 30$ in practice, to assume the distribution of sample mean approximated to the normal distribution [Plane and Gordon, 1982; Chang and Chen, 2008]. The shapes of probability distributions may vary for $N \leq 30$ [Chang and Chen, 2008].

Finally, to determine the variability among the instantaneous U-values of each time series for all investigated buildings, the following parameters were calculated: the mean ($\bar{U}$), the standard deviation (SD or σ), and the coefficient of variation (CV). Subsequently, the 95% confidence intervals were also statistically estimated to observe whether the readings of each time series were equal to each other. In other words, the aim was to evaluate whether there was a relevant difference among average measured U-values resulting from 120, 60 and 30 minutes. The following expression (Equation 18) was applied to calculate the 95% confidence intervals (CI), taking into account that *n* is the specific number of thermograms or data points to be analyzed:

$$CI\ (95\%) = \bar{U} \pm 1.96 \cdot \frac{\sigma}{\sqrt{n}} \tag{18}$$

7.2.2 Implementation of the proposed data-processing method

Roughly speaking, the data-processing method reported in Section 7.2.1. might allow observing tendencies of the IRT signal with the reduction of the sampling duration. In other words, it could provide enough statistical information to detect if the IRT signal draws cycles, which could indicate that the quantitative internal IRT test is being executed under a transitory regime and consequently, more observations should be required with a data acquisition interval of 1 minute in order to achieve reliable values. The results of each building façade are shown in Figures 22-28 and Tables 15 - 16.

Table 15. Summary of results. Average measured U-values ($\bar{U}$), standard deviation (σ), coefficient of variation (CV) and validation of the hypothesis of a constant signal plus white noise

	ΔT [ºC]	**Time** [min]	**$\bar{U}$** [W/m²·K]	**σ** [W/m²·K]	**CV** [%]	**Hypothesis**
F1	6.80 < ΔT < 8.70	120	0.665	0.047	7.08	Fulfilled
		60	0.654	0.047	7.29	Fulfilled
		30	0.645	0.052	8.13	Fulfilled
F2	7.60 < ΔT < 9.10	120	0.396	0.050	12.70	Fulfilled
		60	0.399	0.056	13.97	Fulfilled
		30	0.418	0.054	12.99	Fulfilled
F3	5.80 < ΔT < 8.20	120	0.481	0.032	6.67	Fulfilled
		60	0.481	0.030	6.34	Fulfilled
		30	0.480	0.031	6.42	Fulfilled
F4	8.70 < ΔT < 9.60	120	0.430	0.031	7.25	Fulfilled
		60	0.431	0.033	7.69	Fulfilled
		30	0.425	0.034	8.12	Fulfilled
F5	18.30 < ΔT< 19.60	120	0.557	0.028	4.97	Fulfilled
		60	0.566	0.028	5.02	Fulfilled
		30	0.554	0.031	5.68	Fulfilled
F6	8.20 < ΔT < 10.40	120	0.257	0.018	7.16	Fulfilled
		60	0.260	0.019	7.32	Fulfilled
		30	0.265	0.019	7.18	Fulfilled

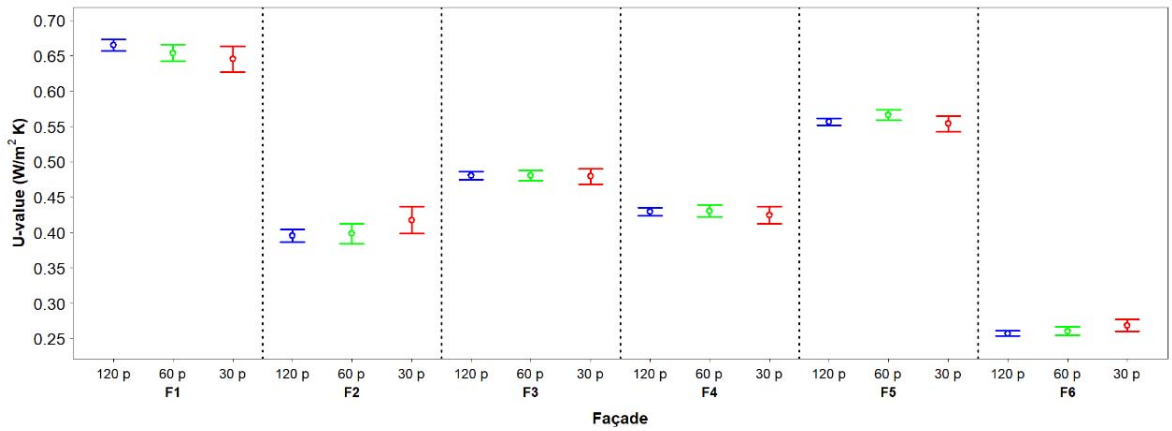

Figure 22. Graphical representation of 95% confidence intervals for U-value estimations

Table 16. Estimation variability

	F1	F2	F3	F4	F5	F6
Estimation mean [W/m²·K]	0.654	0.404	0.480	0.428	0.559	0.261
$\lvert \bar{U}_{120} - \bar{U}_{60} \rvert$	0.011	0.003	0.000	0.001	0.010	0.003
$\lvert \bar{U}_{60} - \bar{U}_{30} \rvert$	0.009	0.019	0.001	0.006	0.012	0.006
$\lvert \bar{U}_{120} - \bar{U}_{30} \rvert$	0.020	0.022	0.001	0.005	0.003	0.008
Estimation standard deviation [W/m²·K]	0.049	0.053	0.031	0.033	0.029	0.019
$\lvert \sigma_{120} - \sigma_{60} \rvert$	0.000	0.005	0.002	0.002	0.001	0.001
$\lvert \sigma_{60} - \sigma_{30} \rvert$	0.005	0.001	0.000	0.001	0.003	0.000
$\lvert \sigma_{120} - \sigma_{30} \rvert$	0.005	0.004	0.001	0.003	0.004	0.001
Estimation coefficient of variation [%]	7.49	13.22	6.48	7.69	5.22	7.22
$\lvert CV_{120} - CV_{60} \rvert$	0.18	1.27	0.33	0.43	0.04	0.16
$\lvert CV_{60} - CV_{30} \rvert$	0.87	0.97	0.09	0.43	0.66	0.13
$\lvert CV_{120} - CV_{30} \rvert$	1.05	0.29	0.24	0.87	0.70	0.02

The façade F1 was characterized by an average thermal transmittance of 0.665 W/m²·K for 120 minutes, 0.654 W/m²·K for 60 minutes and 0.645 W/m²·K for 30 minutes (Table 15). The left graphs of Figure 23 plot the noise [$e_k(t)$] of in-situ measured U-values as a function of time. Discontinuous black lines represent the average value, that is 0, and the discontinuous blue lines represent ±σ. The e_k values reached peaks between 0±0.08 W/m²·K and 0±0.12 W/m²·K. From the above aspects, it can be state that the IRT tests were reliable. In accordance with Table 16, the deviation of the results was low with respect to the average value obtained from the three times series ($\bar{U}$=0.654 W/m²·K). As seen in Figure 23, the results of the ACF revealed that some lags fell outside the 95 % confidence interval (2 for 120 minutes, 3 for 60 minutes and 1 for 30 minutes). Nevertheless, these lags did not exceed the expected values. Moreover, no cycles or trends were observed in the three time series. Only one peak in the CP was detected, but it was of minor importance. Hence, it can be affirmed that the measurements can be regarded as a constant signal plus white noise.

The analysis of the graphical representation of 95% confidence intervals (Table 15; Figure 22), revealed that there was no significance among the measured U-values for the three test durations. In addition, the other statistical parameters related to the variability of the measurements indicated a similar dispersion (Figure 23; Tables 15-16). The standard deviations were found to be between 0.047 W/m²·K and 0.052 W/m²·K. The coefficients of variation (CV) ranged from 7.08 % to 8.13 %.

In accordance with the aspects described above, the in-situ thermal transmittance of F1 might have been determined after only 30 minutes.

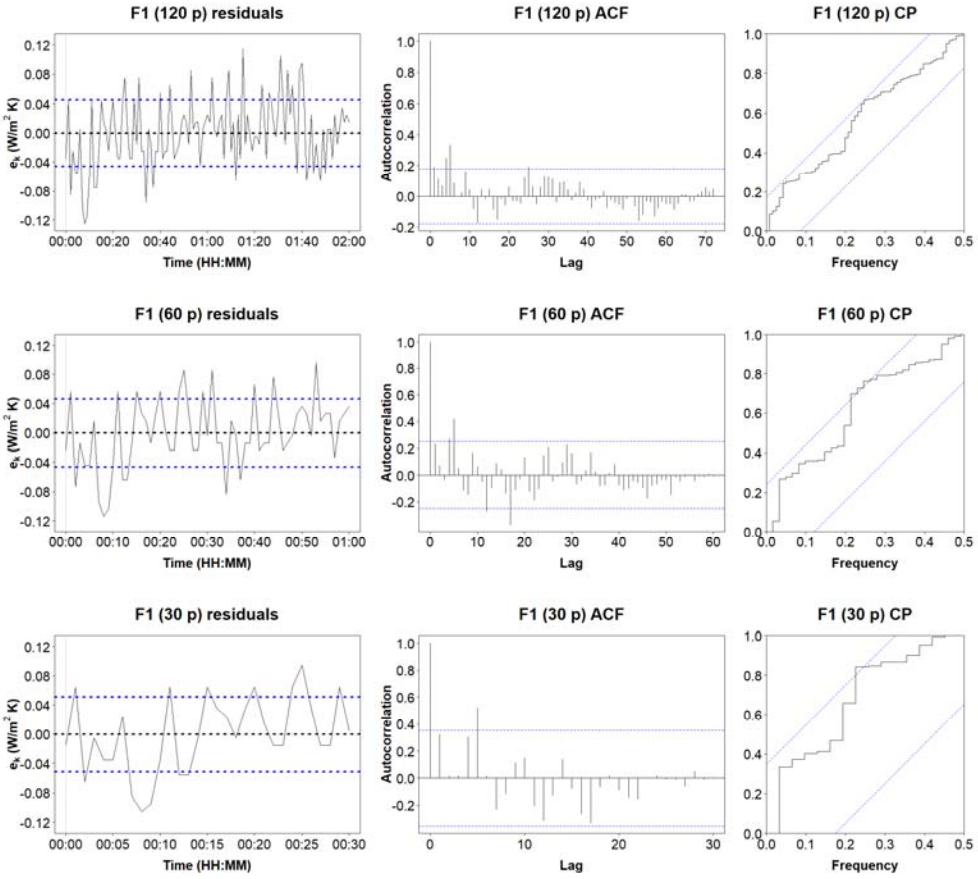

Figure 23. The left column shows the residuals of the measured data for F1. The middle column presents the ACF plot for F1. The right column indicates the CP for F1

Most residuals of the quantitative internal IRT measurements of F2 were found to be reliable for the three sampling durations. The average measured U-value of F2 was 0.404 ± 0.053 W/m^2·K (Table 16) and the partial data were: 0.396 W/m^2·K for 120 minutes, 0.399 W/m^2·K for 60 minutes and 0.418 W/m^2·K for 30 minutes (Table 15). Hence, the IRT tests can be deemed acceptable. However, the difference between the partial average measured thermal transmittances for 120 and 60 minutes was only 0.003 W/m^2·K, whereas $| \bar{U}_{120} - \bar{U}_{30} |$ increased to 0.022 W/m^2·K (Table 16). Indeed, and considering all façades, this last value was noted as the highest.

The ACFs did not have any peak and the CPs provided a similar information (Figure 24). The values were fit to the top confidence interval band. Considering the aspects mentioned above, the quantitative internal IRT measurements of F2 could be accepted as a constant signal plus white noise and a constant sigma independent from the test duration for heavy multi-leaf walls with a low U-value.

The analysis of the variability of measurements obtained for this building envelope (Tables 15-16) leads to the conclusion that this façade wall presented worse values of standard deviation (σ=0.050-0.056 W/m^2·K) and coefficient of variation (12.70 % < CV < 13.97 %) than the other investigated samples. There

was substantially more variation for the test with 30 data points, as indicated in Figure 22 and Table 16. However, the outcomes of the three test durations might be accepted as valid.

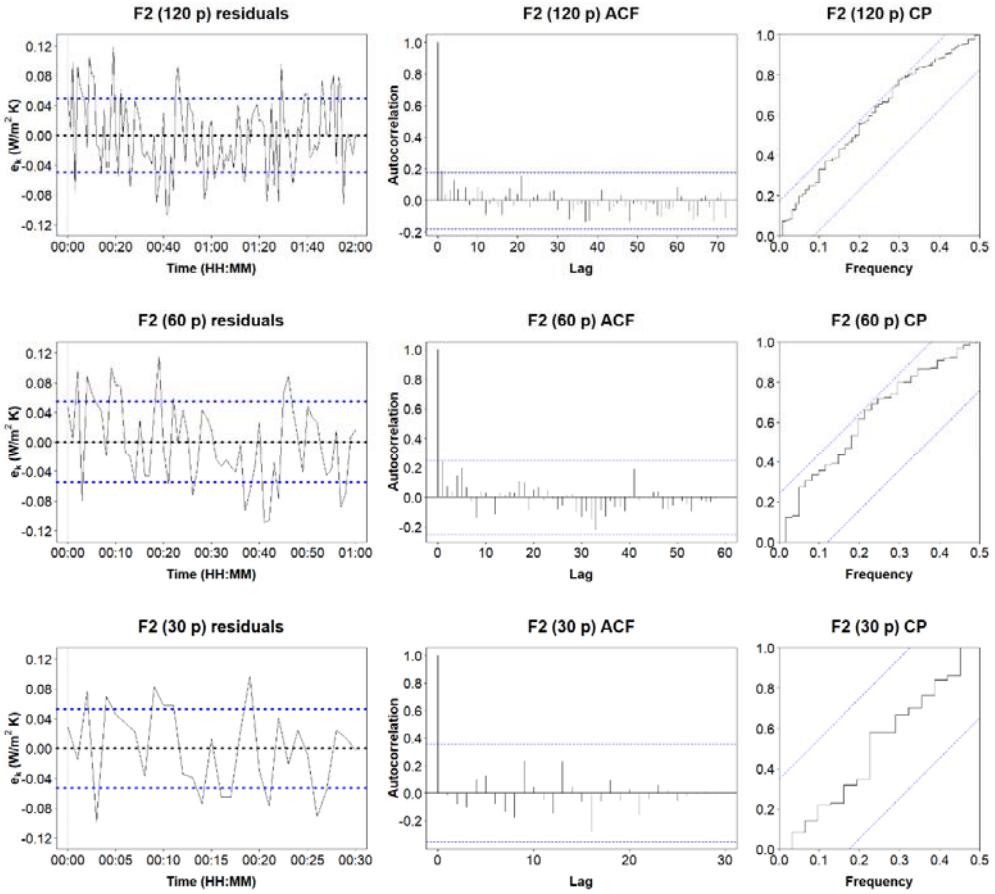

Figure 24. The left column shows the residuals of the measured data for F2. The middle column presents the ACF plot for F2. The right column indicates the CP for F2

The best results were gathered for F3, since the collected data for this building envelope showed extremely similar signals (Table 15): 0.481±0.032 W/m^2·K for 120 minutes; 0.481±0.030 W/m^2·K for 60 minutes; and 0.480±0.031 W/m^2·K for 30 minutes. As seen in Table 16, the deviations among the results were minimal (Table 16) and only four residual peaks presented a value over $e_k = 0 + 0.06$ W/m^2·K (Figure 25).

The above aspects were corroborated with the time series analysis. No significant term was detected in the ACF plots (Figure 25; the middle column). In addition, the CPs of F3 (Figure 25; the right column) were slightly better than the rest of the investigated buildings (the signal described almost a straight line in the middle of the space defined by the two lines of the 95% confidence level band). Hence, it can be affirmed that U-value measurements could be considered a signal with a constant mean plus white noise for each test duration. Regarding the variability (Table 15), the CV was found to be between 6.34% and 6.67%. Therefore, the difference of variability on instantaneous readings was set at 0.24% (Table 16). The standard deviation showed the same value ($\sigma \sim 0.030$ W/m^2·K), regardless of the sampling duration to be validated.

These aspects were supported by the graphical representation of the 95% confidence intervals (Figure 22), which were practically the same size. In other words, the same degree of dispersion and skewness was produced in all data.

Considering the aforementioned aspects, it can be extrapolated that 30 minutes might be enough to calculate the in-situ thermal transmittance of F3.

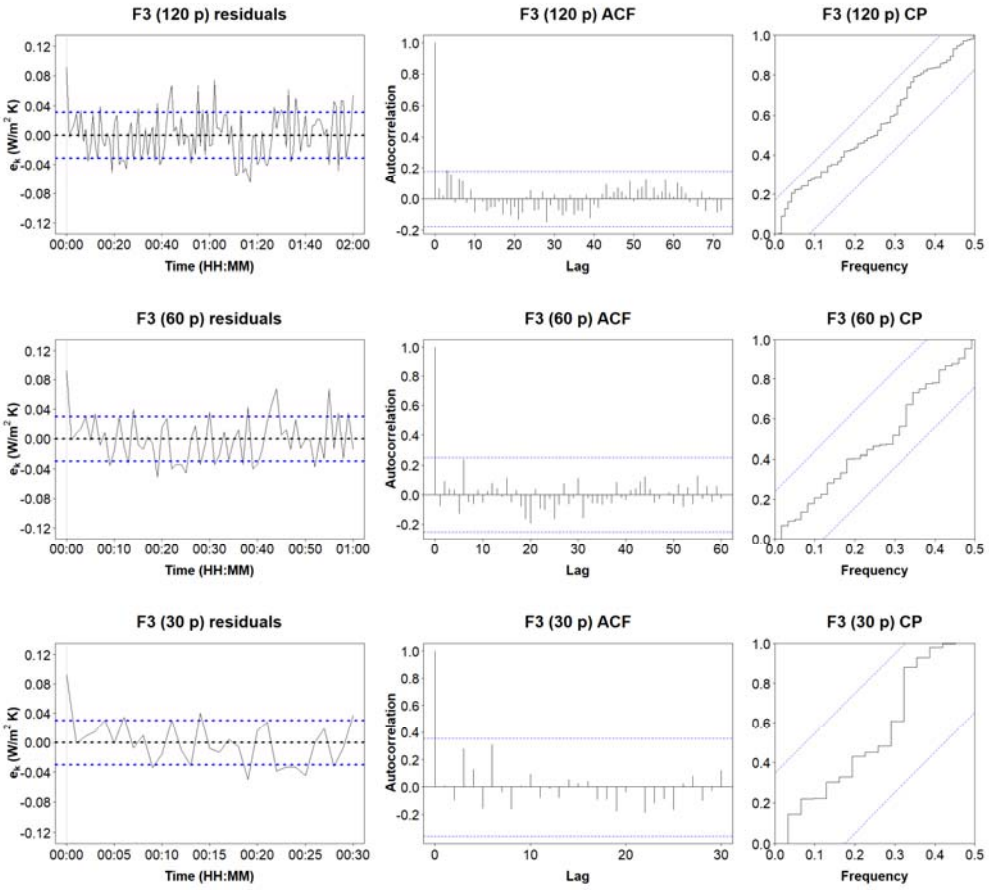

Figure 25. The left column shows the residuals of the measured data for F3. The middle column presents the ACF plot for F3. The right column indicates the CP for F3

In the representation of the residuals of the U-values for F4 as a function of time (Figure 26), some peaks were distinguished outside of the range [0±σ]. However, they remained under e_k= 0±0.06 W/m^2·K. The partial measured U-values were: 0.430±0.031 W/m^2·K for 120 minutes, 0.431±0.033 W/m^2·K for 60 minutes, and 0.425±0.034 W/m^2·K for 30 minutes (Tables 15-16). To evaluate in-depth whether the outcomes of this building envelope might be considered reliable, the results needed to be compared with the time series analysis and the study of data variability.

In the ACF plot, one significant term was noted for all test durations (Figure 26). Actually, a slight cyclical trend might be described for 60 lags in the graph, but the signals obtained for 120 minutes and 30 minutes discarded this aspect. It can be extrapolated that practically all readings were inside the 95% confidence interval band, as seen in the CP.

The analysis on the variability of the results (Figure 22; Tables 15-16) presented similar standard deviations for all signals (σ=0.031-0.034 W/m^2·K) and coefficients of variation (7.25 % < CV < 8.12 %). In the graphical representation of the 95% confidence intervals for the U-value estimations, the dispersion of data were slightly higher for the test that took 30 minutes. These aspects revealed that the hypothesis of a signal with constant mean plus white noise can be adopted for quantitative IRT measurements.

Overall, the results revealed that the procedure for all tests was correct and the minimum sampling duration might be adopted for F4.

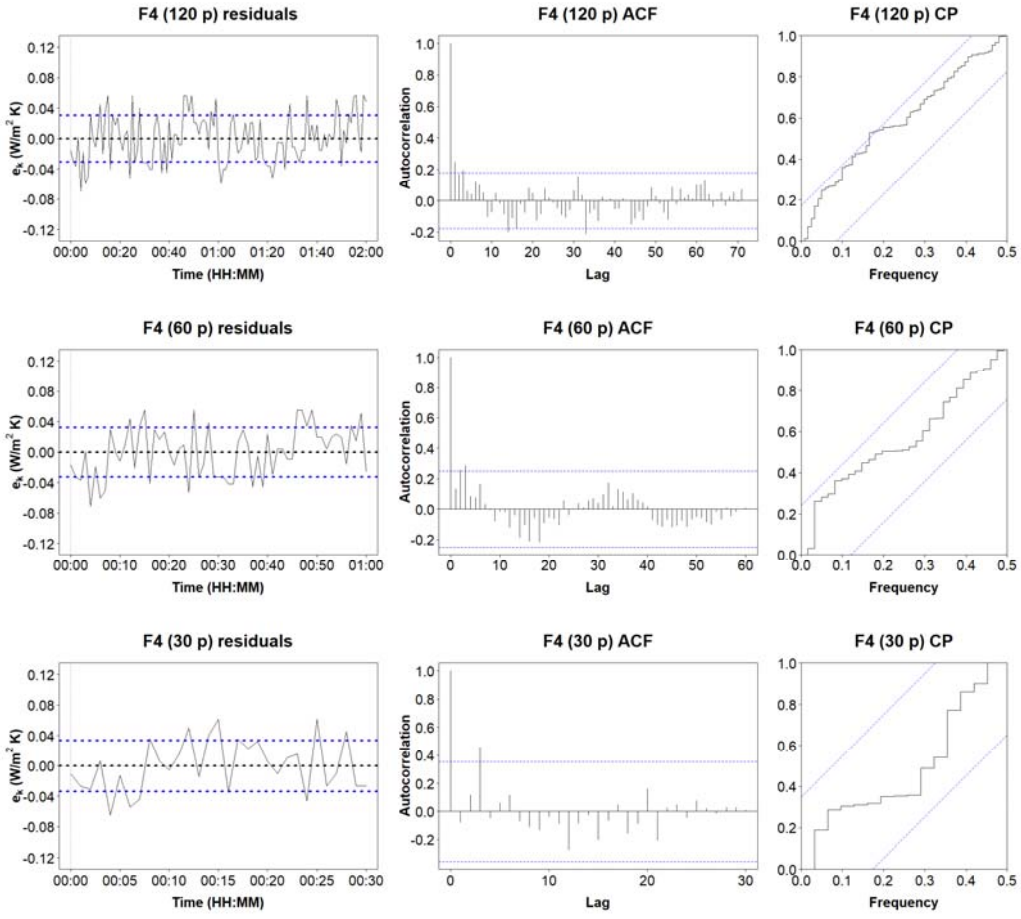

Figure 26. The left column shows the residuals of the measured data for F4. The middle column presents the ACF plot for F4. The right column indicates the CP for F4

Most residuals of U-values for F5 plotted against time were found to be far closer to sigma over the tests. The intervals of the U-value measurements were: 0.557±0.028 W/m^2·K for 120 minutes; 0.566±0.028 W/m^2·K for 60 minutes; 0.554±0.031 W/m^2·K for 30 minutes (Tables 15-16). The statistical parameters were all inside the acceptable range (Table 15), but the data points did not tail away to zero very quickly at the beginning of the tests, especially when the test duration was set at 120 minutes (see the ACF -Figure 27-). Nine significant terms were detected. The residuals of measured U-values fell slightly outside the top band of the 95% confidence interval (see the CP -Figure 27-). It should be noted that the behavior of the signals over time was better for 60 or 30 minutes.

From the analysis of variability (Table 15 and Figure 22), it can be extrapolated that façade F5 had the lowest CV, reaching values between 4.97% and 5.68%. This means that the dispersion of the probability distribution was low. Notably, the difference between the minimum and maximum values of this last statistical parameter was found to be 0.71% (Table 16). The standard deviations were found to be 0.028 W/m^2·K for 120 and 60 minutes and 0.031 W/m^2·K for 30 minutes. These facts support the statement that 120 data points are not necessary and the required test duration might be reduced to 30 minutes, as also shown in the graphical representation of 95 % confidence intervals (Figure 22).

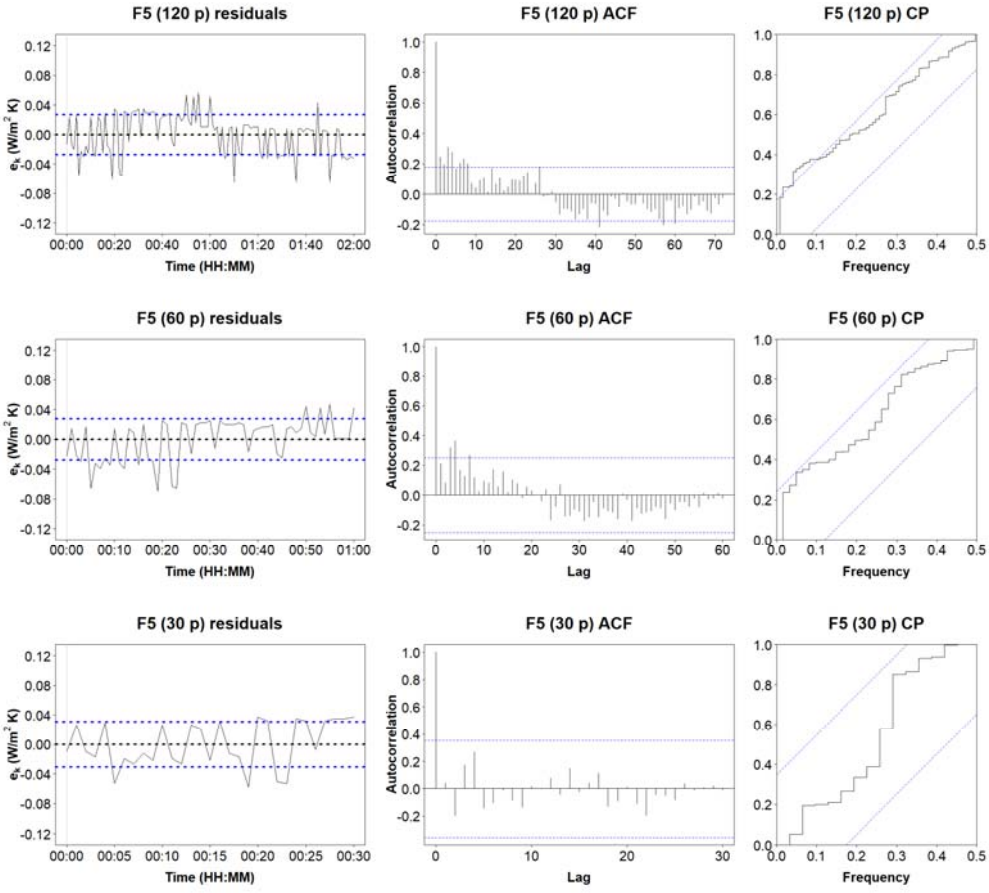

Figure 27. The left column shows the residuals of the measured data for F5. The middle column presents the ACF plot for F5. The right column indicates the CP for F5

In the graphical representation of the residuals of U-values for F6 in function of time (Figure 28), most of the data points showed minor e_k values throughout the tests in comparison with other façades. The average thermal transmittance values were 0.257 W/m^2·K for 120 minutes, 0.260 W/m^2·K for 60 minutes and 0.265 W/m^2·K for 30 minutes (Tables 15-16). According to Figure 28, some peaks of minor importance were observed in both ACF and CP for 120 points. As seen, it could be stated that the gathered measurements can be regarded as a constant mean plus white noise and this façade presented stationarity throughout the tests. In contrast with other heavy multi-leaf walls, some aspects related to the analysis of variability can be highlighted (Tables 15-16). F6 had the lowest values of standard deviation, reaching a maximum value of 0.019 W/m^2·K. The CVs were around 7% like other evaluated samples, but the variation among partial data were extremely low (0.02 % -Table 16-). Indeed, the results of both statistical parameters were expected, since F6 showed minor residual values (e_k) throughout the tests in comparison with other façades (Figure 28). Taking into account these aspects, it can be assumed that all time series defined a signal with constant mean plus white noise and the hypothesis of stationarity can be fulfilled. Concerning the graphical representation of the 95% confidence intervals (Figure 22), the outcomes showed a downward trend of the average measured U-value and its confidence intervals were far smaller for a greater sampling duration. Therefore, only 30 minutes might be required to determine the in-situ measured U-value.

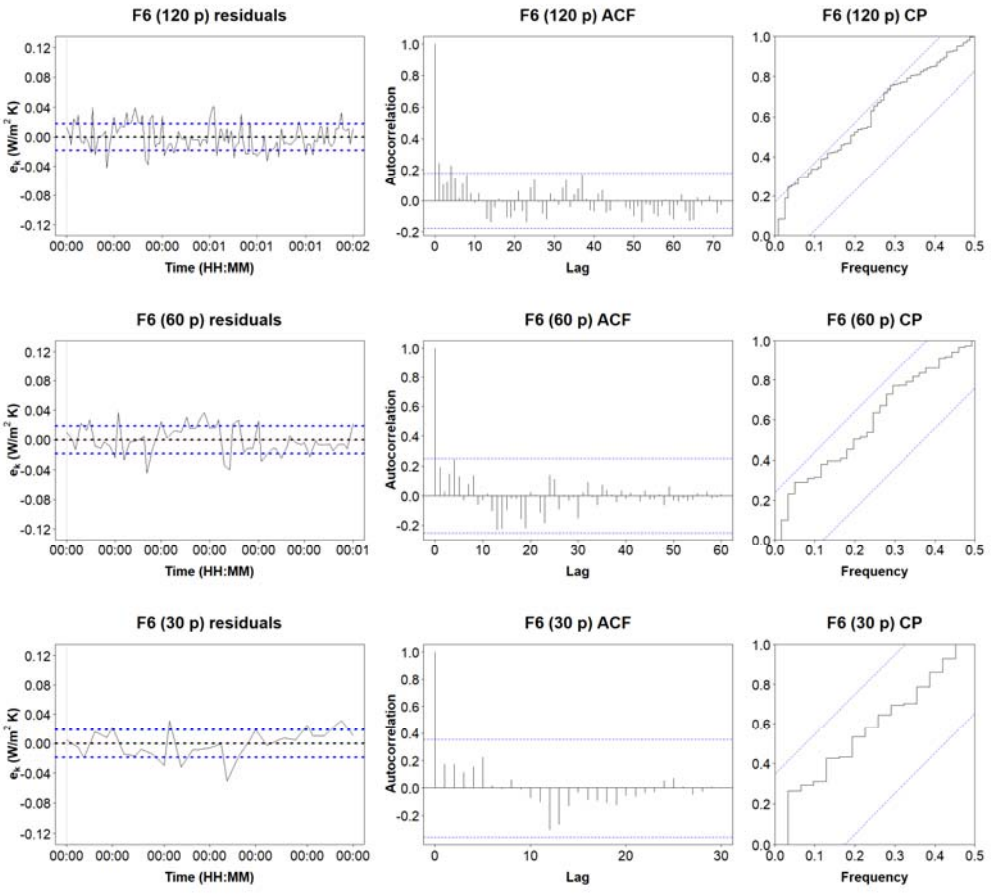

Figure 28. The left column shows the residuals of the measured data for F6. The middle column presents the ACF plot for F6. The right column indicates the CP for F6

Overall, it can be concluded that all statistical results reported reasonable values. Hence, it can be stated that 30 minutes might be enough to determine in-situ measured U-values. The proposed hypothesis for the U-values time series analysis was fulfilled for all investigated samples, to obtain a signal with a constant mean plus white noise. The deviation in the three means ($\bar{U}$) for each façade was low compared to the average value of calculated in Table 16. This aspect was in line with the results of the ACF and CP plots, where some lags fell outside the 95% confidence interval but were less than 5% (Figures 22-28).

The graphical representation of the 95% confidence intervals of all investigated façades suggested that the variability in the measurements did not differ significantly among the three selected sampling durations (Table 15-16; Figure 22). In fact, confidence intervals were extremely similar among samples (i.e. F1 and F2; F3 to F6) and were slightly greater for 30 points. This last aspect was expected due to a reduction in the sample size for the time series. In other words, the confidence interval is defined as CI = f ($\bar{U}$, σ, n) in accordance with Section 7.2.1. If the mean and sigma remained practically constant among tests, the only parameter that entailed an increase or decrease in CI length was the number of thermograms to be analysed. Moreover, the comparative analysis among sigma values gathered for each time series (Table 16) showed that the differences ranged around zero, reaching 0.005 $W/m^2 \cdot K$ as a maximum. The CVs were also low (from 4.97 to 8.13% for façades F1, F3-F6), except façade F2 (12.70 to 13.97%). As seen in Table 16, the differences in CVs among time series were found to be under 1% in most cases. Therefore, the execution time that was commonly applied by other researchers would not represent an improvement in the results. Moreover, the test duration might not be undertaken as an influential factor in the determination of measured U-values. This leads to consider the possibility of evaluating short test durations with a higher sampling frequency in future steps of the research.

A thorough literature review showed that quantitative internal IRT did not have a limit for the CV. Nevertheless, the results of this research were consistent with previous studies on other techniques, such as the standardized HFM method [Roulet et al., 1987; Flanders et al., 1992; ASTM C1555-95 (2013) -American Society for Testing Materials, 2013-; ISO 9869:2014 -International Organization for Standardization, 2014-; Ahmad et al., 2014; Ficco et al., 2015; Meng et al., 2015; Atsonios et al., 2017; Gaspar et al., 2018].

7.3 Validation of the proposed data-processing method

7.3.1 Definition of the validation process

To validate the results obtained by the U-value time series analysis, it is required to apply an alternative and recognised method. Wiener [1949] and Brown et al. [1996] carried out several studies about extrapolation, interpolation or smoothing of stationary and transient time series for engineering applications. Within the enhancement of the heat transfer measurements, some authors compared inverse heat conduction problems (IHCP) using experimental data to determine thermal properties [Beck et al., 1996; Ilyinsky et al., 1997; Le Niliot et al., 1998; Rainieri et al., 1998; Rainieri et al., 2002]. Le Niliot et al. [1998] combined thermographic measurements with numerical techniques to identify unknown heat line sources and boundary conditions for the transient diffusion problem. Ilyinsky et al. [1997] and Rainieri et al. [2002] determined the local distribution of the heat transfer coefficient in thermal systems, applying a filtering technique to remove the undesired noise assumed as random uncertainties in temperature measurements. Their methods were based on the Fourier Transform technique to estimate the heat source distribution in a square domain, taking the surface map recorded by an IR camera as a starting point. Rainieri et al. [2002] applied this type of analysis to compact heat exchangers. They concluded that Wiener filter might be more efficient compared to other traditional filtering procedures, using the "Signal Processing Toolbox" and the "Image Processing Toolbox" of MATLAB software [Mathworks, 1998]. Jiménez et al. [2008] used the "IDENT Toolbox" of MATLAB Software [Mathworks, 2006] to calculate the thermal properties of building elements for tests undertaken from outside the building under transient conditions. In this case, the authors exposed how RC-network models can be formulated as ARMAX or ARX models by means of MATLAB. It should be noted that only ARX models might simplify the analysis without loss of generality. They stated that if the predictions were correctly calculated, then the one-step prediction error or residual could be considered as a white noise sequence. Despite this, similar approaches have not been used to reduce the test duration of quantitative internal IRT tests under stationary conditions. Only Biddulph et al. [2014] combined physical models and Bayesian networks to reduce the U-value monitoring period under dynamic conditions for the HFM.

Taking into account the aspects mentioned above, the "System Identification Tool" of MATLAB Software [Mathworks, 2018] was applied in this study. Firstly, operation pre-processes of the signal (i.e. filters) and several models (i.e. ARX, ARMAX etc) were developed, introducing the IRT data into the "System Identification Tool" of MATLAB Software [Mathworks, 2018]. Secondly, to detect if the results provided by reduced order models were correct, the following aspects were checked: the stability of the model, the resonance state in the frequency response plot, the distribution of zeros and pols and the ACF of the residuals at 95% confidence level.

7.3.2 Validation results

As mentioned above, a validation process was conducted on this study using the "System Identification Tool" of MATLAB Software [Mathworks, 2018] in order to support the results obtained by the U-value time series analysis.

The comparative analysis among the developed models and the original IRT signals showed that the modelled signal was practically stable and continuous with only 30 minutes of test duration (Figure 29). In addition, the respective U-values were slightly the same. Hence, these results confirm the assumption set previously (Section 7.2). The details of the development of the model by MATLAB are reported below.

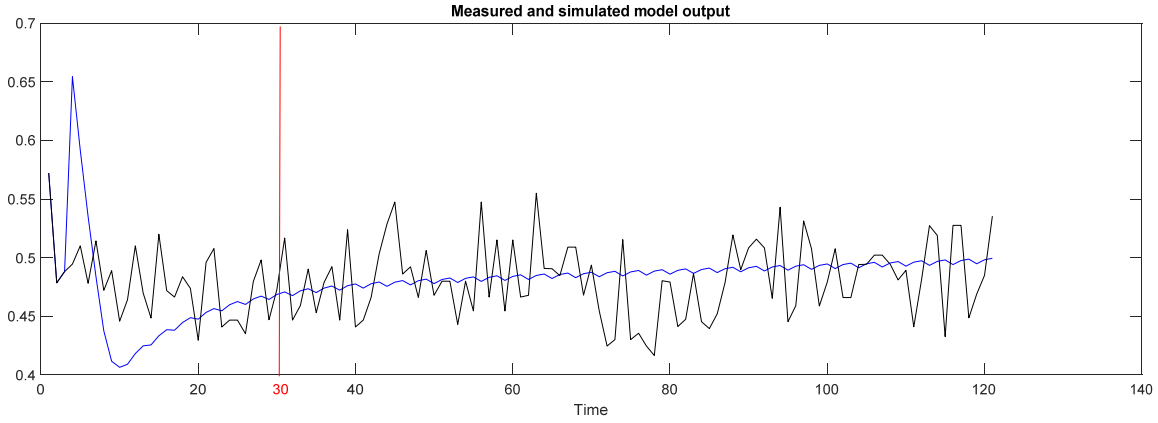

Figure 29. Façade 3. IRT measurements and model output

In the operation pre-processes, several options were tested: "remove means", "remove trends" and "filters. However, the obtained results for each façade were worse than the original IRT signals provided by the quantitative internal IRT measurements. These options led to instable models with peaks of resonance. Furthermore, the residuals fell totally outside the confidence intervals bands at 95%.

Regarding the modelling of the working data, "Transfer Function Model" and "Polynomial Models" among others were checked. The results revealed that the models that better fitted with the reference signal were ARX or ARMX. The current U-value [A(z)y(t)] on the ARX model only depended on the previous U-value [B(z)u(t)], since the exponent of the term [B(z)u(t)] was 1. The model was stable for all heavy multi-leaf walls if it was constituted by a simple structure (na=1, nb=4, nk=7). According to Jiménez et al. [2008], na denotes the order of polynomial $A(q)$, nb the order of polynomial $B(q)$, and nk the delay between output and input. In this thesis, the analysis was limited to models with na, nb and nk, varying between 1 and 10.

By way of example, the results of façade F3 are presented. Figure 30 shows the typical model structure for this building envelope. The models indicated as "Best Fit" (red) by the "System Identification Tool" were those characterized by *na=10*, *nb= 10* and *nk=8*. Nevertheless, the MDL Choice (green) was enough for this study, since the biggest change in the model was generated at the beginning and provided less complexity in the execution.

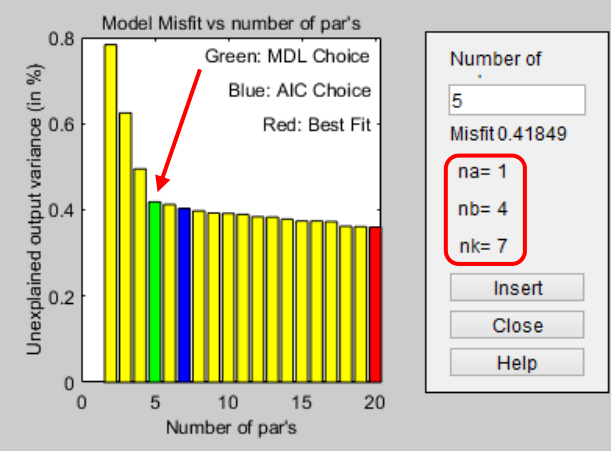

Figure 30. Façade 3. ARX model structure

According to Figure 31, the model ARX was stable, because all zeros and pols were located inside the unit circle. The frequency function does not show signals of instability for a simple model structure. However, several peaks of resonance were detected when the complexity of the model increased (Figure 32). In the ACF of the residuals, all observations were inside the confidence interval bands at 95% (Figure 33).

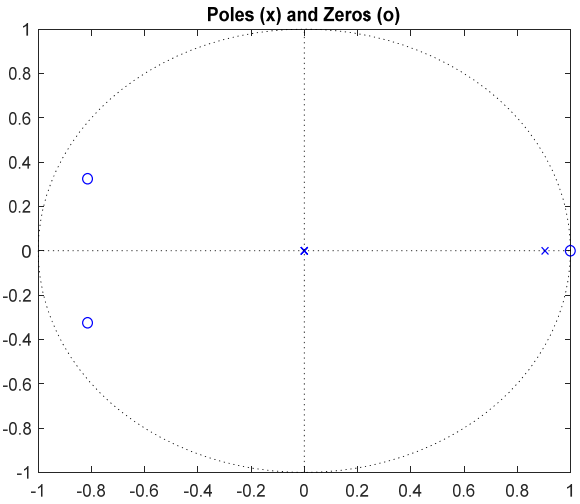

Figure 31. Zeros and pols plot for façades F3

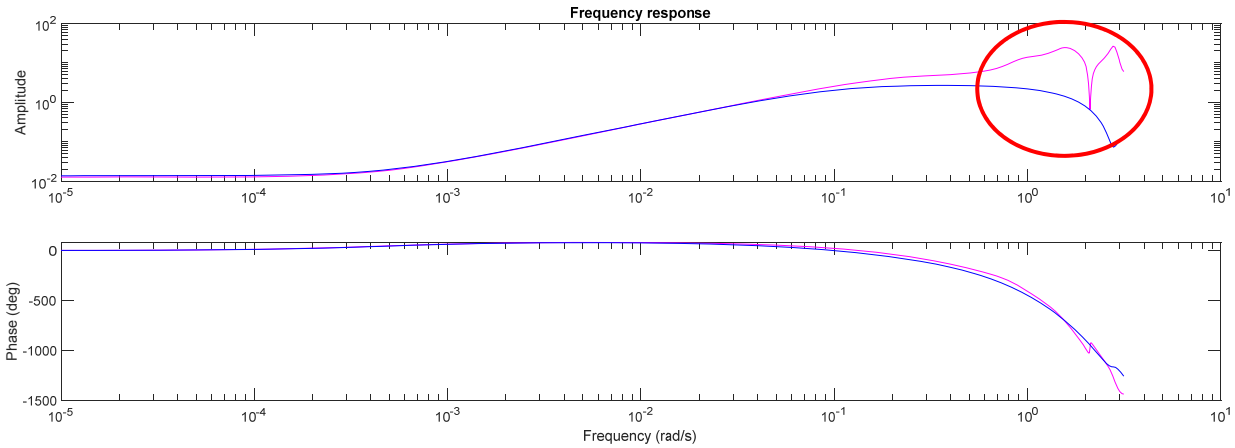

Figure 32. Frequency response for façade F3. Peaks of resonance when the complexity of the model increased

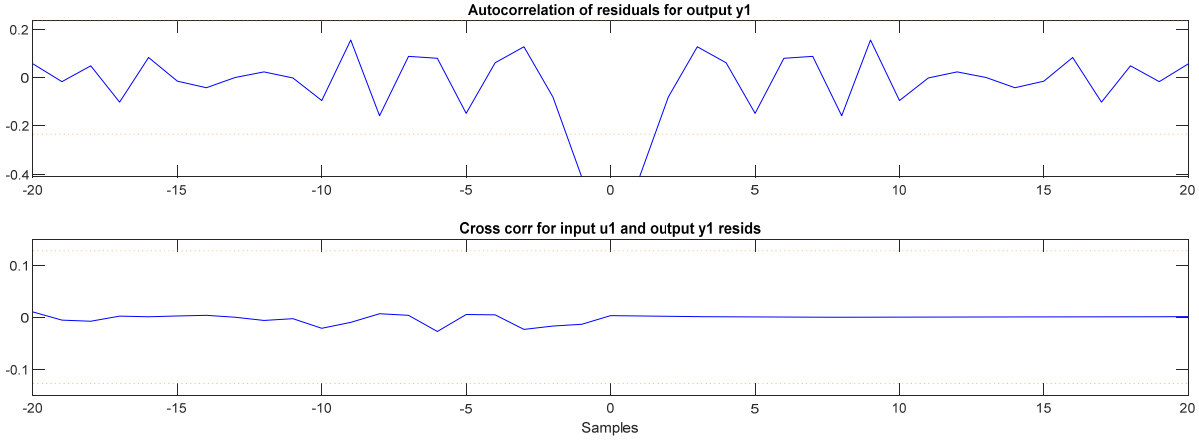

Figure 33. ACF of residuals for façades F3

Chapter 8: Conclusions and further research

This chapter concludes the dissertation with a summary of the main contributions of this research and their possible impact on the field of quantitative internal IRT, adopting the measured thermal transmittance as an indicator of the built quality. During the dissertation undertaken, interesting questions were raised although could not be addressed. These issues are presented as possible future research lines.

8.1 The main contributions of the research

The main findings and implications of this dissertation are presented below, demonstrating how the objectives stated at the beginning have been achieved by the undertaken research.

The first and the second specific objectives of this thesis were focused on identifying the contributory factors of the Energy Performance Gap as well as examining the measurement techniques that are used to assess the thermal behaviour of façades.

The third specific objective consisted of proposing a quantitative internal IRT method in order to determine the in-situ measured thermal transmittances of building envelopes under steady-state conditions. Subsequently, a validation of the method was conducted on two steps: (i) execution of preliminary studies in a laboratory of thermal engineering, to calibrate the numerical model; (ii) implementation of the proposed method on real built environments. In this sense, the aforementioned aspects and their respective results were presented in Journal Paper I. The main contributions are summarized as follows:

- A quantitative internal IRT method for in-situ measurements within the building diagnostics field was developed in this dissertation. The validation procedures demonstrated that the proposed technique was suitable for façades with heavy walls, reaching a deviation between the theoretical and measured U-value of 1.24% up to 3.97% under a test duration of 2-3h.

- Despite of having an advanced software for the monitoring process of façades with an IR camera in the second step of the model validation, the average method is found to be less complex than the dynamic method for the data analysis. Taking into account the quantity of data to be post-processed is established at 180 thermograms per test, the dynamic method implies greater time of statistical analysis. Hence, it is not suitable in terms of efficiency and cost of the method in a future industrial market.

- Construction project documents for existing buildings, especially the oldest ones, are not available. Hence, and in accordance with the results, this method may provide information about the building envelope for future refurbishment. In the case of new buildings, the method might allow the thermal behaviour of building façades to be checked according to the design parameters. These initial conclusions were supported with further assessments, as seen in the enhancement of the applicability range of techniques based on quantitative IRT within the construction industry field.

- In previous investigations conducted by other researchers, new buildings were not evaluated and inner rooms of existing buildings needed to be at a uniform level of temperature at least 48 h. The current method is characterized by not having this limitation if the building has not been used recently, since it behaves like a system that operates under steady-state conditions.

- The proposed method also represented a significant improvement on current regulations, especially for walls with low U-values (i.e. multi–leaf walls) where the use of tabulated values led to overestimated thermal transmittances (around 40%).

- Concerning the thermal behaviour of walls, it was observed that façades with low U-values presented a higher degree of uniformity. This last aspect ensured homogeneity of the heat flux and temperature of the material, as well as minimum influence of the wall area that was being analysed in the thermogram during the post-processing stage to determine the measured U-value.

The fourth specific objective of this thesis was to improve the applicability range of techniques based on quantitative internal IRT in the construction industry and consequently, to fill out the gap in the standardization of the method. For the first time, an in-depth assessment of the most influential operating conditions and non-transient thermophysical properties as well as a reduction of test duration in real built environments was developed. The framework and results were extensively described in Chapters 5 to 7. The key features are summarized below:

- The study based on the analysis of the operating conditions revealed that the measured U-values were significantly related to the outer air temperature (T_{OUT}) for temperature differences (ΔT) under 16ºC. When the inner air temperature increased considerably ($16<\Delta T<21$ºC), the variance in the measured U-value could be attributed to changes in wall surface temperature (T_{WALL}). The analysis highlighted that the optimum temperature difference range was from 7 to 16ºC. Measured U-values were found to be highly overestimated when the temperature difference was around 3-4ºC and slightly underestimated when ΔT ranged between 16 to 21ºC.

- The study based on the influence of non-transient thermophysical properties of the wall, and undertook in real unoccupied buildings, mainly showed three aspects: (i) multi-leaf walls are less

sensitive and provide more reliable results than single-leaf walls for low temperature difference values (ΔT<7ºC); (ii) quantitative internal IRT is found to be more accurate for multi-leaf walls with high values of heat capacity per unit of area, reaching maximum deviations of 0.20%; (iii) multi-leaf walls with lower U-values might entail deviations of around 9%. These results were consistent with previous studies generally conducted on laboratories or experimental buildings where other techniques were applied.

- The study based on the data collection and post-processing revealed that the accuracy of quantitative internal IRT measurements did not increase with a greater test duration. Subsequently, the proposal of a data-processing method taken as a common criterion for stopping the IRT survey showed that there was no difference in the estimation of in-situ U-values with test durations of 120 minutes, 60 minutes and 30 minutes and a sampling frequency of 1 minute. The hypothesis of a constant signal plus white noise can be adopted, regardless of the heavy multi-leaf wall configuration. The values of the autocorrelation function (ACF) and the cumulated periodogram (CP) were inside the 95% confidence intervals bands. In addition, the results of the data-processing method were consistent with those provided by the model ARX performed on "System Identification Tool" of MATLAB [Mathworks, 2018] during the validation process. Consequently, the test duration could be reduced to 30 minutes.

In terms of applicability, this research might help to streamline the decision-making in real built environments. In this way, the execution of the refurbishment process in buildings might be enhanced, increasing the European renovation rate in the mid-term that it is estimated at 1% per year. This statement is supported by the following aspects:

- Having evaluated the influence of operating conditions and non-transient thermophysical properties, mistakes in relation to operating conditions might be avoided if quantitative internal IRT is used as an energy audit tool. Moreover, technical staff might be able to estimate the possible deviation of thermal transmittance depending on the wall type and check if the measurement is in line with expectations. Possible discrepancies might be related to bad workmanship, a lack of insulation, and ageing of the building materials, among other factors.

- The findings also suggest that this proposed method might allow the assessment of aspects related to the determination of the U-value of unoccupied buildings (without electric and heating systems) for ΔT under 10ºC, especially in Spain or European countries with a Mediterranean climate where these test conditions might represent a limitation. Nevertheless, further research is required in this area.

- The U-value time series analysis entails a considerable reduction of the sampling duration that had been used in previous studies (2 - 3 h). In addition, the data-processing method proposed in this thesis could help to advance the standardization of quantitative IRT: (i) a common measurement pattern can be drawn up; (ii) the data analysis can be simplified, since only a short time period for data collection and post-processing of thermograms is needed. Consequently, the entire procedure gains efficiency and could be incorporated into the industrial market.

- The quantitative internal IRT method might provide a solution to the limitations showed by the heat flux meter (HFM), the current standardized method and commonly used in the construction industry field. The combination of qualitative and quantitative IRT in the same inspection makes possible an in-depth evaluation of the building envelope, instead of providing a local measurement. Moreover, the proposed method provides accurate results from non-homogeneous building elements, taking 30 minutes in comparison with the minimum of 72h and maximum of one week for the HFM.

8.2 Further research

During the development of this research, some interesting issues to be evaluated were emerged. However, they were not addressed within this dissertation, since the level of analysis had been beyond the scope of this dissertation. The most urgent research questions seeking for answers and explanations are listed below:

- The findings of the U-value time series analysis (Chapter 7) suggested that the test duration might not become a source of discrepancy in the determination of the measured U-value, in contrast to the operating conditions and the non-transient thermophysical properties that were assumed as influential factors in previous studies. Nevertheless, future steps of this research should include the assessment of minor test durations with a greater sampling frequency, since the current analysis with a data acquisition interval of 1 minute only allowed the hypothesis to be adopted for $N \geq 30$ measurements.

- According to the Chapter 7, it could be reliable to perform tests in 30 minutes. If future steps of research demonstrate that a minor test duration with a greater sampling frequency is valid, two new proposals of research might be performed. The first one is that solar irradiation might be assumed as a constant parameter under the premises of a cloudy day and short test duration. Hence, the proposed method would not only be limited to northern façades. The second one is that the effects of the wind speed in the material surface might be adopted as minimum for a short period of time. This fact might allow to validate the proposed method for light walls. Roughly speaking, this wall

type has less thermal mass and the impact of the wind speed may be greater, since they cool down faster. However, both research proposals require to be validated.

- As commented on Chapter 2, the numerical model has not still been validated in Summer, since a cooler unit system is required inside the buildings. Most existing units of air conditioner provide a non-stationary regime as well as a non-homogeneity of heat flux and temperature on the material to be assessed. Cold air current peaks might not be given when the inner air temperature is greater than the set point temperature. Therefore, a short sampling frequency might lead to reject the current restriction of the proposed method for the summer season.

- To enhance the combined standard uncertainty associated with the measuring equipment, an assessment focused on the influence of the outer temperature sensor location and the type of external measuring equipment (i.e. weather station, thermocouple type K, PT probe, a thermistor encapsulated in epoxy-filled aluminium etc) in the determination of in-situ measured U-value should be required.

- As seen in Chapter 6 and Journal Paper II, the combined standard uncertainty associated with the measuring equipment increased in walls with high heat capacity per unit of area. Nevertheless, this type of wall presented the minimum deviation between theoretical and measured U-value. In addition, and taking into account the results of the U-value time series analysis (Chapter 7), some aspects were highlighted: (i) the collected data for this façade showed extremely similar signals and the same degree of dispersion for the residuals, regardless the sampling duration to be validated; (ii) the autocorrelation function plot and the cumulated periodograms were slightly better than the rest of investigated buildings. Therefore, it should be necessary to carry out a specific study to improve the uncertainty that derived from the measuring equipment in relation to the aforementioned thermophysical parameter and the thermal inertia of the wall.

- Microsoft developed HoloLens glasses to integrate BIM with virtual reality. These type of glasses are designed for scanning and measuring the 3D space in order to establish BIM solutions. It might be interesting to incorporate an electronic circuit with a small infrared camera in the glasses for in-situ building diagnosis. The electronic circuit should be able to read input data on real time, using: measurements of the IR camera; the inner air temperature by an encapsulated sensor that would be installed in the external surface of the glasses; the outer air temperature by a wire-less sensor installed temporarily outside the building by the technician. Subsequently, the electronic circuit should also be able to determine the measured U-value with the numerical model of the proposed method. In this way, BIM and quantitative IRT would be completely integrated for in-depth analysis in the operation stage of the building.

References

[1] Itard and Meijer, 2008. *Towards a sustainable Northern European Housing Stock. Figures, facts and future*. Available at: < https://www.arct.cam.ac.uk/Downloads/towards-a-sustainable-northern-european-housing.pdf> (accessed 31.10.17)

[2] Dowson, M; Poole, A; Harrison, D; Susman, G. *Domestic UK retrofit challenge: barriers, incentives and current performance leading into the Green Dale*. Energy Policy 50 (2012) 294-305

[3] Gangolells, M; Casals, M. *Resilience to increasing temperatures: Residential building stock adaptation through codes and standards.* Building Research & Information 40 (2012) 645-664

[4] Gangolells, M; Casals, M; Forcada, N; Macarulla, M; Cuerva, E. *Energy mapping of existing building stock in Spain*. Journal of Cleaner Production 112 (2016) 3895 -3904

[5] BPIE -Buildings Performance Institute Europe-, 2011. *Europe's Buildings Under The Microscope. A country-by-country review of the energy performance of buildings*. Available at: < http://bpie.eu/wp-content/uploads/2015/10/HR_EU_B_under_microscope_study.pdf> (accessed 31.10.17)

[6] EIU –Economist Intelligence Unit-, 2013. *Investing in energy efficiency in Europe's buildings. A view from the construction and real estate sectors*. Available at: <http://www.gbpn.org/sites/default/files/06.EIU_EUROPE_CaseStudy_0.pdf > (accessed 31.10.17)

[7] European Parliament's Committee on Industry, Research and Energy [ITRE], 2016. *Boosting Building Renovation: What potential and value for Europe*. Available at: <http://www.europarl.europa.eu/RegData/etudes/STUD/2016/587326/IPOL_STU(2016)587326_EN.pdf> (accessed 31.10.17)

[8] Interreg Europe, 2017. *Improving energy efficiency in buildings*. Available at: <https://www.interregeurope.eu/fileadmin/user_upload/2017-09-11_TO4_policy_brief__EE_in_existing_buildings_v3_KM_kp_final.pdf > (accessed 31.10.17)

[9] IEA –International Energy Agency-, 2013. *Transition to Sustainable Buildings. Strategies and Opportunities to 2050*. Available at: < http://www.iea.org/publications/freepublications/publication/transition-to-sustainable-buildings.html> (accessed 31.10.17)

[10] O'Grady, A.M.; Lechowska, A.A; Harte, A.M. *Quantification of heat losses through building envelope thermal bridges influenced by wind velocity using the outdoor infrared thermography technique*. Applied Energy 108 (2017) 1038 – 1052

[11] Taylor, T; Counsell, J; Gill, S. *Energy efficiency is more than skin deep: Improving construction quality control in new-building housing using thermography*. Energy and Buildings 66 (2013) 222-231

[12] Bordass, B; Cohen, R; Field, J. *Energy Performance of Non-Domestic Buildings: Closing the Credibility Gap.* International Conference on Improving Energy Efficiency in Commercial Buildings, 2004

[13] Demanuele, C; Tweddell, T; Davies, M. *Bridging the gap between predicted and actual energy performance in schools*. World Renewable Energy Congress XI, Abu Dhabi, UAE, 2010

[14] Menezes, A.C.; Cripps, A; Bouchlaghem, D; Buswell, R. *Predicted vs. actual energy performance of non-domestic buildings: using post-occupancy evaluation data to reduce the performance gap*. Applied Energy 97 (2012) 355-364

[15] Dimitrijevic, B; Bros Williamson, J; Purdie, C; Morrison, G. *The Gap between Design and Build: Construction compliance towards 2020 in Scotland*. CIC START ONLINE 2012

[16] Guerra-Santín, O; Tweed, C; Jenkins, H; Jiang, S. *Monitoring the performance of low energy dwellings: Two UK case studies*. Energy and Buildings 64 (2013) 32-40

[17] De Wilde, P. *The gap between predicted and measured energy performance of buildings: a framework for investigation*. Automation in Construction 41 (2014) 40-49

[18] Zalejska -Jonsson, A. *Evaluation of low-energy and conventional residential buildings from occupants' perspective.* Building Environment 58 (2012) 135-144

[19] European Union, 2010. *Directive 2010/31/EU of the European Parliament and of the Council of 19 May 2010 on the energy performance of buildings*. Available at: <http://eur-lex.europa.eu/legal-content/EN/TXT/PDF/?uri=CELEX:32010L0031&from=en> (accessed 04.10.16)

[20] Albatici, R; Tonelli, A.M. *Infrared thermovision technique for the assessment of thermal transmittance value of opaque building elements on site*. Energy and Buildings 42 (2010) 2177-2183

[21] Ficco, G; Iannetta, F; Ianniello, E; d'Ambrosio, F.R.; Dell'Isola, M. *U-Value in situ measurement for energy diagnosis of existing buildings.* Energy and Buildings 104 (2015) 108-121

[22] European Union, 2012. *Directive 2012/27/EU of the European Parliament and of the Council of 25 October 2012 on energy efficiency, amending Directive 2009/125/EC and 2010/30/EU and replacing Directives 2004/8/EC and 2006/32/EC*. Available at: http://eur-lex.europa.eu/legal-content/EN/TXT/PDF/?uri=CELEX:32012L0027&from=en (accessed 04.10.16)

[23] Spain, 2013. *Royal Degree RD 235/2013. Procedure for the certification of building energy efficiency*. Available at:https://www.boe.es/buscar/pdf/2013/BOE-A-2013-3904-consolidado.pdf (accessed 04.10.16)

[24] Spain, 2016. *Royal Degree RD 56/2016. Energy efficiency related to energy audits*. Available at: https://www.boe.es/buscar/pdf/2016/BOE-A-2016-1460-consolidado.pdf (accessed 04.10.16)

[25] Cuerda, E; Pérez, M; Neila, J. *Façade typologies as a tool for selecting refurbishment measures for the Spanish residential building stock*. Energy and Buildings 76 (2014) 119-129

[26] Littlewood, J.R.; Smallwood, I. *Testing building fabric performance and the impacts upon occupant safety, energy use and carbon inefficiencies in dwellings*. Energy Procedia 83 (2015) 454-463

[27] Tronchin, L; Fabbri, K. *Energy performance evaluation in Mediterranean countries: Comparison between software simulations and operating rating simulation*. Energy and Buildings 40 (2008) 1176-1187

[28] Fitton, R. *Energy monitoring in retrofit projects: strategies, tools and practices. Retrofitting the built environament*. John Wiley and Sons, 2013, pp 141-153

[29] Ahern, C; Norton, B; Enright, B. *The statistical relevance and effect of assuming pessimistic default overall thermal transmittance coeficients on dwelling energy performance certification quality in Ireland*. Energy and Buildings 127 (2016) 268-278

[30] Marshall, A; Fiiton, R; Swan, W; Farmer, D; Johnston, D; Benjaber, M; Ji, Y. *Domestic Building fabric performance: Closing the gap between the in-situ measured and modelled performance*. Energy and Buildings 150 (2017) 307-317

[31] Ferrari, S; Zanotto, V. *The thermal performance of walls under actual service conditions: Evaluating the results of climatic chamber tests*. Construction and Building Materials 43 (2013) 309-316

[32] Nardi, I; Sfarra, S; Ambrosini, D. *Quantitative thermography for the estimation of the U-Value: state of art and a case study.* 32nd IUT (Italian Union of Thermo-fluid-dynamics) Heat Transfer Conference, Journal of Physics, Conference Series 547 (2014) 012016

[33] Soares, N.; Martins, C; Gonçalves, M; Santos, P; Simões da Silva, L; Costa, J.J. *Laboratory and in-situ non-destructive methods to evaluate the thermal transmittance and behaviour of walls, windows and construction elements with innovative materials: A review*. Energy and Buildings 182 (2019) 88 – 110

[34] Emmel, M.G; Abadie, M.O.; Mendes, N. *New external convective heat transfer coefficient correlations for isolated low -rise buildings*. Energy and Buildings 39 (2007) 335-342

[35] Prada, A; Cappelletti, F; Baggio, P; Gasparella, A. *On the effect of material uncertainties in envelope heat transfer simulations*. Energy and Buildings 71 (2014) 53-60

[36] Rossi, M; Rocco, V.M. *External walls design: The role of periodic thermal transmittance and internal areal heat capacity.* Energy and Buildings 68 (2014) 732 -740

[37] Liu, J; Heidarinejad, M; Gracik, S; Srebric, J. *The impact of exterior surface convective heat transfer coefficients on the building energy consumption in urban neighbourhoods with different plan area densities.* Energy and Buildings 86 (2015) 449-463

[38] Asdrubali, F; Baldinelli, G; Bianchi, F. *A quantitative methodology to evaluate thermal bridges in buildings.* Applied Energy 97 (2012) 365-373

[39] Vereecken, E; Roels, S. *A comparison of the hygric performance of interior insulation systems: A hot box-cold box experiment.* Energy and Buildings 80 (2014) 37-44

[40] Kumar, A; Suman, B.M. *Experimental evaluation of insulation materials for walls and roofs and their impact on indoor thermal comfort under composite climate*. Building and Environment 59 (2013) 635-643

[41] Anderson, B.R. *The measurement of U-values on site*. Proceedings of the ASHRAE/DOE/BTECC Conference (1985)

[42] Roulet, C; Gass, J; Markus, I. *In-situ U-value measurement: reliable results in short time by dynamic interpretation of measured data*. Proceedings Thermal Performance of the Exterior Envelopes of Buildings III. ASHRAE (1985) 777-784

[43] Flanders, S.N. *In-situ Heat Flux Measurements in Buildings. Applications and Interpretations of Results*. CRREL Special Report 91-3, U.S. Army Corps of Engineers, Cold Regions Research and Engineering Laboratory (1991)

[44] Flanders, S.N. *The convergence criterion in measuring building R-values*. Proceedings Thermal Performance of the Exterior Envelopes of Buildings V. ASHRAE (1992) 204-209

[45] Ahmad, A; Maslehuddin, M; Al-Hadhrami, L.M. *In situ measurement of thermal transmittance and thermal resistance of hollow reinforced precast concrete walls.* Energy and Buildings 84 (2014) 132 -141

[46] Gaspar, K; Casals, M; Gangolells, M. *A comparison of standardized calculation methods for in situ measurements of façades U-value*. Energy and Buildings 130 (2016) 592-599

[47] Atsonios, I.A.; Mandilaras, I.O; Kontogeorgos, A.D.; Founti, M.A. *A comparative assessment of the standardized methods for the in-situ measurement of the thermal resistance of building walls*. Energy and Buildings 154 (2017) 198-206

[48] Anderson, L.J. *Energy conservation with thermography*. Proceedings of the Infrared Information Exchange. AGA Corporation (1977) 61-62

[49] Burch, D.M; Kusuda, T; Blum, D.G. *An infrared technique for heat loss measurement*. NBS Technical Note 933, U.S. Government Printing Office (1977)

[50] Burn, K; Schuyler, G. *Applications of infrared thermography in locating and identifying building faults*. Journal of International Institute for Conservation 4 (1980) 3-14

[51] Flanders, S.N; Marshall, S.J. *Interpolating R-Values from thermograms*. Proceedings of Thermosense IV, SPIE –The International Society for Optical Engineering- (1981) 157-164

[52] McIntosh, G.B. *Recent advances in the quantification of heat loss using thermography*. Proceedings of Thermosense IV, SPIE –The International Society for Optical Engineering- (1981) 213-218

[53] Straube, J; Burnett, E.F.P. *Rain control and design strategies*. Journal of Building Physics 23 (1999) 41-56

[54] Kalamees, T. *Air tightness and air leakages of new lightweight single-family detached houses in Estonia*. Building and Environment 42 (2007) 2369-2377

[55] Madding, R. *Finding R-values of stud frame constructed houses with IR thermography*. Proceedings of InfraMation (2008)

[56] Lucchi, E. *Non-invasive method for investigating energy and environmental performances in existing buildings*. PLEA Conference on Passive and Low Energy Architecture (2011)

[57] Meola, C; Carlomagno, G.M. *Infrared thermography to evaluate impact damage in glass/epoxy with manufacturing defects*. International Journal of Impact Engineering 67 (2014) 1-11.

[58] Fox, M; Coley, D; Goodhew, S; de Wilde, P. *Time- lapse thermography for building defect detection.* Energy and Buildings 92 (2015) 95-106

[59] Barreira, E; Almeida, R.M.S.F; Delgado, J.M.P.Q. *Infrared thermography for assessing moisture related phenomena in building components.* Construction and Building materials 110 (2016) 251-269

[60] Lehman, B; Ghazi Wakili, K; Frank, Th; Vera Collado, B; Tanner, Ch. *Effects of individual climatic parameters on the infrared thermography of buildings*. Applied Energy 110 (2013) 29-43

[61] Tzifa, V; Papadakos, G; Papadopoulou, A.G.; Marinakis, V; Psarras, J. *Uncertainty and method limitations in a short-time measurement of the effective thermal transmittance on a building envelope using an infrared camera*. International Journal of Sustainable Energy (2014) 1-19

[62] Albatici, R; Tonelli, A.M.; Chiogna, M. *A comprehensive experimental approach for the validation of quantitative infrared thermography in the evaluation of building thermal transmittance*. Applied Energy 141 (2015) 218-228

[63] Meng, X; Yan, B; Gao, Y; Wang, J; Zhang, W; Long, E. *Factors affecting the in-situ measurement accuracy of the wall heat transfer coefficient using the heat flow meter method*. Energy and Buildings 86 (2015) 754-765

[64] Nardi, I; Paoletti, D; Ambrosini, D; de Rubeis, T; Sfarra, S. *U-Value assessment by infrared thermography: A comparison of different calculation methods in a Guarded Hot Box*. Energy and Buildings 122 (2016) 211-221

[65] Haralambopoulos, D; Paparsenos, G.F. *Assessing the thermal insulation of old buildings –The need for in-situ spot measurements of thermal resistance and planar infrared thermography*. Energy Conversion and Management 39 (1998) 65-79

[66] Kisilewicz, T; Wróbel, A. *Quantitative infrared wall inspection*. 10th International Conference on Quantitative Infrared Thermography (2010)

[67] Fokaides, P.A.; Kalogirou, S.A. *Application of infrared thermography for the determination of the overall heat transfer coefficient (U-Value) in building envelopes*. Applied Energy 88 (2011) 4358-4365

[68] Dall'O, G; Sarto, L; Panza, A. *Infrared screening of residential buildings for energy audit purposes: results of a field test*. Energies 6 (2013), 3859-3878

[69] De Freitas, S.S.; de Freitas, V.P.; Barreira, E. *Detection of façade plaster detachments using infrared thermography –A non destructive technique.* Construction and Building Materials 70 (2014) 80-87

[70] Danielski, I; Fröling, M. *Diagnosis of buildings' thermal performance -a quantitative method using thermography under non-steady state heat flow*. 7th Internacional Conference on Sustainability in Energy and Buildings. Energy Procedia (2015) 320-329

[71] Albatici, R; Passerini, F; Tonelli, A.M.; Gialanella, S. *Assessment of the thermal emissivity value of building materials using an infrared thermovision technique emissometer*. Energy and Buildings 66 (2013) 33-40

[72] International Organization for Standardization, 2014. *ISO 9869:2014 Thermal insulation. Building elements. In –situ measurement of thermal resistance and thermal transmittance. Part 1: Heat flow meter method*

[73] Carbonez, K; Van Den Bossche, N; Steeman, M; Van De Vijver, S; Janssens, A. *On the applicability of quantitative infrared thermography on window glazing.* 10th Nordic Symposium on Building Physics, Proceedings (2014) 313-320

[74] Tejedor, B; Casals, M; Gangolells, M; Roca, X. *Quantitative internal infrared thermography for determining in-situ thermal behaviour of façades.* Energy and Buildings 151 (2017) 187-197

[75] Infrared Training Center and FLIR Systems, 2015. *Level I Infrared Thermography Certification Manual. Publication number 1560093_G-es-ES.* Spain, 2016

[76] International Organization for Standardization, 1998. *EN 13187:1998 (ISO 6781:1983 modified). Thermal Performance of Buildings. Qualitative detection of thermal irregularities in building envelopes. Infrared method*

[77] RESNET –Residential Energy Services Network-, 2010. *RESNET Interim Guideline for Thermographic Inspections of Buildings*. Available at: <http://www.resnet.us/standards/RESNET_IR_ interim_guidelines. pdf > (accessed 04.10.16)

[78] Nardi, I; Ambrosini, D; de Rubeis, T; Sfarra, S; Perilli, S; Pasqualoni, G. *A comparison between thermographic and flow-meter methods for the evaluation of thermal transmittance of different wall constructions.* Journal of Physics, Conference Series 655 (2015) 012007

[79] Tejedor, B; Casals, M; Gangolells, M. *Assessing the influence of operating conditions and thermophysical properties on the accuracy of in-situ measured U-values using quantitative internal* infrared *thermography.* Energy and Buildings 171 (2018) 64-75

[80] Dall'O, G; Lucchi, E; Poliseno, G. *Infrared scanning on buildings as a tool for evaluating pathologies and suggesting energy retrofit actions.* 47th AiCARR International Conference on Systems. Energy and Built Environment toward a Sustainable Comfort (2009)

[81] Fox, M; Goodhew, S; De Wilde, P. *Building defect detection: External versus internal thermography.* Building and Environment 105 (2016) 317-331

[82] Palyvos, J.A. *A survey of wind convection coefficient correlations for building envelope energy systems' modelling.* Applied Thermal Engineering 28 (2008) 801-808

[83] Hoyano, A; Asano, K; Kanamaru, T. *Analysis of the heat flux from the exterior surface of buildings using time sequential thermography.* Atmospheric Environment 33 (1999) 3941-3951

[84] Rabadiya, A.V.; Kirar, R. *Comparative analysis of wind loss coefficient (wind heat transfer coefficient) for solar plate collector.* International Journal of Emerging Technology and Advanced Engineering (IJETAE). ISSN 2250-2459, Volume 2, Issue 9, 2012

[85] Sham, J.F.C; Lo, T.Y.; Memon, S.A. *Verification and application of continuous surface temperature monitoring technique for investigation of nocturnal sensible heat release characteristics by building fabrics.* Energy and Buildings 53 (2012) 108-116.

[86] International Organization for Standardization, 2012. *UNE EN ISO 6946:2012 Building components and building elements. Thermal resistance and thermal transmittance. Calculation method*

[87] Asdrubali, F; D'Alessandro, F; Baldinelli, G; Bianchi, F. *Evaluating in situ thermal transmittance of green buildings masonries –A case study*. Case Studies in Construction Materials 1 (2014) 53-59

[88] Biddulph, P; Gori, V; Elwell, C.A.; Scott, C; Rye, C; Lowe, R; Oreszczyn, T. *Inferring the thermal resistance and effective thermal mass of a wall using frequent temperature and heat flux measurements*. Energy and Buildings 78 (2014) 10-16

[89] Kylili, A; Fokaides, P.A.; Christou, P; Kalogirou, S.A. *Infrared thermography (IRT) applications for building diagnostics: A review*. Applied Energy 134 (2014) 531 -549

[90] Taylor, T; Counsell, J; Gill, S. *Combining thermography and computer simulation to identify and assess insulation defects in the construction of building façades.* Energy and Buildings 76 (2014) 130-142

[91] Fox, M; Coley, D; Goodhew, S; de Wilde, P. *Thermography methodologies for detecting energy related building defects*. Renewable and Sustainable Energy Reviews 40 (2014) 296-310

[92] Barreira, E; Almeida, R.M.S.F; Moreira, M. *An infrared thermography passive approach to assess the effect of leakage points in buildings*. Energy and Buildings 140 (2017) 224-235

[93] Cesaratto, P.G; De Carli, M. *A measuring campaign of thermal conductance in situ and possible impacts on net energy demand in buildings*. Energy and Buildings 59 (2013) 29-36

[94] American Society for Testing and Materials, 2013. *Standard ASTM C177-13. Standard test method for steady-state heat flux measurements and thermal transmission properties by means of the guarded hot plate apparatus*. 2013

[95] American Society for Testing and Materials, 2011. *Standard ASTM C1363-11. Standard test method for thermal performance of building materials and envelope assemblies by means of a hot box apparatus*

[96] International Organization for Standardization, 1997. *UNE-EN ISO 8990:1997. Thermal insulation. Determination of steady-state thermal transmission properties. Calibrated and guarded hot box*

[97] International Organization for Standardization, 2008. *ISO 18434-1:2008. Condition monitoring and diagnostic of machines. Thermography –Part 1: General procedures*

[98] Balaras, C.A; Argiriou, A.A. *Infrared thermography for building diagnostics.* Energy and Buildings 34 (2002) 171-183

[99] Datcu, S; Ibos, L; Candau, Y; Mattei, S. *Improvement of building wall surface temperature measurements by infrared thermography.* Infrared Physics & Technology 46 (2005) 451-467

[100] Charlier, L. *Utilisation de la thermographie infrarouge pour la determination des déperditions thermiques d'un bâtiment.* Université de Liége (2007)

[101] Van De Vijver, S; Steeman, M; Van Den Bossche, N; Carbonez, K; Janssens, A. *The influence of environmental parameters on the thermographic analysis of the building envelope.* 12th International Conference on Quantitative Infrared Thermography, Proceedings (2014)

[102] Lucchi, E. *Applications of the infrared thermography in the energy audit of buildings: A review.* Renewable and Sustainable Energy Reviews 82 (2018) 3077-3090

[103] Vavilov, VP. *A pessimistic view of the energy auditing of building structures with the use of infrared thermography.* Russian Journal of Nondestructive Testing 46 (2010) 906-910

[104] Nardi, I; Lucchi, E; De Rubeis, T; Ambrosini, D. *Quantification of heat energy losses through the building envelope: a state-of-the-art analysis with critical and comprehensive review on infrared thermography*. Buildings and Environment 146 (2018) 190-205

[105] Marshall, A; Francou, J; Fitton, R; Swan, R; Owen, W; Benjaber, M. *Variations in the U-value measurements of a whole dwelling using infrared thermography under controlled conditions*. Buildings 8, 46 (2018)

[106] Bienvenido-Huertas, D; Rodríguez-Álvaro, R; Moyano, J.J; Rico, F; Marín, D. *Determining the U-value of façades using the thermometric method: potentials and limitations*. Energies 11 (2018) 1-17

[107] Marinetti, S; Cesaratto, P.G. *Emissivity estimation for accurate quantitative thermography*. NDT&E International 51 (2012) 127-134.

[108] FLIR Systems, 2015. FLIR TOOLS+ Software

[109] O'Grady, A.M.; Lechowska, A.A.; Harte, A.M. *Infrared thermography technique as an in-situ method of assessing heat loss through thermal bridging*. Energy and Buildings 135 (2017) 20 – 32

[110] Grinzato, E; Vavilov, V; Kauppinen, T. *Quantitative infrared thermography in buildings*. Energy and Buildings 29 (1998) 1-9

[111] Martin Ocaña, S; Cañas Guerrero, I; Gonzalez Requena, I. *Thermographic survey of two rural buildings in Spain*. Energy and Buildings 36 (2004) 515-523

[112] Aelenei, D; Henriques, F.M.A. *Analysis of the condensation risk on exterior surface of building envelopes*. Energy and Buildings 40 (2008) 1866 -1871

[113] Desogus, G; Mura, S; Ricciu, R. *Comparing different approaches to in situ measurement of building components thermal resistance.* Energy and Buildings 43 (2011) 2613-2620

[114] Bagavathiappan, S; Lahiri, B.B.; Saravanan, T; Philip, J; Jayakumar, T. *Infrared thermography for condition monitoring –A review*. Infrared Physics and Technology 60 (2013) 35-55

[115] Byrne, A; Byrne, G; Davies, A; Robinson, A.J. *Transient and quasi-steady thermal behaviour of a building envelope due to retroffited cavity wall and ceiling insulation*. Energy and Buildings 61 (2013) 356-365

[116] Bisegna, F; Ambrosini, D; Paoletti, D; Sfarra, S; Gugliermetti, F. *A qualitative method for combining thermal imprints to emerging weal points of ancient wall structures by passive infrared thermography –A case study*. Journal of Cultural Heritage 15 (2014) 199-202

[117] Latif, E; Anca Ciupala, M; Chitral Wijeyesekera, D. *The comparative in situ hygrothermal performance of Hemp and Stone Wool insulations in vapour open timber frame wall panels*. Construction and Building Materials 73 (2014) 205-213

[118] Pisello, A.L.; Castaldo, V.L.; Taylor, J.E.; Cotana, F. *Expanding Inter-Building Effect Modelling to Examine Primary Energy for Lighting.* Energy and Buildings 76 (2014) 513-523

[119] Stazi, F; Tittarelli, F; Politi, G; Di Perna, C.; Munafo, P. *Assessment of the actual hygrothermal performance of glass mineral wool insulation applied 25 years ago in masonry cavity walls*. Energy and Buildings 68 (2014) 292-304

[120] Pérez –Bella, J.M.; Domínguez-Hernández, J; Cano-Suñén, E; del Coz-Díaz, J.J; Álvarez Rabanal, F.P. *A correction factor to approximate the design thermal conductivity of building materials. Application to Spanish façades*. Energy and Buildings 88 (2015) 153-164

[121] Maroy, K; Carbonez, K; Steeman, M; Van Den Bossche, N. *Assessing the thermal performance of insulating glass units with infrared thermography: Potencial and limitations.* Energy and Buildings 138 (2017) 175 - 192

[122] Astarita, T; Cardone, G; Carlomagno, G.M.; Meola, C. *A survey on infrared thermography for convective heat transfer measurements.* Optics and Laser Technology 32 (2000) 593-610

[123] Avdelidis, N.P.; Moropoulou, A. *Emissivity considerations in building thermography*. Energy and Buildings 35 (2003) 663-667

[124] Porras-Amores, C; Mazarron, F.R.; Cañas, I. *Using quantitative infrared thermography to determine indoor air temperature*. Energy and Buildings 65 (2013) 292 -298

[125] Ohlsson, K.E.A.; Olofsson, T. *Quantitative infrared thermography imaging of the density of heat flow rate through a building element surface*. Applied Energy 134 (2014) 499-505

[126] ASHRAE. *Handbook: Fundamentals.* American Society of Heating, Refrigerating and Air-Conditioning Engineers, 2005. ISBN 1-931-86271-0

[127] Touloukian, Y.S.; Liley, P.E.; Saxena, S.C. *Thermophysical Properties of Matter. Volume 3. Thermal Conductivity.* IFI/Plenum. New York, 1970. ISBN 978-0-306-67020-6

[128] Touloukian, Y.S.; Saxena, S.C.; Hestermans, P. *Thermophysical Properties of Matter. Volume 11. Viscosity.* IFI/Plenum. New York, 1970. ISBN 978-1-475-71630-6

[129] Keenan, J.H; Chao, J; Kaye, J. *Gas Tables –International Version.* John Wiley & Sons. New York, 1983. ISBN 0-471-08874-9

[130] Dixon, C. *The Shock Absorber Handbook. Appendix B. Properties of air.* Second Edition. John Wiley & Sons. New York, 2007. ISBN 978-0-470-51020-9

[131] Serth, R.W. *Process heat transfer: Principles and Applications. Chapter 2: Convective heat transfer*. Elsevier, 2007, p.43-84, ISBN 978-0-12-373588-1.

[132] F-Chart Software, 2016. EES Software

[133] Spain, 2006. *Royal Decree 314/2006 approving the Spanish Technical Building Code CTE-DB-HE1*. Available at: < http://www.boe.es/boe/dias/2006/03/28/pdfs/A11816-11831.pdf > (accessed 04.10.16)

[134] International Organization for Standardization, 2012. *UNE EN ISO 10456:2012 Building materials and products –Hygrothermal properties –Tabulated design values and procedures for determining declared and design thermal values*, 2012

[135] International Organization for Standardization, 2008. *ISO/IEC Guide 98-3:2008. Uncertainty of Measurement. Part 3: Guide to the Expression of Uncertainty in Measurement (GUM: 1995)*. 1998

[136] Spain, 1979. *Royal Decree 2429/1979 approving the Basic Building Norm on Thermal Conditions in Buildings NBE-CT-79*. Available at: < https://www.boe.es/boe/dias/1979/10/22/pdfs/A24524-24550.pdf> (accessed 04.10.16)

[137] IBM, 2017. SPSS Statistics v.24 Software

[138] Love, P. *Influence of project type and procurement method on rework costs in building construction projects*. Journal of Construction Engineering and Management 128 (2002) 18-29

[139] Forcada, N; Macarulla, M; Fuertes, A; Casals, M; Gangolells, M; Roca, X. *Influence of building type on post-handover defects in housing.* Journal of Performance of Constructed Facilities 26 (2012) 433-440

[140] International Organization for Standardization, 2011. *UNE EN ISO 13786:2011 Thermal performance of building components –Dynamic thermal characteristics –Calculation methods*

[141] Yaffee, R.A.; McGee, M. *Introduction to time series analysis and forecasting: with applications of SAS and SPSS*. Academic Press (2000)

[142] Mahan, M.Y; Chron, C.R; Georgopoulos, A.P. *White noise test: detecting autocorrelation and nonstationarities in long time series after ARIMA modelling*. Proceedings of the 14th Python in Science Conference (SCYPY 2015)

[143] Andersen, K.K.; Madsen, H; Hansen, L.H. *Modelling the heat dynamics of a building using stochastic differential equations*. Energy and Buildings 31 (2000) 13-24

[144] Bacher, P; Madsen, H. *Identifying suitable models for the heat dynamics of buildings*. Energy and Buildings 43 (2011) 1511-1522

[145] Macarulla, M; Casals, M; Carnevali, M; Forcada, N; Gangolells, M. *Modelling indoor air carbon dioxide concentration using grey-box models*. Building and Environment 117 (2017) 146-153

[146] Macarulla, M; Casals, M; Forcada, N; Gangolells, M; Giretti, A. *Estimation of a room ventilation air change rate* using *a stochastic grey-box modelling approach.* Measurement 124 (2018) 539-548

[147] Meko, D. *Notes on Autocorrelation, Notes 3, GEOS 585A*, *from the course Applied Time Series Analysis*. University of Arizona, 2010. Available at: <http://www.ltrr.arizona.edu/~dmeko/geos585a.html#chandout> (accessed 20.02.18)

[148] Fuller, W.A. *Introduction to statistical time series*. John Wiley and Sons. pp. 363-366. New York 1996

[149] Rust, B.W; O'Leary, D.P. *Residual periodograms for choosing regularization parameters for ill-posed* problems. IOP Science. Inverse Problems 24 (2008)

[150] Box, G.; Jenkins, G. *Time series analysis: forecasting and control*. Holden Day, 2nd Edition (1976)

[151] Anderson, O.D. *The Box-Jenkins approach to time series analysis*. RAIRO 11 (1977) 3-29

[152] Huitema, B.E.; McKean, J.W. *Autocorrelation estimation and inference with small samples*. Physicological Bulletin 110 (1991) 291-304

[153] De Carlo, L.T.; Tryon, W.W. *Estimating and testing autocorrelation with small samples: a comparison of the C-Statistic to a modified estimator*. Behav. Res. Ther. 31 (1993) 781-788

[154] Lúnden, O; Bäckström, M. *Stirrer efficiency in FOA reverberation chambers. Evaluation of correlation coefficients and chi-squared tests*. Proc. IEEE Int.Symp.Electromagn.Compat. 1 (2000) 11-16

[155] Plane, D.R.; Gordon, K.R. *A simple proof of no applicability of the central limit theorem to finite populations.* The American statistician 36 (1982) 175-176

[156] Chang, H-J; Chen, P-Y. *On sample size in using central limit theorem for gamma distribution*. Information and Management Sciences 19 (2008) 153-174

[157] American Society for Testing and Materials, 2013. *Standard ASTM C1555-95 (2013). Standard practice for determining thermal resistance of building envelope components from the in-situ data*

[158] Gaspar, K; Casals, M; Gangolells, M. *In-situ measurement of façades with a low U-value: Avoiding deviations*. Energy and Buildings 170 (2018) 61-73

[159] Wiener, N. *Extrapolation, Interpolation and Smoothing of Stationary Time Series*. John Wiley & Sons. New York, 2013 (Reprint of 1949 Edition). ISBN 1-614-27517-3

[160] Brown, R.G.; Hwang, P. *Introduction to Random Signals and Applied Kalman Filtering*. John Wiley & Sons. New York, 1996. ISBN 0-471-12839-2

[161] Beck, J.V.; Blackwell, A; Haji-Sheich. *Comparison of some inverse heat conduction methods using experimental data*. International Journal of Heat Mass Transfer 39 (1996) 3649-3657

[162] Ilyinsky, A.L.; Rainieri, S; Farina, A; Pagliarini, G. *New Experimental Tecnhique for Enhancement of Spatial Resolution in Heat Transfer Measurements*. Proceedings 4th World Conference on Experimental Heat Transfer, Fluid Mechanics and Thermodynamics, vol.1 (1997) 93-100

[163] Le Niliot, C; Gallet, P. *Infrared thermography applied to the resolution on inverse heat conduction problems: recovery of heat line sources and boundary conditions*. Revue Générale de Thermique 37 (1998) 629-643

[164] Rainieri, S; Pagliarini, G. *Performance Analysis of a FPA IR Camera for Surface Heat Flux Restoration*. Proceedings of the 8th International Symposium on Flow Visualization Sorrento (1998) 1-4

[165] Rainieri, S; Pagliarini, G. *Data filtering applied to infrared thermographic measurements intended for the estimation of local heat transfer coefficient*. Experimental Thermal and Fluid Science 26 (2002) 109-114

[166] MathWorks, 1998. Signal Processing Toolbox, MATLAB Software

[167] MathWorks, 1998. Image Processing Toolbox, MATLAB Software

[168] Jiménez, M.J; Madsen, H; Andersen, K.K. *Identification of the main thermal characteristics of building components using MATLAB*. Building and Environment 43 (2008) 170-180

[169] MathWorks, 2006. IDENT Toolbox, MATLAB Software

[170] MathWorks, 2018. System Identification Tool, MATLAB Software